

AD-A187 187

HIGH-RESOLUTION REAL-TIME RADIOGRAPHY (RTR) SYSTEM
DESIGN(U) LOCKHEED MISSILES AND SPACE CO INC PALO ALTO
CA RESEARCH AND D L M KLYNN ET AL JUL 87
LMSC-D067282 AFMIL-TR-87-4055

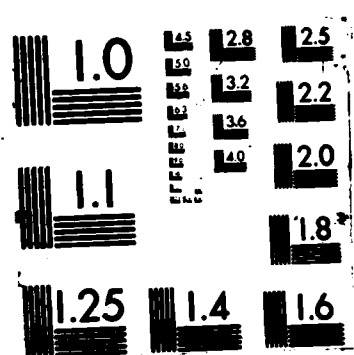
1/2

UNCLASSIFIED

F/G 14/2

NL



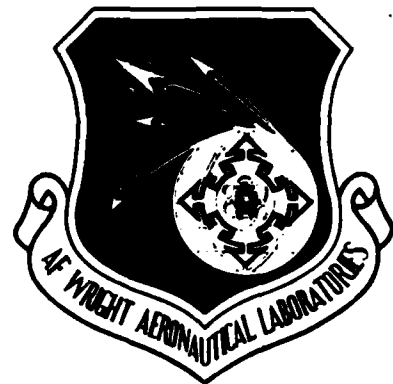


DTIC FILE COPY

(2)

AD-A187 107

AFWAL-TR-87-4055



HIGH-RESOLUTION
REAL-TIME RADIOGRAPHY (RTR)
SYSTEM DESIGN

Lockheed Missiles & Space Company, Inc.
Research & Development Division
3251 Hanover Street
Palo Alto, California 94304

DTIC
ELECTE
NOV 09 1987
S D

July 1987

Final Report for Period July 1983 - November 1986

Approved for Public Release: Distribution Unlimited

MATERIALS LABORATORY
AIR FORCE WRIGHT AERONAUTICAL LABORATORIES
AIR FORCE SYSTEMS COMMAND
WRIGHT-PATTERSON AIR FORCE BASE, OHIO 95433-6533

87 10 14

43

NOTICE

When Government drawings, specifications, or other data are used for any purpose other than in connection with a definitely related Government procurement operation, the United States Government thereby incurs no responsibility nor any obligation whatsoever; and the fact that the government may have formulated, furnished, or in any way supplied the said drawings, specifications, or other data, is not to be regarded by implication or otherwise as in any manner licensing the holder or any other person or corporation, or conveying any rights or permission to manufacture, use, or sell any patented invention that may in any way be related thereto.

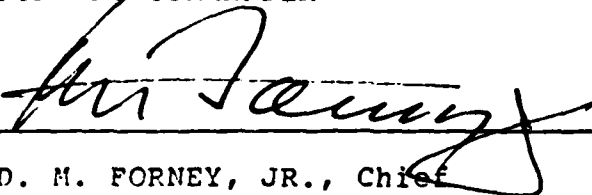
This report has been reviewed by the Office of Public Affairs (ASD/PA) and is releasable to the National Technical Information Service (NTIS). At NTIS, it will be available to the general public, including foreign nations.

This technical report has been reviewed and is approved for publication.



JAMES A. HOLLOWAY
Nondestructive Evaluation Branch
Metals and Ceramics Division

FOR THE COMMANDER



D. M. FORNEY, JR., Chief
Nondestructive Evaluation Branch
Metals and Ceramics Division

"If your address has changed, if you wish to be removed from our mailing list, or if the addressee is no longer employed by your organization, please notify AFWAL/MLLP, W-PAFB OH 45433-6533 to help us maintain a current mailing list."

Copies of this report should not be returned unless return is required by security considerations, contractual obligations, or notice on a specific document.

Unclassified

SECURITY CLASSIFICATION OF THIS PAGE

REPORT DOCUMENTATION PAGE				Form Approved OMB No 0704-0188	
1a. REPORT SECURITY CLASSIFICATION Unclassified			1b. RESTRICTIVE MARKINGS None		
2a. SECURITY CLASSIFICATION AUTHORITY			3. DISTRIBUTION/AVAILABILITY OF REPORT Approved for public release; distribution is unlimited		
2b. DECLASSIFICATION/DOWNGRADING SCHEDULE N/A					
4. PERFORMING ORGANIZATION REPORT NUMBER(S) LMSC-D067282			5. MONITORING ORGANIZATION REPORT NUMBER(S) AFWAL-TR-87-4055		
6a. NAME OF PERFORMING ORGANIZATION Lockheed Missiles & Space Company, Inc.		6b. OFFICE SYMBOL (If applicable) 93-60	7a. NAME OF MONITORING ORGANIZATION Air Force Wright Aeronautical Laboratories Materials Laboratory (AFWAL/MLLP)		
6c. ADDRESS (City, State, and ZIP Code) NDT Technology Laboratory 815 E. Middlefield Road Mountain View, CA 94304			7b. ADDRESS (City, State, and ZIP Code) Wright-Patterson AFB, Ohio 45433-6533		
8a. NAME OF FUNDING/SPONSORING ORGANIZATION		8b. OFFICE SYMBOL (If applicable)	9. PROCUREMENT INSTRUMENT IDENTIFICATION NUMBER Contract F33615-83-C-5087		
8c. ADDRESS (City, State, and ZIP Code)			10. SOURCE OF FUNDING NUMBERS		
			PROGRAM ELEMENT NO. 62102F	PROJECT NO. 2418	TASK NO. 02
			WORK UNIT ACCESSION NO. 19		
11. TITLE (Include Security Classification) High-Resolution Real-Time Radiography (RTR) System Design Unclassified					
12. PERSONAL AUTHOR(S) Klynn, L. M.; Barry, R. C.; Barker, M. D.; Bueno, C.; Maple, T. G.					
13a. TYPE OF REPORT Final		13b. TIME COVERED FROM 7-20-83 to 11-20-86		14. DATE OF REPORT (Year, Month, Day) July 1987	
15. PAGE COUNT 140					
16. SUPPLEMENTARY NOTATION					
17. COSATI CODES			18. SUBJECT TERMS (Continue on reverse if necessary and identify by block number)		
FIELD	GROUP	SUB-GROUP			
14	02		Real-time radiography; Display Screens; X-ray converters		
19. ABSTRACT (Continue on reverse if necessary and identify by block number)					
<p>A high-resolution real-time radiography (RTR) system was designed for aerospace component x-ray inspections in the 20 to 300 kV range. Particulate and glass x-ray converters, image intensifiers, and video camera components were performance tested for resolution greater than 10 lp/mm, dynamic range greater than 1000, contrast sensitivity of 1%, and image size of 12 x 12 in. A breadboard RTR system, constructed with optimized components, produced 1024 x 1024 pixels per image with 8 bits per pixel. Computer controlled optical zooming achieved horizontal fields of view from 12.8 to 0.5 in. and corresponding resolutions of 3 to 80 pixels mm. Conceptual high-resolution RTR prototype systems were designed using the test results.</p>					
20. DISTRIBUTION/AVAILABILITY OF ABSTRACT <input type="checkbox"/> UNCLASSIFIED/UNLIMITED <input checked="" type="checkbox"/> SAME AS RPT <input type="checkbox"/> DTIC USERS			21. ABSTRACT SECURITY CLASSIFICATION		
22a. NAME OF RESPONSIBLE INDIVIDUAL J. A. Halloway			22b. TELEPHONE (Include Area Code) (513) 255-5309		22c. OFFICE SYMBOL AFWAL/MLLP

TABLE OF CONTENTS

Section		Page
1	INTRODUCTION	1-1
2	TECHNICAL REQUIREMENTS/TASKS	2-1
	2.1 TASK I - TESTING AND EVALUATION OF THE X-RAY CONVERTER DEVICES	2-1
	2.2 TASK II - BREADBOARD RTR SYSTEM CONSTRUCTION/ DEMONSTRATION	2-2
	2.3 TASK III - RTR PROTOTYPE SYSTEM DESIGN	2-3
3	TASK I - X-RAY CONVERTER DEVICE EVALUATION	3-1
	3.1 X-RAY CONVERTER DEVICES	3-1
	3.1.1 Particulate Screen X-ray Converters	3-1
	3.1.2 Commercial Fluorescent Glass	3-1
	3.1.3 Commercial Fiber-Optic Fluorescent Glass	3-2
	3.1.4 Gadolinium Oxysulfide Films	3-2
	3.1.5 LMSC-Proprietary Fluorescent Glass	3-3
	3.2 X-RAY CONVERTER EVALUATION CRITERIA	3-3
	3.2.1 Quantum Efficiency	3-4
	3.2.2 Dynamic Range	3-5
	3.2.3 MODULATION TRANSFER FUNCTION	3-5
	3.2.4 Contrast Sensitivity	3-7
	3.2.5 Figure of Merit Criteria	3-8
	3.3 X-RAY CONVERTER PERFORMANCE	3-9
	3.3.1 Effective Quantum Efficiency (EQE) Measurements	3-9
	3.3.2 Dynamic Range of X-ray Converters	3-15
	3.3.3 Modulation Transfer Function (MTF) Measurements	3-15
	3.3.4 Contrast Sensitivity of X-Ray Converters	3-28
	3.4 EXTERNAL FACTORS AFFECTING X-RAY CONVERTER PERFORMANCE	3-36
	3.4.1 Geometrical Unsharpness	3-37
	3.4.2 Spectral Distribution of the X-Ray Source	3-37
	3.4.3 Spectral Distribution of the Visible Light	3-38

TABLE OF CONTENTS (Continues)

Section	Page
3.4.4 Performance of the Measuring Equipment	3-38
3.4.5 Scattered Radiation	3-39
3.4.6 Radiation Damage of Converter Materials	3-40
3.5 PERFORMANCE OF LOW-LIGHT-LEVEL VIDEO CAMERAS	3-40
3.6 SUMMARY AND CONCLUSIONS	3-42
3.7 FIGURES OF MERIT CONVERTER PERFORMANCE	3-49
4 TASK II - BREADBOARD RTR SYSTEM	4-1
4.1 CONSTRUCTION OF THE BREADBOARD HIGH-RESOLUTION RTR SYSTEM	4-1
4.1.1 X-Ray Source	4-2
4.1.2 X-Ray Converter Screen	4-4
4.1.3 Lens	4-4
4.1.4 Camera	4-8
4.1.5 Camera Positioner	4-12
4.1.6 Host Computer System	4-14
4.1.7 Image Processor	4-17
4.1.8 Software	4-21
4.1.9 Displays	4-23
4.1.10 Video Image Printer	4-24
4.1.11 Object Positioner	4-24
4.1.12 Overall Configuration	4-26
4.2 BREADBOARD PERFORMANCE	4-30
4.2.1 Resolution	4-30
4.2.2 Dynamic Range	4-32
4.2.3 Penetrameter Sensitivity	4-33
4.3 INDUSTRY RTR DEMONSTRATION	4-57
5 RTR PROTOTYPE SYSTEM DESIGN	5-1
5.1 X-RAY SYSTEM	5-1
5.2 CAMERA SYSTEM	5-1
5.2.1 X-Ray Converter Screen	5-1

TABLE OF CONTENTS (Concluded)

Section	Page
5.2.2 Lens	5-2
5.2.3 Video Camera	5-3
5.2.4 Camera Positioners	5-4
5.3 IMAGE PROCESSING AND CONTROL COMPUTER	5-6
5.3.1 Host Computer	5-6
5.3.2 Image Processor	5-6
5.3.3 Video Digitizer	5-7
5.3.4 Software	5-7
5.4 OBJECT MANIPULATION SYSTEM	5-8
5.5 OVERALL CONFIGURATION	5-11



Accession For	
NTIS CRA&I	<input checked="" type="checkbox"/>
DTIC TAB	<input type="checkbox"/>
Unannounced	<input type="checkbox"/>
Justification	
By	
Distribution /	
Availability Codes	
Dist	Avail and/or Special
A-1	

LIST OF ILLUSTRATIONS

Figure		Page
1	Instrumentation to Test and Evaluate X-Ray Converter Devices	3-6
2	Experimental Setup for Measuring Effective Quantum Efficiency	3-10
3	Efficiency of Particulate Screens	3-10
4	Efficiency of Commercial Glass Screens (420 kV, 10 mA x-ray source)	3-11
5	Efficiency of Commercial Glass and Fine Particulate Screens (420 kV, 10 mA x-ray source)	3-12
6	Efficiency of Commercial Glass and Fine Particulate Screens 160 kV, 4 mA x-ray source)	3-12
7	Efficiency of Commercial Glass Screens (160 kV, 4 mA x-ray source)	3-13
8	Screen Brightness Versus Dose Rate for Fine Particulate Screens, Commercial Glass, and Commercial Fiber-Optic Plates	3-14
9	Screen Efficiency of GOS Film	3-16
10	GOS Screen Brightness Versus Dose Rate	3-16
11	Block Diagram of MTF Measurement	3-18
12	Modulation Transfer Function for Several Screens	3-19
13	System Modulation Transfer Function Measurement	3-21
14	Modulation Transfer Function of Real-Time Radiographic System	3-22
15	Modulation Transfer Function of Particulate Screens	3-22
16	Modulation Transfer Function of High-Speed Particulate Screen	3-23
17	Modulation Transfer Function of 1/4-in. Commercial Glass Plate	3-24
18	Modulation Transfer Function of 1/2-in. Commercial Fiber-Optic Plate	3-25
19	Modulation Transfer Function for Gadolinium Oxysulfide Film	3-25
20	Funk Grid Resolution	3-27
21	Contrast Sensitivity Measurement	3-29
22	Contrast Sensitivity Versus Shim/Absorber Ratio for Regular Particulate Screen	3-35

LIST OF ILLUSTRATIONS (Continues)

Figure		Page
23	Contrast Sensitivity Versus Shim/Absorber Ratio for Fine Particulate Detail Screen	3-37
24	Spectral Emission of (A) Lockheed Fluorescent Proprietary Glass, (B) Commercial Fluorescent Glass, and (C) Commercial Proprietary Screen	3-39
25	Varo 25-mm Image Intensifier Transfer Characteristics	3-42
26	Limiting Resolution Versus Scene Brightness	3-43
27	Screen Resolution Comparison Examples	3-45
28	Contrast Sensitivity Measurement Technique	3-46
29	Screen Efficiency Versus Tube Voltage	3-48
30	Screen Light-Output Measurements	3-49
31	Figures of Merit for Converter Screen Materials	3-51
32	Side View of Lens Manipulator System	4-6
33	Requirements to Focus Lens for Each Field Size	4-6
34	Limiting Resolution Characteristics of Low-Light-Level Cameras	4-8
35	Isocon Image Tube Performance	4-9
36	Top View of Manipulator	4-13
37	Side View of Manipulator	4-13
38	Digital Motor Indexers and Limit Switch Electrical Wire Interconnect Configuration	4-14
39	Functional Block Diagram of the Computer System	4-16
40	Front View of Computer and Image Processor	4-17
41	Trappix System Block Diagram	4-18
42	Honeywell Video Graphic Recorder	4-24
43	Overall RTR System	4-26
44	Back View of Fluorescent Screen Bulkhead	4-27
45	Side View of Festooning System	4-27
46	Computer, Camera, and Operator Console Electrical Wire and Cable Interconnect Configuration	4-29
47	Front View of Operator's Console Work Area	4-30
48	Front View of Indexers and Joysticks for X, Y, Z, and F	4-30

LIST OF ILLUSTRATIONS (Concluded)

Figure		Page
49	Film Density Versus Aluminum Thickness for 100 kV, Type M Film	4-34
50	Digital Level Versus Aluminum Thickness for 100 kV, 2-mA, RTR System	4-34
51	Penetrameter Sensitivity of Film and RTR for 20 kV, Plastic	4-53
52	Penetrameter Sensitivity of Film and RTR for 60 kV, Aluminum	4-53
53	Penetrameter Sensitivity of Film and RTR for 100 kV, Aluminum	4-54
54	Penetrameter Sensitivity of Film and RTR for 140 kV, Aluminum	4-54
55	Penetrameter Sensitivity of Film and RTR for 180 kV, Steel	4-55
56	Penetrameter Sensitivity of Film and RTR for 220 kV, Steel	4-55
57	Penetrameter Sensitivity of Film and RTR for 260 kV, Steel	4-56
58	Penetrameter Sensitivity of Film and RTR for 300 kV, Steel	4-56
59	Camera Positioner Configuration	5-5
60	The Camera, Optics, and X Ray: Concept 1	5-9
61	The Camera, Optics, and X Ray: Concept 2	5-10
62	The Camera, Optics, and X Ray: Concept 3	5-12
63	The Camera, Optics, and X Ray: Concept 4	5-13
64	The Camera, Optics, and X Ray: Concept 5	5-14
65	Operator's Console: Air Force RTR System	5-15

LIST OF TABLES

Table		Page
1	High-Speed Particulate Screen Contrast Sensitivity and Signal-to-Noise Ratio	3-30
2	Commercial Glass Fiber-Optic Screen Contrast Sensitivity and Signal-to-Noise Ratio	3-31
3	One Percent Contrast Sensitivity of $Gd_{202}S:Tb$ Film, 1 Percent Shim	3-33
4	Contrast Sensitivity of Fine Particulate Detail Screen, 1 Percent Shim	3-33
5	Contrast Sensitivity of Commercial Fiber-Optic Screen, 1 Percent Shim	3-34
6	Contrast Sensitivity of Commercial Glass Plane, 1/4 in. Thick, 1 Percent Shim	3-34
7	1/1 Variation, Regular Particulate Screen	3-35
8	1/1 Variation, Fine Particulate Detail Screen	3-36
9	Low-Energy Contrast Sensitivity Measurements	3-50
10	Figure of Merit Conclusion	3-52
11	Breadboard High-Resolution RTR System Performance Goals	4-2
12	X-Ray System Specifications	4-3
13	Lens Specification, Lens 60-mm f/0.7	4-5
14	Penn Video Isocon Camera Functions	4-10
15	Resolutions for 800 and 1024 TV Lines for Various Fields of View	4-11
16	Film Data	4-33
17	RTR Penetrameter Data	4-36
18	RTR Penetrameter Data	4-37
19	RTR Penetrameter Data	4-38
20	RTR Penetrameter Data	4-39
21	RTR Penetrameter Data	4-40

LIST OF TABLES (Concluded)

Table		Page
22	RTR Penetrameter Data	4-41
23	RTR Penetrameter Data	4-42
24	RTR Penetrameter Data	4-43
25	Film Penetrameter Data	4-45
26	Film Penetrameter Data	4-46
27	Film Penetrameter Data	4-47
28	Film Penetrameter Data	4-48
29	Film Penetrameter Data	4-49
30	Film Penetrameter Data	4-50
31	Film Penetrameter Data	4-51
32	Film Penetrameter Data	4-52
33	X-Ray Converter Screens for Various Applications	5-3

Section 1 INTRODUCTION

The objective of this program was the functional design of an all-electronic, high-resolution prototype real-time radiography (RTR) system for inspecting aerospace components, with the performance parameters and image size of film-based radiography. A major part of this program dealt with the selection, evaluation, and optimization of commercially available x-ray-to-light/electron converter devices. Several commercially available converter devices and associated advanced-technology devices with sensitivity in the x-ray region of the electromagnetic spectrum were evaluated. The evaluation concentrated on obtaining devices that showed the greatest promise of attaining a resolution, dynamic range, and contrast sensitivity equivalent to industrial x-ray film (resolution ≥ 10 lp/mm, dynamic range $> 10^3$, contrast sensitivity 1 percent), and also showed the most promise of being able to provide an image size equivalent to that of current radiographic film (at least 10 in. by 12 in.). A breadboard RTR system was constructed and its performance tested and optimized. Conceptual RTR systems were designed, using the results of the testing and optimization of the breadboard system. The system designs may be the basis for a multisource, follow-on manufacturing technology program which will construct a production prototype real-time radiography system with the performance characteristics listed above. This system will be applicable to the inspection of aerospace components at x-ray energy levels less than 300 kVp at manufacturing, remanufacturing, and depot-maintenance facilities.

This program consisted of three tasks.

In Task I, we tested and evaluated commercially available x-ray converter devices, representing the most advanced state of the art in this technology, in order to determine their performance characteristics as compared to x-ray film. Each converter device was conceptually different, not minor variations

of the same device. The devices were modified as necessary, and were tested and evaluated over an energy range from 20 to 300 kVp. From the results of this evaluation, we selected converter devices having high "figures of merit".

In Task II, a "breadboard" RTR system was constructed, utilizing the converter devices chosen in Task I with the required associated x-ray source, electronics, and data-processing capability. This system was tested, evaluated, and optimized so that its performance on radiographic standards was equal to or better than that of a film-based radiographic system. A demonstration of the capability of the breadboard system will be held at LMSC to show the results of this performance as well as the image quality achieved in the inspection of actual aerospace hardware specimens.

In Task III, design concepts were developed for complete RTR systems incorporating the x-ray converter device selected in Task I. The design included all necessary image processing instrumentation, image-display electronics, recorders, data-processors, and image-storage equipment required for inspecting aerospace components in a manufacturing, remanufacturing, and depot-maintenance environment.

Section 2

TECHNICAL REQUIREMENTS/TASKS

2.1 TASK I - TESTING AND EVALUATION OF THE X-RAY CONVERTER DEVICES

The criteria for testing and evaluation of the x-ray converter devices were: resolution ≥ 10 lp/mm, dynamic range of 10^3 without x-ray energy adjustment, and contrast sensitivity of 1 percent over an x-ray energy range from 20 to 300 kVp. The devices chosen are capable of being used or are practically capable of being developed for use and are at least a 10-in. x 12-in. format.

An evaluation procedure was established and utilized, including the required instrumentation for measuring the performance of each particular device. The procedure is such that the devices can be rated against one another on an equivalent basis with industrial x-ray film over an energy range from 20 to 300 kVp using selected kilovoltage increments of 25-30 kVp.

As part of the test and evaluation, devices were fabricated or modified as necessary to either improve performance characteristics of the x-ray converter devices or facilitate the device evaluation. Simple fixturing or scanning mechanisms required for evaluating the performance of the individual devices were constructed.

During the establishment and utilization of the evaluation procedure, the external factors that adversely affect the performance of the x-ray converter devices being evaluated were defined and approaches for minimizing the effects of these factors were developed and applied.

A figure of merit was developed for each device tested. The figures of merit represent the total performance capability of the devices, together with other factors such as the complexity of the device, ease and cost of fabrication,

and potential for improvement. The converters with the highest figure of merit were selected for further test, evaluation, and optimization in Task II.

2.2 TASK II - BREADBOARD RTR SYSTEM CONSTRUCTION/DEMONSTRATION

A breadboard RTR system was constructed, consisting of the x-ray converter devices selected together with the basic electronic instrumentation and data processing capability required to demonstrate the capability of the converter devices for use in a real-time radiographic system. This breadboard system was used to test, evaluate, and optimize the real-time radiographic technique by using a series of penetrameters in conjunction with different thicknesses of step wedges consisting of plastic, aluminum, and steel. The minimum penetrameter sensitivity was established using penetrameters constructed to conform to the American Society of Testing Materials (ASTM) Specification E-142-77 and a series of step wedges that covered a range of thicknesses appropriate for the x-ray energies being investigated. The minimum penetrameter sensitivity was also established for Class I type x-ray film using the same step-wedge materials, material thicknesses, penetrameter type, and x-ray energy. The evaluation and optimization was accomplished in 40-kVp increments from 20 to 300 kVp. The ability of the device to achieve the same penetrameter image quality as obtained with x-ray film for the same type and thickness of material for all x-ray energies was evaluated. An approach for evaluating and optimizing the system for determining image quality at the lower x-ray energies was devised.

The capability of the RTR-system breadboard will be demonstrated before a group of NDE engineers, chosen by the AFWAL/MLLP program manager, representing both government and industry. The demonstration will review the results obtained during the testing, evaluation, and optimization of the real-time radiography system. The capability of the RTR system breadboard will be demonstrated by displaying the results of inspecting a maximum of five specimens with geometries and dimensions representative of airframe and engine hardware.

2.3 TASK III - RTR PROTOTYPE SYSTEM DESIGN

A high-resolution prototype RTR system incorporating the converter device selected in Task I and the accompanying instrumentation identified in Task II was designed. Instrumentation included the x-ray source, camera equipment, image-processing instrumentation, monitors, tape-recording equipment, and an image-storage system that is suitable for viewing and storage of high-resolution images, and has the required data processing capability. The system designed can be used in a manufacturing and remanufacturing facility and can function in a depot maintenance environment.

Section 3

TASK I - X-RAY CONVERTER DEVICE EVALUATION

X-ray converter devices selected on the basis of the guidelines given in Section 2.1 were purchased or fabricated. Evaluation criteria, evaluation procedures, and test apparatus were established, and performance of the x-ray converters was tested and the results analyzed. Factors that could affect performance were identified. The results were compared and a figure of merit established. X-ray converter selection guidelines were established for RTR applications requiring high resolution.

3.1 X-RAY CONVERTER DEVICES

The x-ray converter devices that were selected for evaluation were all intended to be used in x-ray imaging systems. All produce light or electrons that are converted to light. All were expected to exceed 10 line pairs per millimeter (lp/mm) resolution and have a dynamic range of 1000 and better than 1 percent contrast sensitivity. The devices included commercially available particulate screens, a fluorescent glass plate, and a fluorescent fiber-optic glass plate. In addition, an LMSC-proprietary fluorescent glass and rare-earth films were tested.

3.1.1 Particulate Screen X-Ray Converters

Regular, medium, and fine, and high-speed particulate screens were selected as being representative of this class of screen. Examples were purchased from local x-ray suppliers.

3.1.2 Commercial Fluorescent Glass

The commercial fluorescent glass, one of the brightest high-resolution glasses commercially available, was purchased as samples 0.25 in. thick. Before testing, a mirror coating had to be added to the x-ray side of the plate.

3.1.3 Commercial Fiber-Optic Fluorescent Glass

This fiber-optic x-ray converter is made of the same fluorescent commercial glass as the homogeneous glass plate. The fiber-optics absorb the x-rays and emit light which is collimated and conducted to the output by the fibers. An added mirror coating reflects the light to the output side of the plate.

3.1.4 Gadolinium Oxysulfide Films

Seven films of $\text{Gd}_2\text{O}_2\text{S:Tb}$ were deposited on single-crystal sapphire substrates utilizing radiofrequency sputtering. Intended thicknesses were $5\text{ }\mu\text{m}$ (0.2 mil) for the first film and $25\text{ }\mu\text{m}$ (1 mil) for the other six films.

The sputtering configuration used first was "sputter-down," with the target mounted above the substrate. The target was made by hot pressing $\text{Gd}_2\text{O}_2\text{S:Tb}$ powder at only moderately elevated temperature and pressure to avoid contamination by reaction with the die, and thus was not a dense ceramic disk. Most of the films produced showed evidence of a fine powder deposit which degraded their quality, the powder particles acting as masks to produce numerous pinholes in the films. The effect appeared to worsen with successive films. The source of the powder was particles that eroded from the target and fell onto the substrate.

To correct the problem, the sputtering system was modified to a "sputter-up" configuration. Although films of 1-mil thickness were deposited with the modified system, the films spalled from the sapphire substrate during the subsequent sulfurization treatment, probably the result of an increase of stress with increased film thickness. Unless the spalling problem can be overcome, it appears that, despite the inherently high resolution of these films, they may not be a viable candidate as an image conversion device for this project.

Although the quality of the first thick (1-mil) $\text{Gd}_2\text{O}_2\text{S:Tb}$ film fabricated under this program was considered less than satisfactory - having a

yellowish-brown tone and some visible imperfections - it had at least the merit of being a continuous, transparent film. It was therefore felt that an attempt to measure the resolution of the film might be worthwhile.

To insure optimum luminescent brightness, the film was treated in a sulfurizing atmosphere at 1050°C for 1 h, in accordance with the LMSC-patented process previously used for 1- to 2- μ m-thick films. The brightness was measured after 1 h of treatment and again after 3 h. At 150 kV, 5 mA, the brightness after the total 3-h treatment was 1.51×10^{-2} ft-L, an increase of 41 percent over that for the initial 1-h treatment (1.07×10^{-2} ft-L). This result indicated that the optimum treatment time for thick films is indeed greater than for 2- μ m films, but because only a moderate increase was obtained with the additional treatment, the optimum time for 25- μ m film is probably between 2 and 3 h.

The gadolinium oxysulfide film fabrication was performed under the LMSC Independent Research Program. Evaluation of the films was performed under this contract.

3.1.5 LMSC-Proprietary Fluorescent Glass

A new fluorescent glass was developed and fabricated under the LMSC Independent Research Program. The sample screens were evaluated under this contract.

3.2 X-RAY CONVERTER EVALUATION CRITERIA

The image converter device is the most critical element of a real-time radiographic system because it determines the signal available for acquisition and processing by the system. The image quality of a converter is best represented by the following four parameters:

- Quantum efficiency
- Dynamic range

- Modulation transfer function (spatial resolution)
- Contrast sensitivity

Although these parameters are interrelated, each has meaningful significance to the radiographer; therefore, each of the four parameters must be measured under standardized conditions in order to make a quantitative comparison of different converter devices. A figure of merit, which combines the results of evaluation each of these parameters, must also be developed. The measurement procedures used for each of these parameters and the development of a figure of merit are described in detail in the following subsections.

3.2.1 Quantum Efficiency

Visible light emission is only one of several possible methods of energy dissipation of an incident x-ray beam. Moreover, it is necessary to distinguish between the intrinsic quantum efficiency of the converter material and the effective quantum efficiency of a converter device. Because intrinsic quantum efficiency, which is the fraction of absorbed incident x-ray photons converted to visible light photons, is an intrinsic property of the material, it is independent of thickness.

On the other hand, in a real converter device, the effective quantum efficiency depends upon the linear energy absorption coefficient of the converter material, the thickness of the material, the intrinsic quantum efficiency of the material, and the collection efficiency of the measuring system. For this program, the parameter measured was the effective quantum efficiency (EQE) of the converter device expressed in foot-lamberts of emitted light per rad of incident x-ray energy (ft-L/rad).

The x-ray source was a Seifert Isovolt US-3 with a digitally controlled power supply for regulating the high voltage from 10 to 420 kVp in 1-kVp steps and the cathode current from 1 to 10 mA in 1-mA steps.

A precision dosimeter (Radocon III Model 550 by Victoreen, Inc.) was used to monitor the precise dosage received by the converter device.

The light output from the luminescent surface of the converter device was monitored by a precision light meter (Pritchard Model 1980A-PL photometer from Photo Research Division Killmorgen Corp.). The measurements were taken for several screen thicknesses over the range 30 to 300 kV in 25-kV steps.

3.2.2 Dynamic Range

Dynamic range was measured as effective quantum efficiency, but with the source-to-converter distance varied to measure the dynamic range of the flux to 3 orders of magnitude. The system dynamic range was measured by examining objects over an exposure range equivalent to 1000-to-1 density range on Kodak Type M industrial film.

3.2.3 MODULATION TRANSFER FUNCTION

Although industrial radiographers have used various penetrameters and even Funk grids borrowed from the medical x-ray field to estimate resolution capabilities of image converters, the measurements are highly subjective and do not provide the quantitative results desirable. In the medical x-ray field, modulation transfer function (MTF) measurements have been made for film-screen combinations using narrow slits and scanning the described film with microdensitometers. This method is not applicable to real-time radiography, which does not utilize film. In addition, it is desirable to determine MTFs for the overall system, as well as for the converter device.

The LMSC High-Energy, Real-Time Radiographic Inspection System (HERTIS)* shown schematically in Fig. 1, includes a very sensitive, low-light-level isocon

*B. E. Kinchen, X-Ray Inspection System, LMSC-D811899 (1982) p. 6-215; and B. E. Kinchen, R. C. Barry, X-Ray Inspection System, LMSC-D877109 (1983)

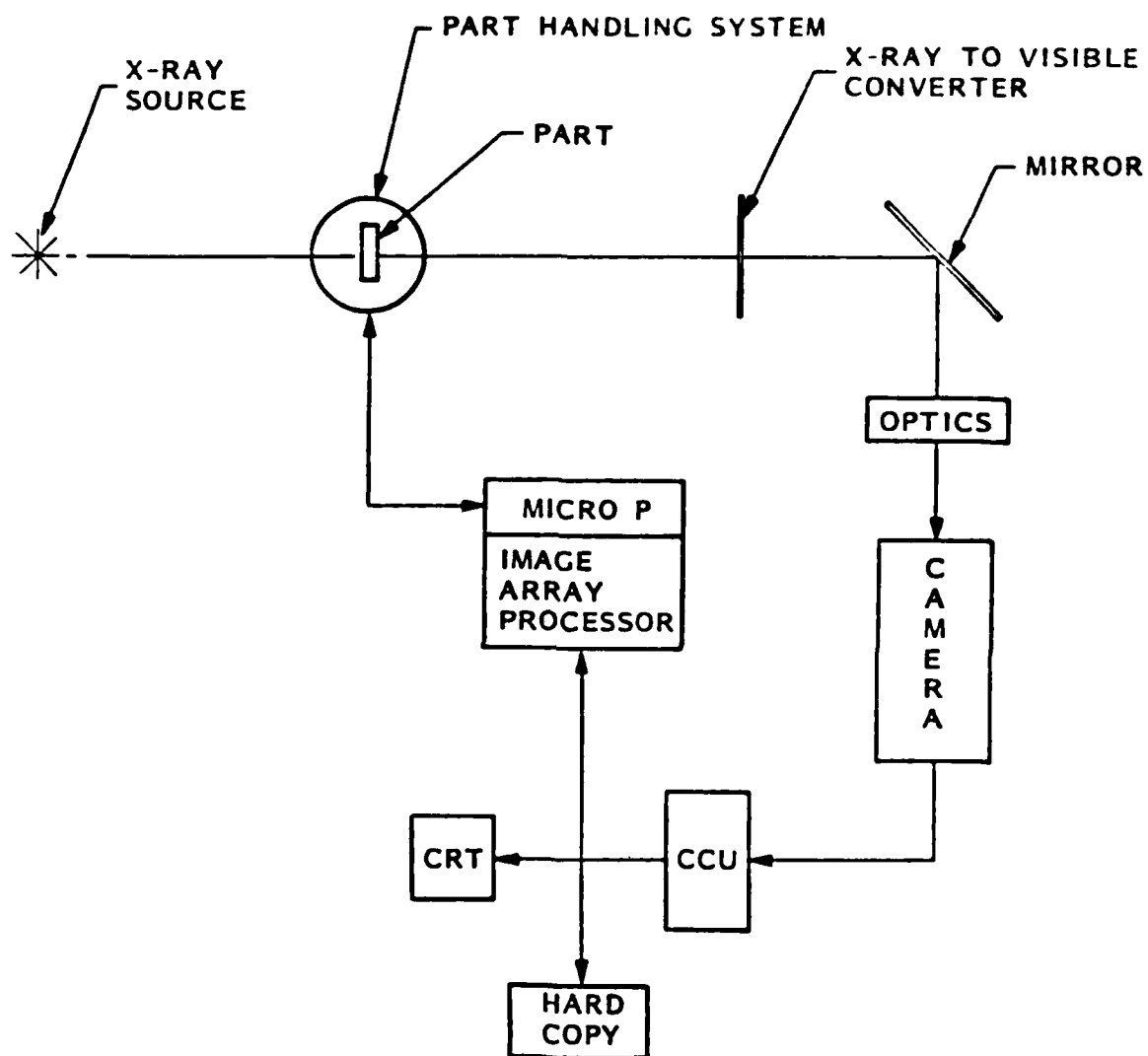


Fig. 1 Instrumentation to Test and Evaluate X-Ray Converter Devices

camera, a fast video digitizer, and a complete digital image-processing system, and provides a considerable capability for accurate MTF measurements. A portion of the converter device can be masked with a metal sheet having a sharp edge, and a digitized intensity profile can be recorded along a line passing from the unmasked to the masked region. The image processor can then be used to transform the square wave function of the profile with the modulation transfer functions. This overall MTF is called the converter-plus-camera MTF for short.

The MTF of the camera can be determined separately by viewing a uniformly illuminated area through a transparency having a portion of the field of view blacked out. The converter MTF can then be determined by dividing the converter-plus-camera MTF by the camera MTF.

3.2.4 Contrast Sensitivity

The digital image processors of the LMSC HERTIS system can be used to measure the contrast sensitivity with the following procedures:

1. Acquire a digital image from the converter device under specified radiographic conditions and store the digital image in an image memory
2. Acquire a second digital image under identical conditions, with about 1/4 of the image converter device covered by a shim of the material under test and between 1 to 5 percent as thick as the sample material under test
3. Subtract the two images to eliminate shadings and irregularities in the imaging system
4. Select an area covered by the shim and perform a histogram analysis, recording the mean m_1 and standard deviation σ_1
5. Select an area not covered by the shim and perform a histogram analysis recording the mean m_0 and standard deviation σ_0
6. The signal produced by the shim is $m_1 - m_0$ and the averaged noise in the image is $(\sigma_0^2 + \sigma_1^2)^{1/2}$. The contrast sensitivity C can then be derived:

$$C = \frac{\Delta l}{l} \frac{(\sigma_0^2 + \sigma_1^2)^{1/2}}{l(m_1 - m_0)} = \frac{\Delta l}{l} \cdot \frac{1}{(S/N)_{\Delta l}}$$

in which l is the sample thickness and Δl is the thickness of the shim, and $(S/N)_{\Delta l}$ is the signal-to-noise ratio caused by the shim.

The advantage in using this procedure is that it is independent of the amplifier gain in the detector electronic circuitry. The shading and local variations in the detector circuitry are also compensated very effectively by the image subtraction.

3.2.5 Figure of Merit Criteria

An important objective of this contract was to define a figure of merit (FM) for characterizing x-ray image-conversion screens. The FM was defined as the product of the modulation transfer function and the effective quantum efficiency:

$$FM = MTF \times EQE$$

This definition has the advantage of combining the resolution properties with the efficiency. The FM is not, however, a single-valued quantity, because the MTF is a function of the spatial frequency (lp/mm) and also the EQE is a function of the x-ray voltage. The FM is therefore best expressed as a set of curves, as for example, FM versus spatial frequency and FM versus x-ray voltage. By referring to such curves for the various screens that may be useful, the radiographer can quickly determine the screen best suited for a particular application. If the object to be examined is relatively thick or dense, then clearly higher kV must be used; in this case, curves for FM versus spatial frequency at a typical higher kV will show which screen will provide the best resolution. For an object of low density, a low kV would be used. Here, again, curves for FM versus spatial frequency at the lower kV will permit comparing resolution capabilities of screens.

3.3 X-RAY CONVERTER PERFORMANCE

The results of evaluating the candidate x-ray converter devices listed in Section 3.1 for the criteria listed in Section 3.2 are reported here.

3.3.1 Effective Quantum Efficiency (EQE) Measurements

The x-ray-to-light conversion efficiency of the converter device is one of several key factors affecting image qualities in a real-time radiographic system. A measure of the converter's efficiency is provided by the effective quantum efficiency (EQE), defined as the ratio of the screen brightness to the input x-ray dose rate. The EQE depends on the total x-ray linear attenuation coefficient, the thickness, and the intrinsic quantum efficiency of the converter material.

We report here measurements of the effective quantum efficiency of several high resolution screens: Regular, medium, and fine particulate screens, two commercial fiber-optic faceplates (1/4 in. and 1/2 in. thick), two commercial fluorescent glass plates (1/8 in. and 1/4 in. thick), and a gadolinium oxysulfide:terbium screen (0.20 mils thick). The measurements were performed with x-ray tube voltages from 30 to 400 kV and with x-ray dose rates up to 12 R/s. Two x-ray sources were used: a Seifert 160/4 x-ray tube with available accelerating voltages from 30 to 160 kV and a Seifert 420/10 with voltages from 70 to 400 kV. Dose rates were controlled by varying the tube current and the distance between the x-ray source and the screen; a Victoreen 500 dosimeter was used to monitor the dose rate. Screen brightness was monitored with a Pritchard 1980A photometer. A schematic diagram of the experiments setup is shown in Fig. 2.

3.3.1.1 Particulate Screens. The effective quantum efficiencies of regular, medium, and fine particulate screens, measured as a function of x-ray tube voltages between 70 and 400 kV, are shown in Fig. 3. The medium particulate screen has only recently been made available. The EQEs of all three screens show a similar voltage dependence - first increasing rapidly at low voltages,

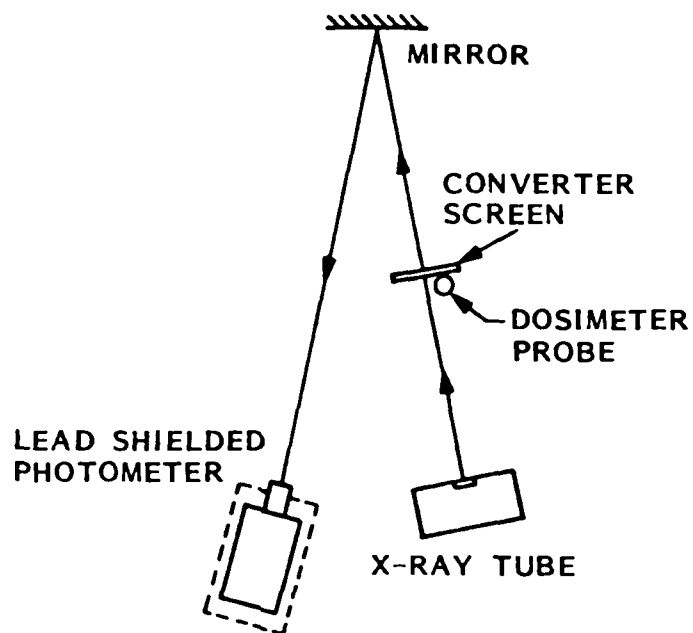


Fig. 2 Experimental Setup for Measuring Effective Quantum Efficiency

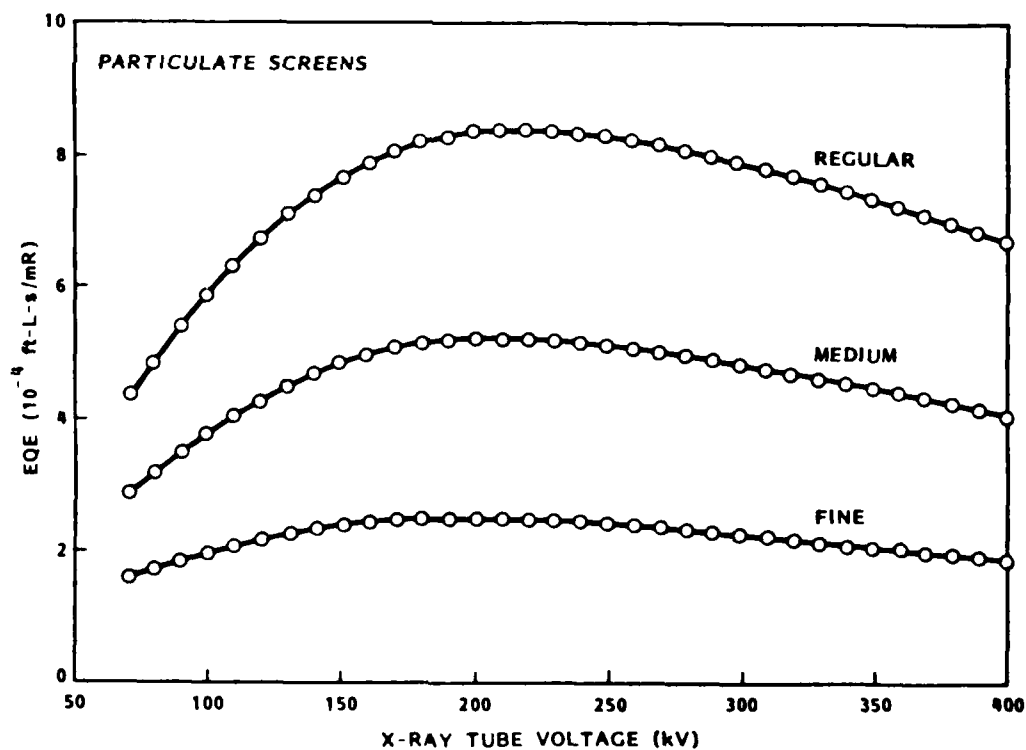


Fig. 3 Efficiency of Particulate Screens

then peaking near 200 kV, followed by a gradual decrease at higher voltages. As might be expected, the EQE of the medium screen is intermediate between that of the regular and fine screens. The overall efficiency of the regular particulate screen is about two and four times greater than that of the medium and fine screens, respectively.

3.3.1.2 Commercial Glass and Fiber-Optic Screens. The effective quantum efficiencies of the commercial glass and fiber-optic screens are shown in Figs. 4 through 7. For comparison, that of the fine particulate screen is also shown in Figs. 5 and 6. The EQEs of commercial fiber-optic and glass plates, which are approximately equal at the same thickness, are generally below that of the Fine Particulate. However, with an aluminized mylar as a reflective backing, which in effect doubles the light output, the commercial glass screens become more efficient than the fine particulate.

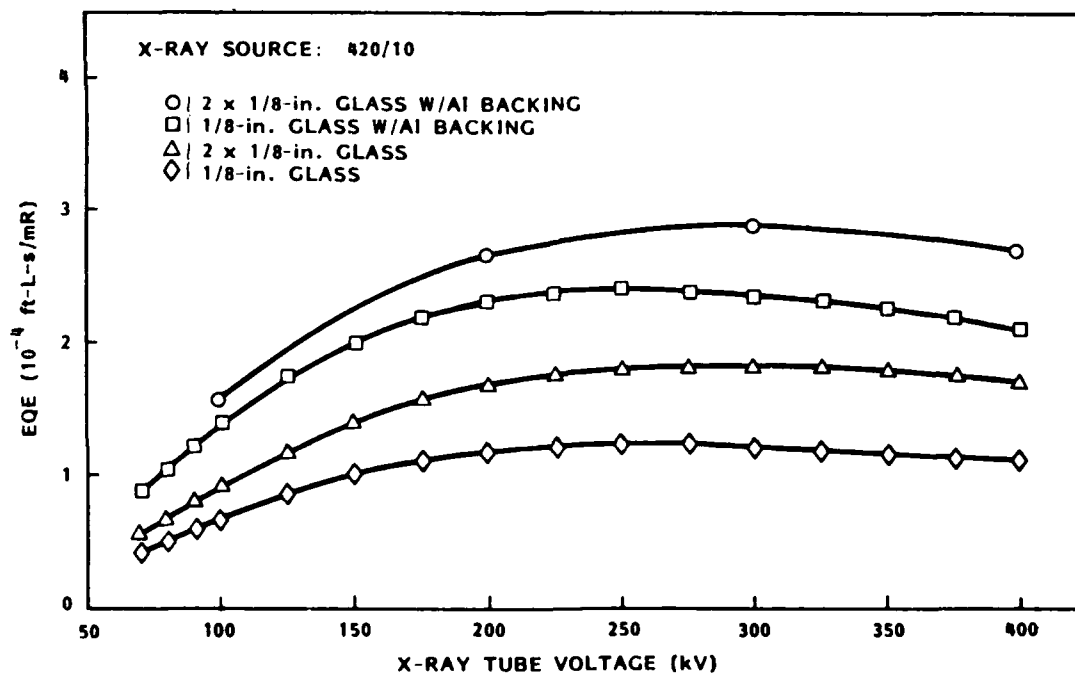


Fig. 4 Efficiency of Commercial Glass Screens (420 kV, 10 mA x-ray source)

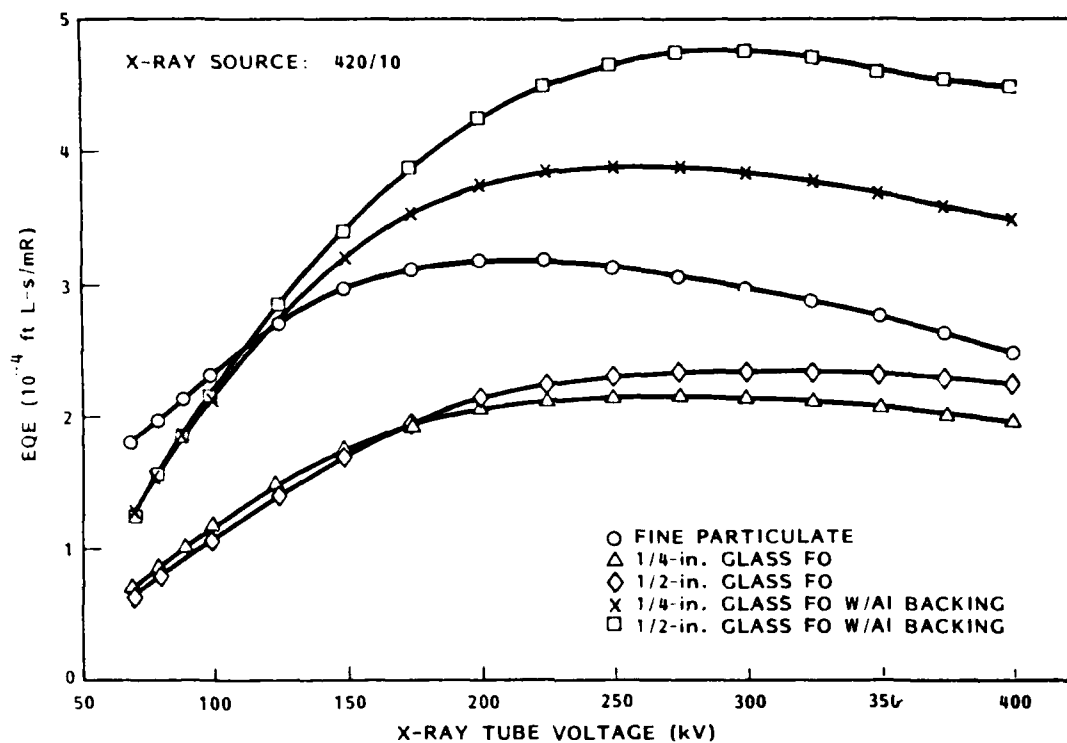


Fig. 5 Efficiency of Commercial Glass and Fine Particulate Screens (420 kV, 10 mA x-ray source)

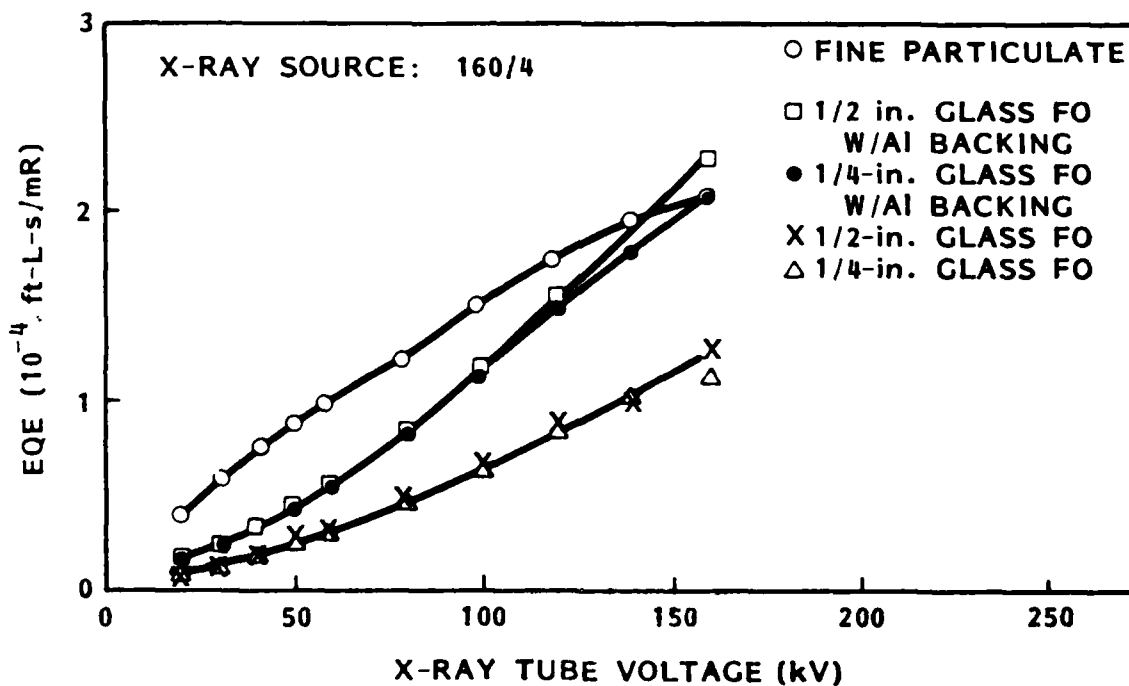


Fig. 6 Efficiency of Commercial Glass and Fine Particulate Screens (160 kV, 4 mA x-ray source)

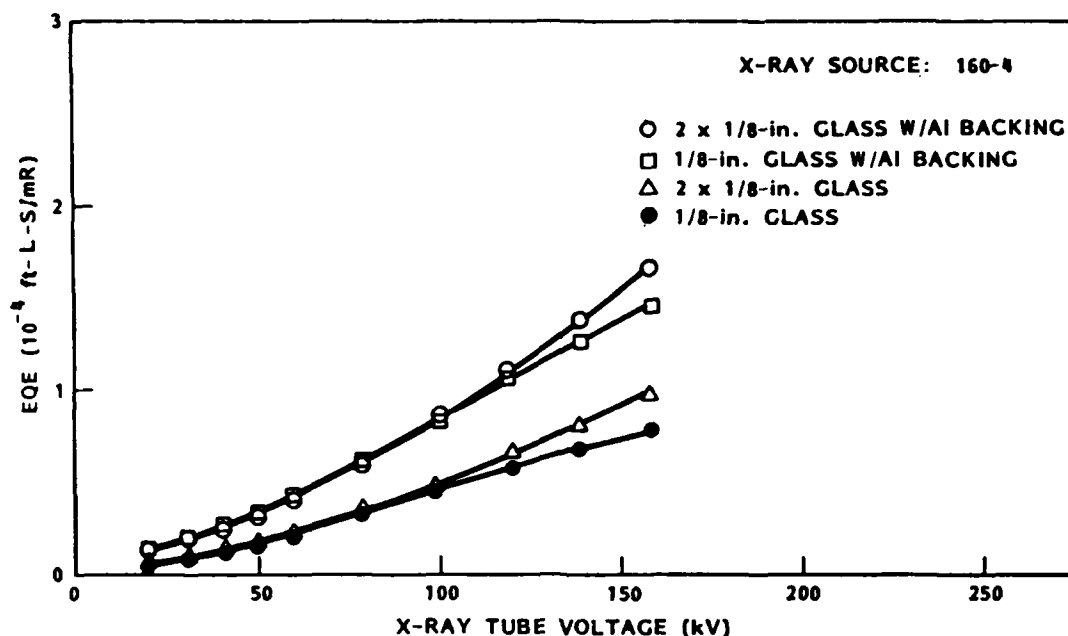


Fig. 7 Efficiency of Commercial Glass Screens (160 kV, 4 mA x-ray source)

The values of the EQE obtained using the Seifert 420/10 x-ray tube are approximately twice those obtained using the smaller Seifert 160/4. The difference is largely due to the different operating characteristics of the tubes. The magnitude and behavior of the EQE below 200 kV strongly suggest that the x-ray energy distribution of the 160/4 source is shifted more toward the lower energy end relative to the 420/10.

Screen brightness was measured at high x-ray dose rate (1-10 R/s) at 100, 200, 300, and 400 kV. Some representative brightness curves obtained with a tube voltage at 200 kV are shown in Fig. 8 for three different screens. All three screens exhibited a linear dependence of the screen brightness on dose rate up to 10 R/s. Fluctuation in the output brightness was observed to be no more than 0.001 ft-L, thus giving a dynamic range of 1000:1 or greater for all three screens.

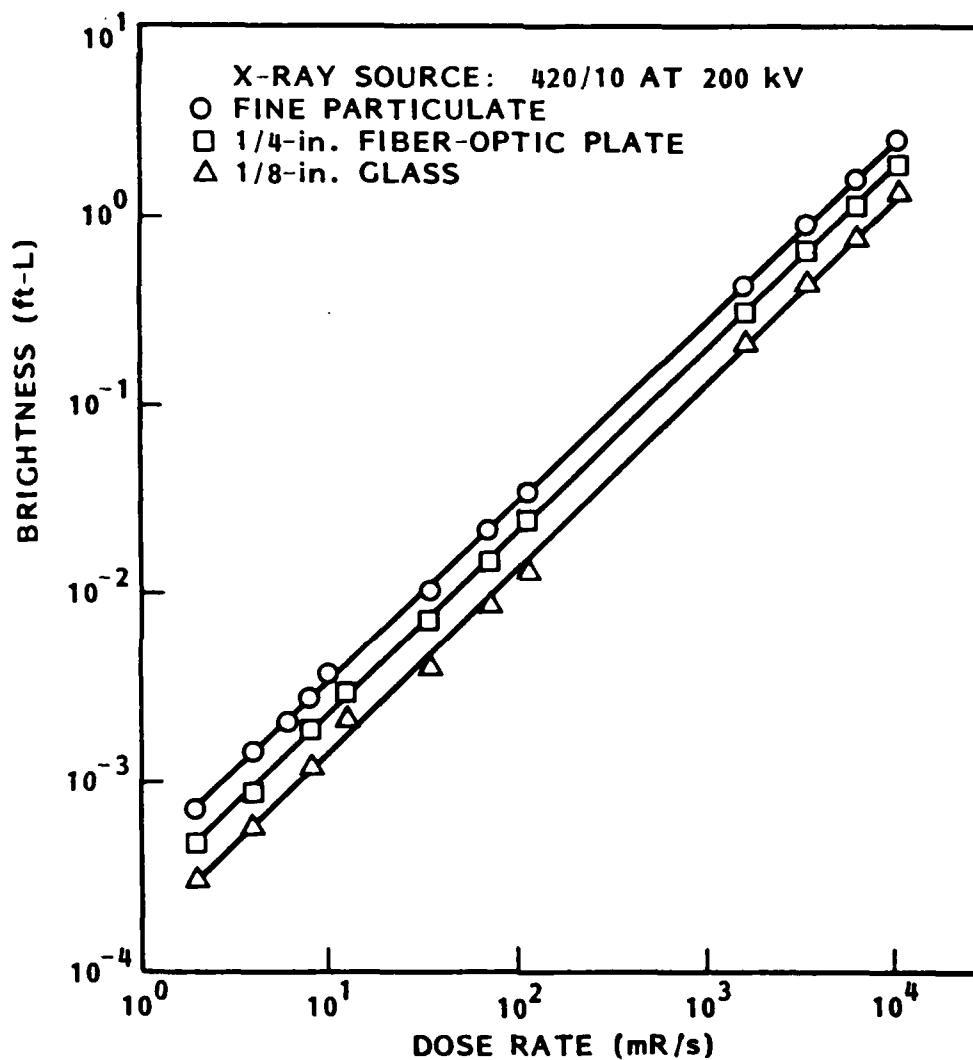


Fig. 8 Screen Brightness Versus Dose Rate for Fine Particulate Screens, Commercial Glass, and Commercial Fiber-Optic Plates

Slight browning of the commercial fiber-optic and glass plate screens was evident after prolonged exposure to x radiation at high dose rates. This, however, does not affect the light output from the glass in the useable range. The glass can be returned to a clear state by annealing at 300°C for 1 h if desired.

3.3.1.3 Gadolinium Oxysulfide Film. The effective quantum efficiency of a gadolinium oxysulfide:terbium (GOS) screen is shown in Fig. 9. The film was sputter-deposited in the "sputter down" configuration. The quality of the film was excellent; only slight traces of particle deposits and surface imperfections were observed. Film thickness was approximately 0.20 mil. Because of its small thickness, the GOS film showed a considerably smaller screen efficiency than the other high-resolution screens tested earlier. The output response of the screen was observed to be linear, as shown in Fig. 10; there was no indication of brightness saturation with dose rates up to 16 R/s.

3.3.2 Dynamic Range of X-Ray Converters

The dynamic range of particulate screens and commercial glass x-ray converters was shown to be over 1000 on Fig. 8 as described in section 3.3.1.2.

3.3.3 Modulation Transfer Function (MTF) Measurements

The two methods used to measure MTF were the Funk grid and square wave response. Although both methods are reported here, nonlinearities in the square wave response will require more extensive linearizing and calibration to guarantee correct results. The video response linearization is being addressed by LMSC.

3.3.3.1 Original Method. Some preliminary modulation transfer function (MTF) measurements for several x-ray conversion screens were obtained from square-wave response (SWR) measurements made by passing x-rays through a variable-frequency lead bar pattern (Funk grid) placed in front of the screens. The screen image was focused onto an isocon camera and the camera

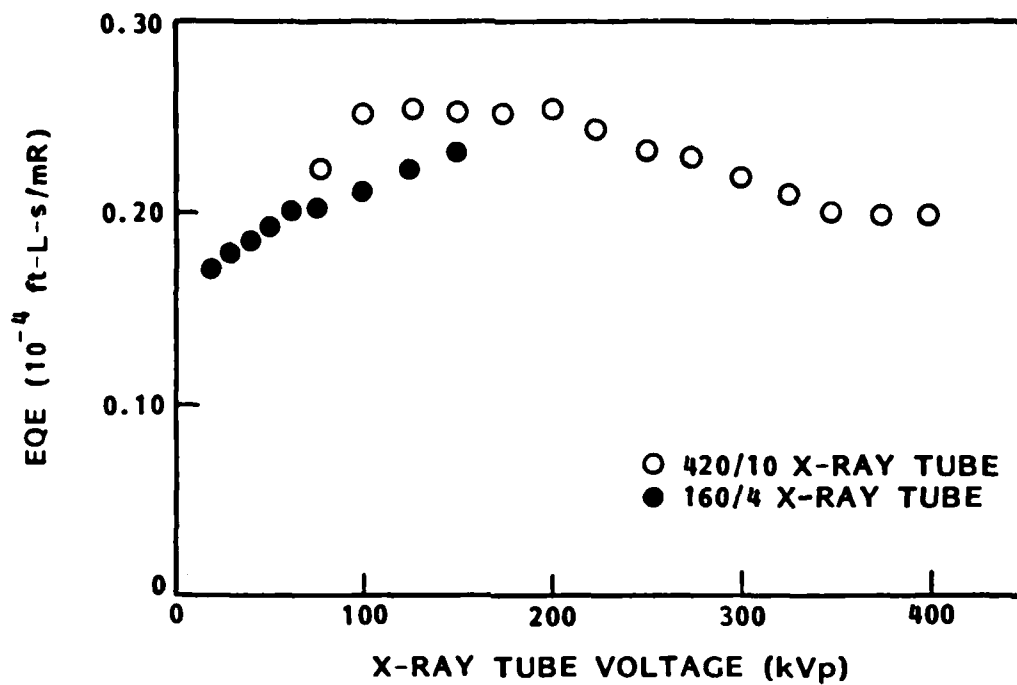


Fig. 9 Screen Efficiency of GOS Film

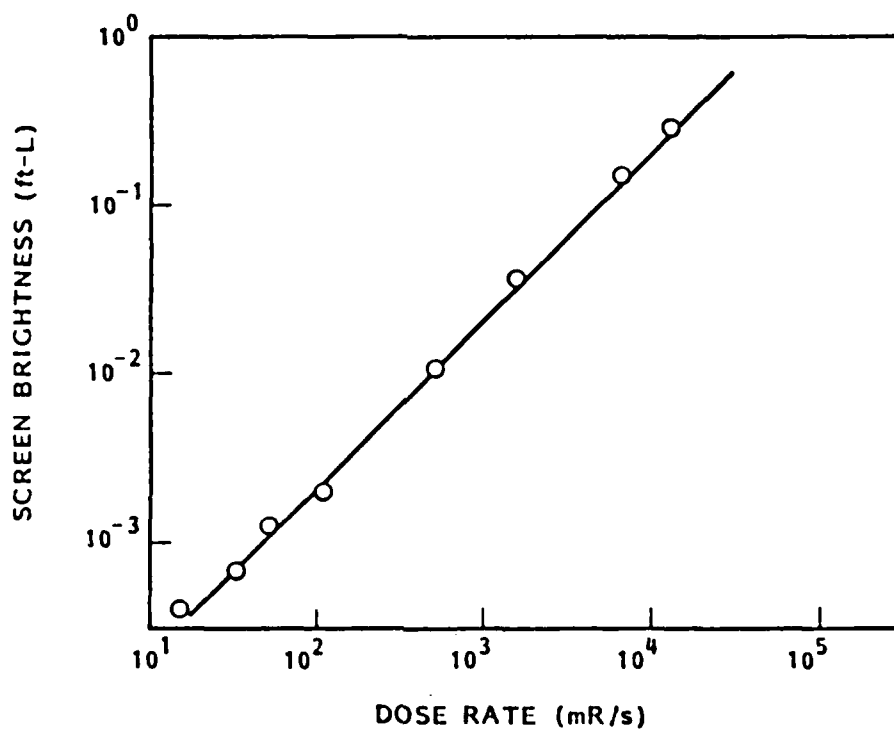


Fig. 10 GOS Screen Brightness Versus Dose Rate

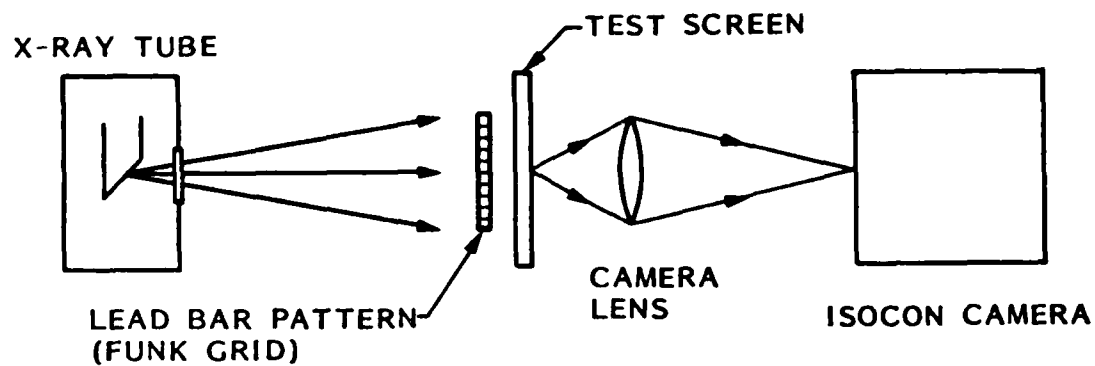
video signal observed on a waveform monitor, as shown schematically in Fig. 11. The SWR at each pattern frequency was taken to be the video signal modulation normalized to the modulation of the lowest frequency. A computer program was then used to fit the SWR data for the screen and camera system with a polynomial function. The screen camera system MTF was then obtained by performing a fast Fourier transform (FFT) on the derivative of the polynomial. The MTFs obtained from these preliminary measurements are shown in Fig. 12.

The MTF of the camera system was similarly determined from an SWR for the Funk grid illuminated with an electroluminescent panel. The screen MTFs were finally obtained by factoring out the MTF of the camera system. The results were not fully satisfactory. No data above 10 lp/mm were available, since the maximum frequency of the Funk grid was 10 lp/mm. Also, at the higher frequencies, the uncertainty became large as a result of decrease in signal-to-noise ratio with increasing frequency; this made it difficult to satisfactorily fit the data with the polynomial function. To obviate these problems, modifications were made in the method of measurement and processing of the data.

3.3.3.2 Improved Method. The Funk grid was replaced with an 0.005-in.-thick tungsten shim covering one-half the field of view.

A reversed 16-mm lens was substituted for the Canon f/0.7 lens normally used with the isocon tube, providing a 10X magnification and hence a better definition of the edge trace. A 256-frame integrated image was recorded with the shim in place, then the shim removed and a second 256-frame integrated image recorded. Subtracting the first image from the second eliminated any isocon-tube localized defects and minimized noise. The reversed 16-mm lens was then replaced with a long-working-distance 20X microscope objective, which provided greater convenience in focusing the image upon the isocon tube. The image-array processor was then used to obtain an intensity profile across the edge. Generally, about 10 lines were averaged to produce the profile. The

SQUARE WAVE RESPONSE OF SCREEN AND CAMERA



SQUARE WAVE RESPONSE OF CAMERA

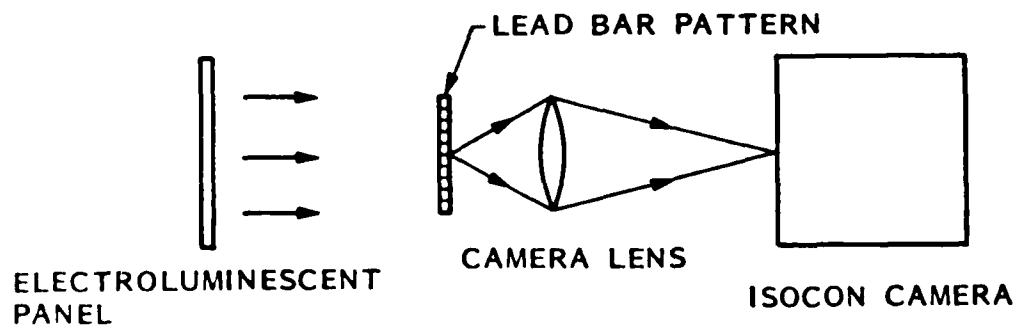


Fig. 11 Block Diagram of MTF Measurement

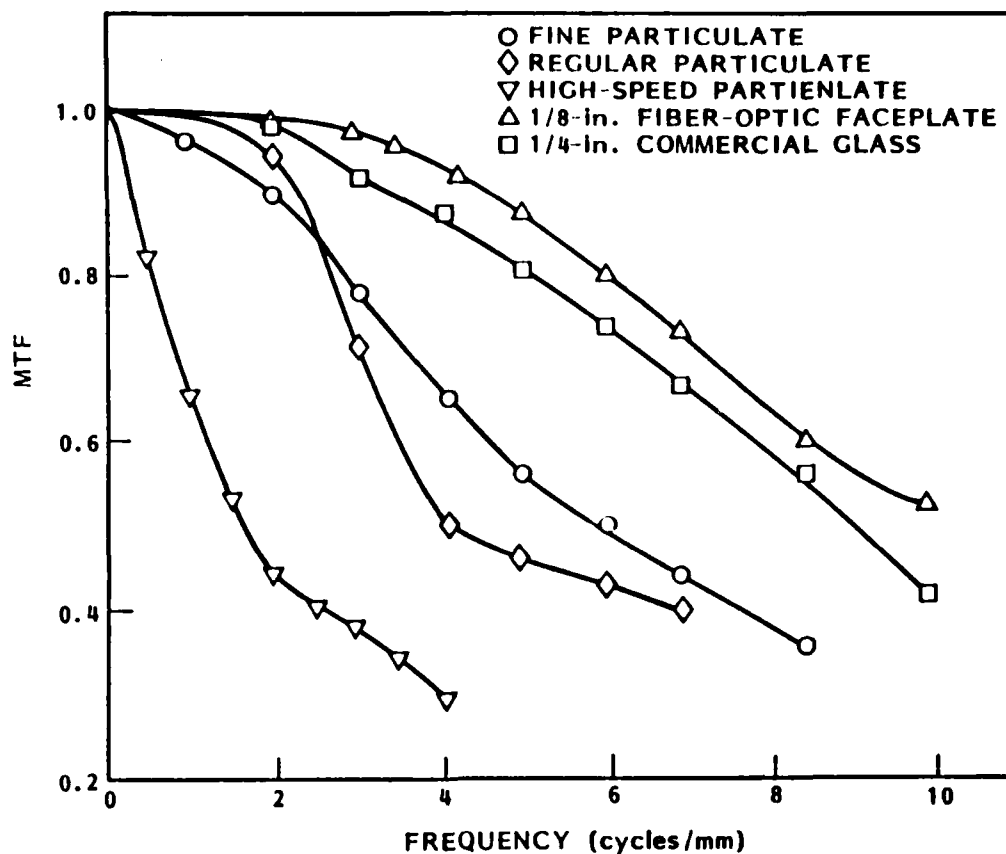


Fig. 12 Modulation Transfer Function for Several Screens

20X objective allowed resolving the edge at 200 to 400 pixels/mm. The edge profile was then fitted with a hyperbolic tangent function.

$$Y = Y_a + \frac{1}{2} \cdot D [1 + \tanh[2S(X - X_m)/D]]$$

Using the cursor mode of the digital image processor, Fortran programs were written that require only placement of cursors under joystick control to do the fitting. The MTF curve was obtained by performing an FFT on the derivative of the hyperbolic tangent function, the results being normalized to zero frequency. By sampling the derivative at 128 points, the window effect and aliasing in performing a finite FFT were made negligible.

The method of fitting the profile with the hyperbolic tangent function was somewhat novel. The change in intensity across the edge was determined by placing cursors on the profile at the left and right of the edge step. The vertical difference in cursor positions corresponded to the parameter D , representing the difference between the asymptotes of the hyperbolic tangent. The slope S in the edge region was measured by overlaying a straight line on the profile, then rotating the line under computer control for best visual fit to the points delineating the edge. When the fit was considered satisfactory, the parameters D and S were read out on the computer console. To verify the goodness of fit, the hyperbolic tangent curve corresponding to the given D and S values was then overlaid on the profile.

Use of 128 points for the FFT provided MTF values over the range 0 to 60 lp/mm.

3.3.3.3 Modulation Transfer Function of the HERTIS System. The overall MTF was measured for the LMSC High-Energy, Real-Time Inspection System (HERTIS), used to characterize the image conversion screens studied under this program. The HERTIS system consists essentially of a low-light-level isocon camera and a digital image processor.

The MTF of the detection system is of importance because it affects the measured (or apparent) MTF of the image-conversion screens. Thus, the apparent MTF of the screen is the product of the intrinsic MTF of the screen and the MTF of the detection system:

$$\text{Screen MTF (apparent)} = \text{Screen MTF (intrinsic)} \times \text{System MTF.}$$

Knowing the system MTF, the intrinsic MTF of the screen can be obtained by dividing the measured MTF of the screen by the system MTF. The measurement setup is shown schematically in Fig. 13. The test pattern was a Kodak high-resolution photographic plate containing an image of several line pairs, the individual lines having a width of 0.005 in. The plate also contained an open rectangle on a blackfield. The plate was illuminated from behind by an electroluminescent panel, not shown in the figure.

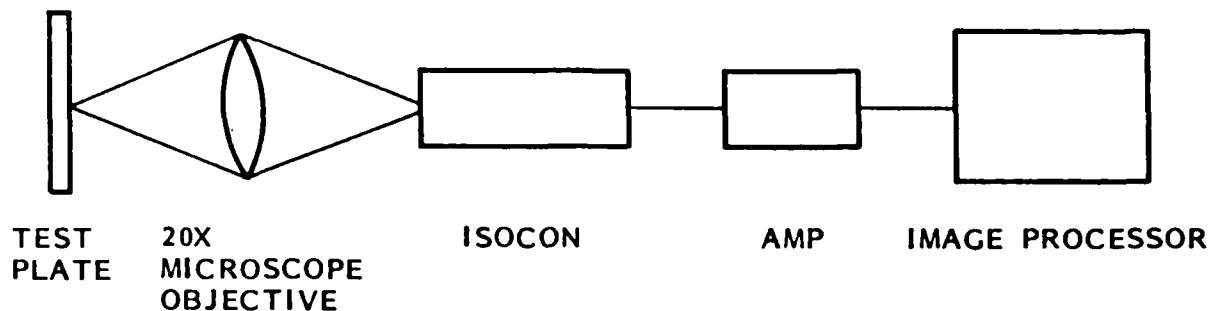


Fig. 13 System Modulation Transfer Function Measurement

The measurement was made in three steps. First, the microscope objective was focused on the line pair group and the number of pixels per mm determined by joystick manipulation of cursors overlaid on the console image.

Next, the plate was translated transversely to bring the edge of the rectangular opening into the field of view. A 256-frame integrated image was recorded; then the plate was removed and a second 256-frame integrated image recorded. The two images were subtracted, minimizing noise and also any localized defects in the isocon tube.

Finally, using the array processor, an intensity profile was recorded for a group of video lines across the rectangle edge. The profile was fitted with a hyperbolic tangent function, as described in section 3.3.3.2. An FFT was next performed on the derivative of the hyperbolic tangent function. The resulting vector magnitudes, when multiplied by pixels per millimeter and normalized to zero frequency, yield the MTF of the system, as shown in Fig. 14.

3.3.3.4 MTF of Intensifier Screens. MTF measurements were performed for regular, medium, and fine particulate screens using the improved method. The results, after factoring out the system MTF, are shown in Fig. 15. The resolution of the particulate regular is only a little less than that of the

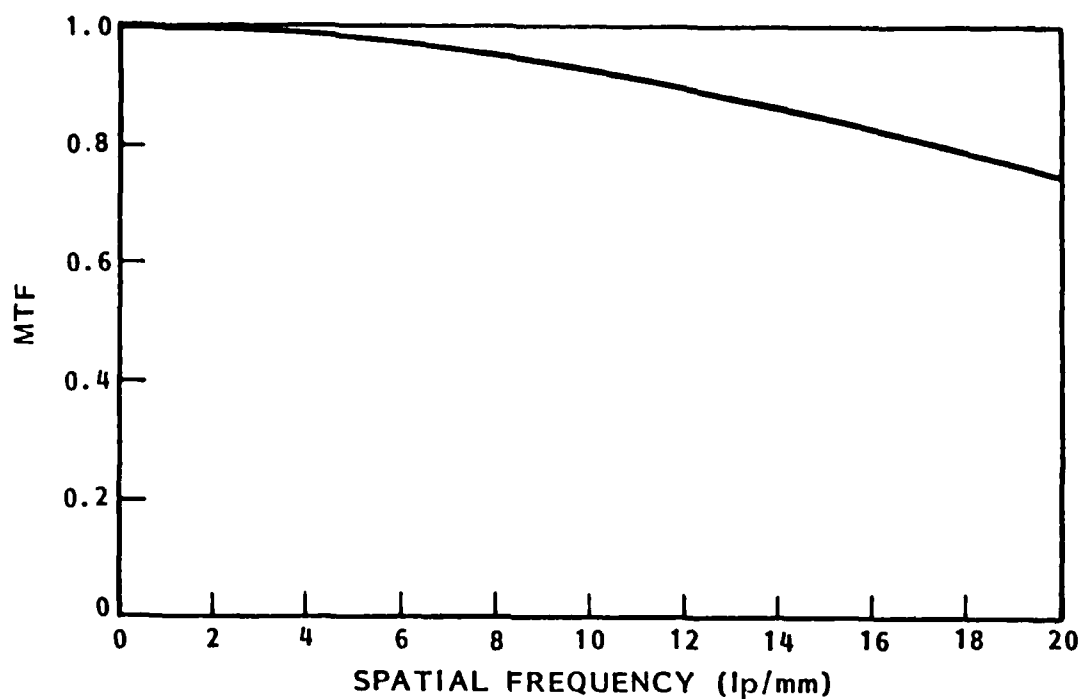


Fig. 14 Modulation Transfer Function of Real-Time Radiographic System

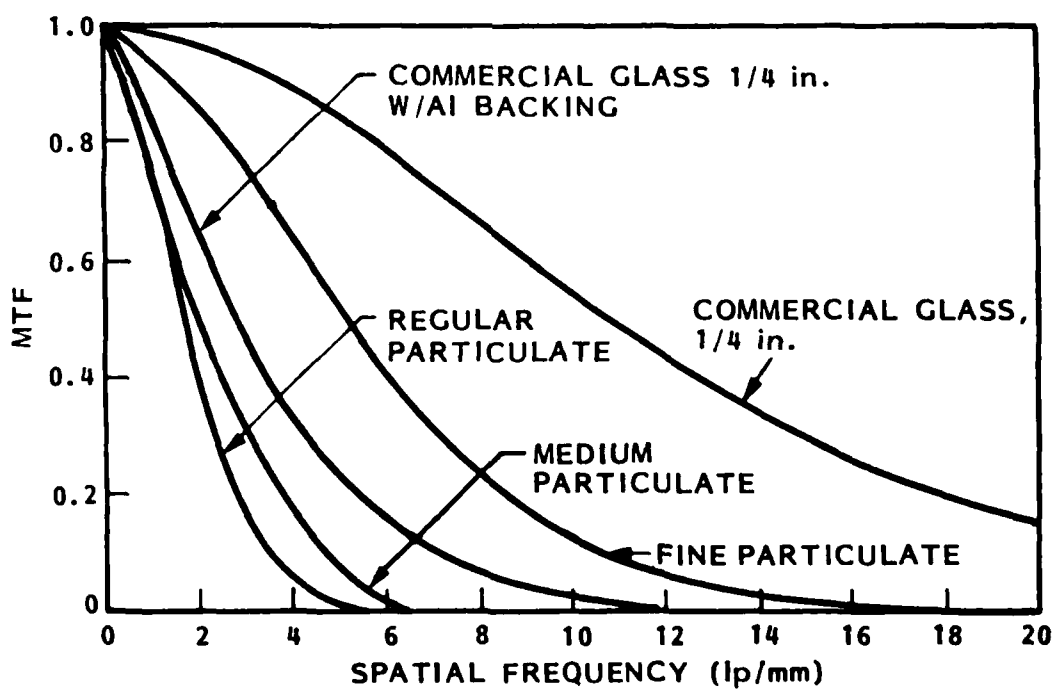


Fig. 15 Modulation Transfer Function of Particulate Screens

medium, and both are considerably lower than for the fine screen. This is indicative of the layer particle sizes of the Regular and Medium screens. The fine screen is also thinner, showing considerable transmission for visible light.

High-Speed Particulate Screen. The MTF measured for a high-speed particulate screen is shown in Fig. 16. The resolution is inferior to that of even the particulate regular screen.

Commercial Glass Plates. The MTF curves for 1/4-in. commercial glass plates, with and without a coating of evaporated aluminum deposited on one face of the plate, are shown in Fig. 17. The x-ray tube voltage was 200 kV. Although the reflective coating increases the screen efficiency, there is a loss of resolution, as the reflected energy is spread out over a larger solid angle. Resolution without the aluminum coating is 10 lp/mm at a 50 percent MTF. With the aluminum coating, resolution is about 3.5 lp/mm at 50 percent MTF. These measurements were made using a 0.005-in. tungsten shim placed on the x-ray-source side of the plate to cover one half of the field of view.

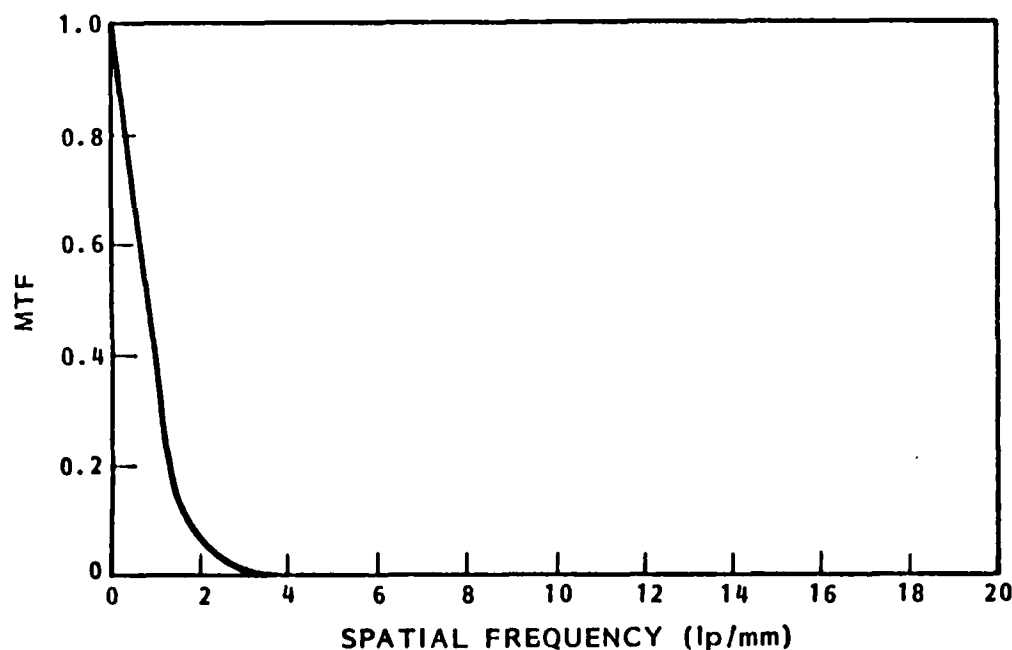


Fig. 16 Modulation Transfer Function of High-Speed Particulate Screen

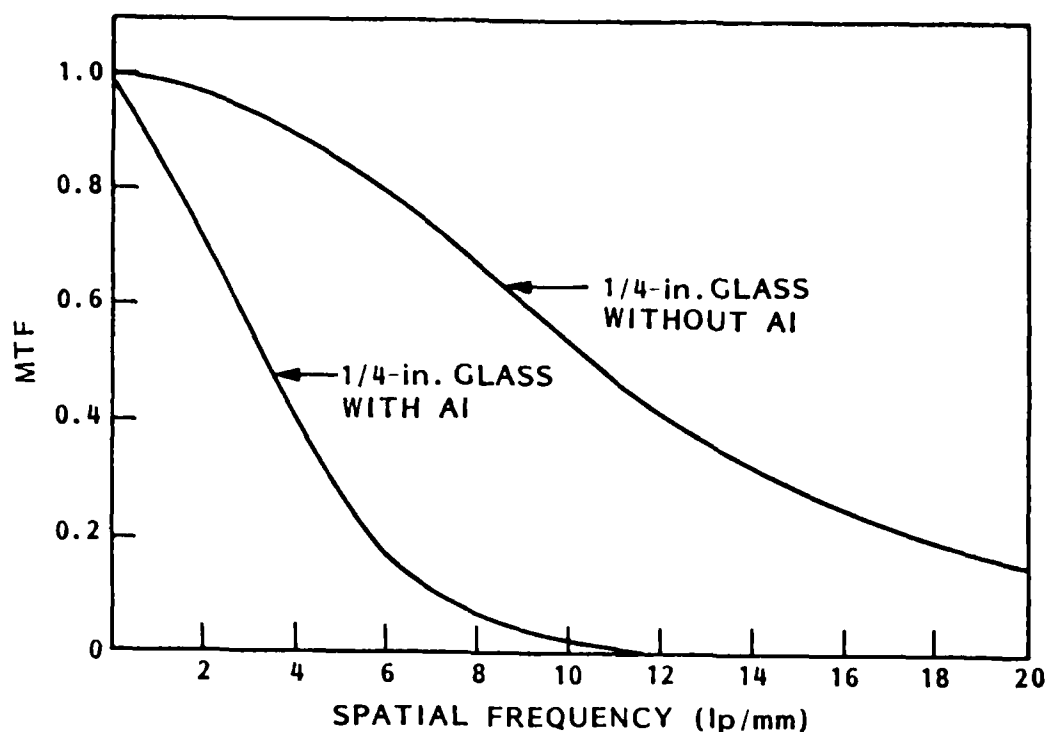


Fig. 17 Modulation Transfer Function of 1/4-in. Commercial Glass Plate

Commercial Fiber-Optic Screens. The MTF curve for a 1/2-in. commercial fiber-optic plate with an aluminum coating on the back surface is shown in Fig. 18. Spatial resolution is close to 9 lp/mm at 50 percent MTF, only a little less than that for the uncoated glass plate of Fig. 17. This demonstrates that when the fiber diameter is sufficiently small, about 0.001 in. in this case, excellent resolution is attainable, while the light output is substantially increased by piping the emitting light down the fiber. A glass plate, on the other hand, useful light output is reduced by light trapping due to internal reflection.

Gadolinium Oxysulfide Film. The system-corrected MTF curve for an 0.2-mil-thick gadolinium oxysulfide:terbium film is shown in Fig. 19. Resolution is better than 9 lp/mm at a 50 percent MTF. The curve is comparable to that of the commercial 1/4-in. glass plate, as might be expected since both materials are free of any optical discontinuities.

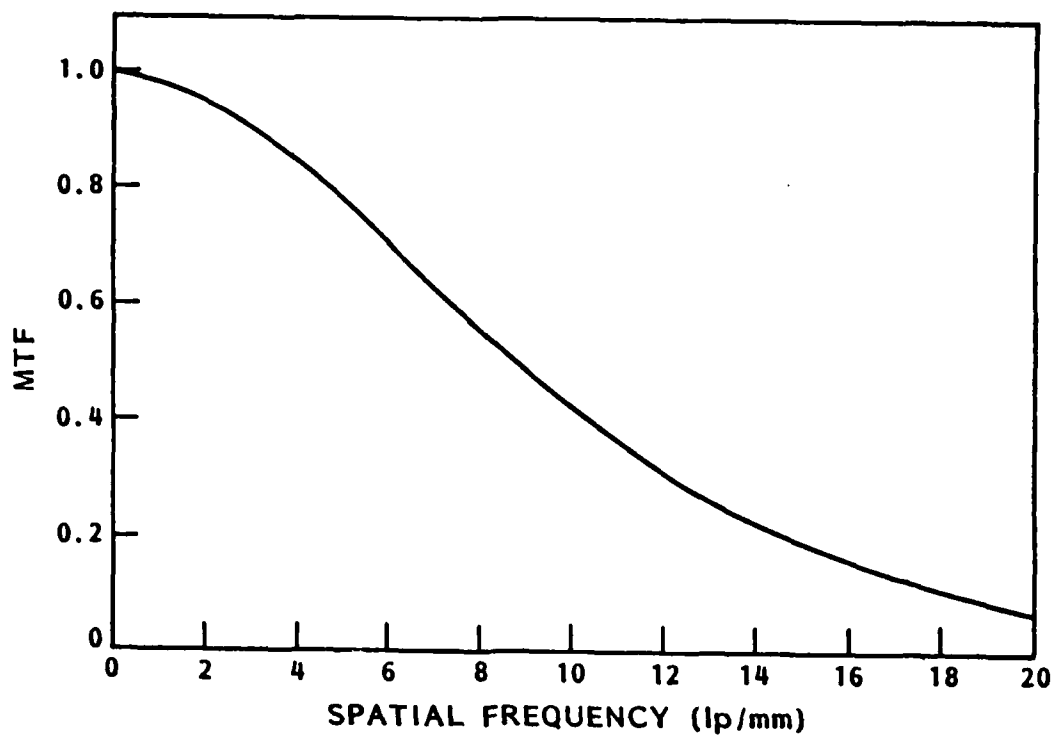


Fig. 18 Modulation Transfer Function of 1/2-in. Commercial Fiber-Optic Plate

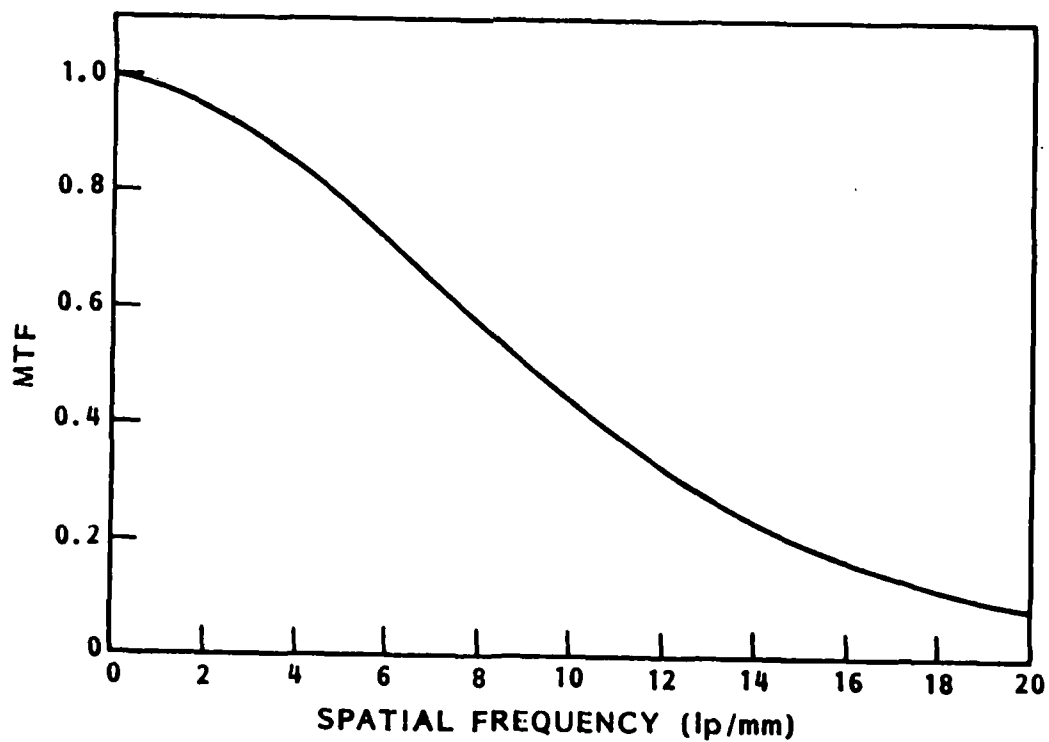


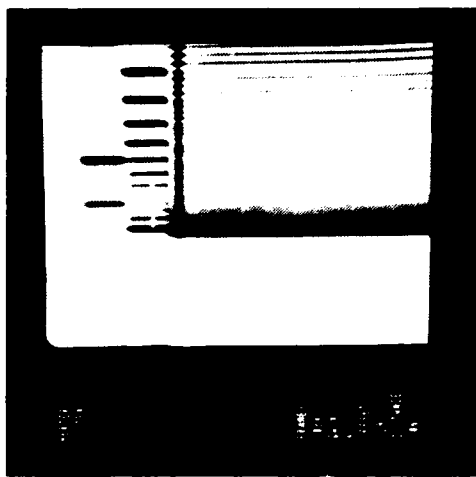
Fig. 19 Modulation Transfer Function for Gadolinium Oxysulfide Film

The resolution of the treated $\text{Gd}_2\text{O}_2\text{S:Tb}$ film was measured using a No. 53 Funk grid at 150 kV and 5 mA. A value of 4.2 lp/mm was obtained, using integration and subtraction of 256 frames. For comparison, 6 lp/mm was measured for a high-speed screen under the same conditions. An x-ray brightness measurement of the high-speed screen yielded a value of 7.91×10^{-1} ft-L as compared to the 1.51×10^{-2} ft-L for the film. This suggested that the apparent resolution of the film might be limited by the low signal from the film relative to system noise. To increase the signal strength, an increase of incident x-ray flux was required. This was accomplished by reducing the sample-to-source distance, increasing the x-ray source current to 10 mA, and increasing the number of integrated frames to 1024. Measurement then demonstrated excellent resolution of the 10 lp/mm patterns of the Funk grid, the limit of the test capability of the grid. Under the same conditions, the resolution of the high-speed screen remained at 6 lp/mm (see Fig. 20).

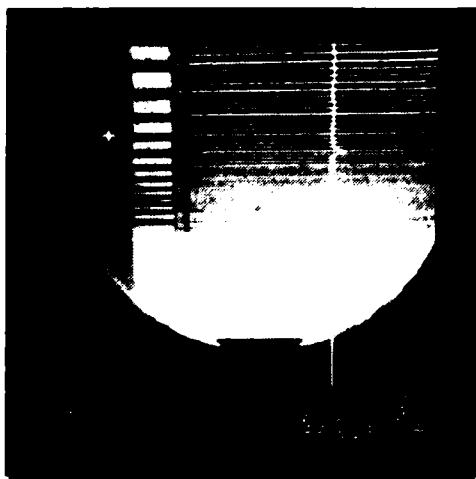
An intensity profile was obtained by scanning across the large index line of the Funk grid. Signal height for the $\text{Gd}_2\text{O}_2\text{S:Tb}$ film was 14 gray levels, and for the high-speed screen 32 gray levels. See Fig. 20, in which individual pixels can be readily distinguished.

The radiographer performing the measurements reported that he was able to distinguish the 10 lp/mm pattern with a single frame for the film in real time (no integration, no subtraction), suggesting that the actual resolution of the $\text{Gd}_2\text{O}_2\text{S}$ film may be well in excess of 10 lp/mm.

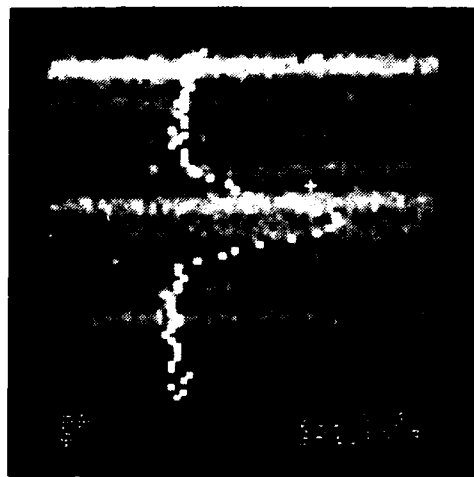
3.3.3.5 MTF Voltage Dependence. A comparison of the spatial frequency value at the 50 percent MTF point for the particulate and glass screens over the range 80 to 400 kV indicates that the MTFs for these screens are not voltage dependent, although the results do not entirely exclude a slight decrease with increasing kV. Additional measurements would be required to determine whether the possible slight decrease with increasing kV actually exists. This trend, if it exists, appears to be similar for both materials.



HIGH-SPEED SCREEN
6 lp/mm



Gd₂O₂S FILM
10 lp/mm



CONDITIONS: 150 kV
20 mA

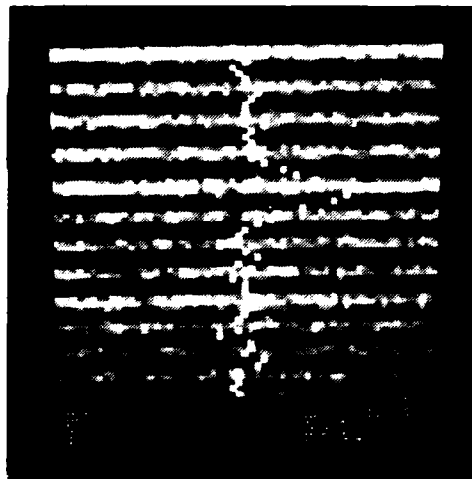


Fig. 20 Funk Grid Resolution

3.3.4 Contrast Sensitivity of X-Ray Converters

Contrast sensitivity, C , is the percent change in object thickness divided by the percent change in the image signal-to-noise ratio. Contrast sensitivity performance was measured for 5 percent and 1 percent changes in object thickness.

3.3.4.1 Five Percent Contrast Sensitivity Measurements

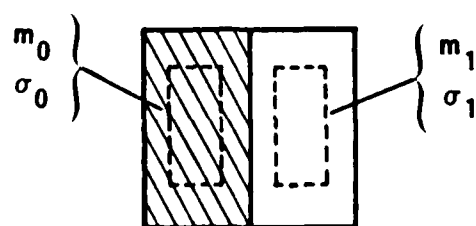
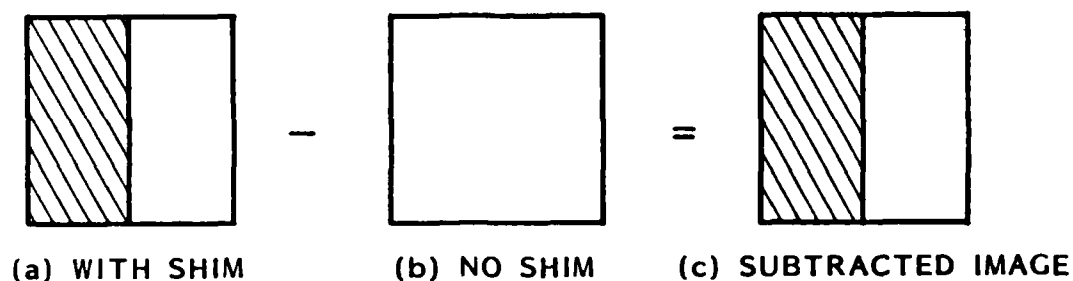
Gadolinium Oxysulfide Film. The contrast sensitivity of the gadolinium oxysulfide film was measured under the following conditions:

- o 0.02-in. aluminum shim covering left half of field
- o 0.375-in. aluminum absorber covering entire field
- o 37-cm x-ray source to test screen distance
- o Small x-ray tube (KB160/4)
- o 0.8-in. field of view for isocon camera tube
- o 150 kV, 20 mA

The shim thickness corresponded to 5.3 percent of the absorber thickness. Measurements were performed at 30, 40, 50, 75, 100, 125, 150, 175, 200, 225, 250, 275, and 300 kV. Current was changed for each kV in order to avoid saturation of the isocon tube. For the 50-kV measurement, an 0.005-in. aluminum shim with an 0.090-in. aluminum absorber was used (shim thickness 5.6 percent of absorber thickness) to avoid excessive reduction of the x-ray flux by the absorber.

At each voltage, images with the shim in place were subtracted from the image without the shim, and the digitized subtracted image recorded on diskettes. Integration frames were 1, 2, 3, 4, 8, 16, 32, 64, 128, 256, 512, and 1024.

Histogram analysis was performed on the shim and no-shim areas of the subtracted image to provide mean and standard-deviation intensity value for the corresponding areas, as shown in Fig. 21. Using this data, the contrast sensitivity was calculated using the equation



HISTOGRAM ANALYSIS

Fig. 21 Contrast Sensitivity Measurement

$$c = \frac{\Delta l (\sigma_0^2 + \sigma_1^2)^{1/2}}{l (m_1 - m_0)} \quad (4-1)$$

where Δl is the shim thickness, l the absorber thickness, m_0 and m_1 the mean intensities for the non-shim and shim areas, respectively, and σ_0 and σ_1 , the corresponding deviations.

The signal-to-noise ratio, S/N , is represented by the equation

$$\frac{S}{N} = \frac{(m_1 - m_2)}{(\sigma_0^2 + \sigma_1^2)^{1/2}} \quad (4-2)$$

Results for the $\text{Gd}_2\text{O}_2\text{S}$ film are summarized in Table 1.

High-Speed Screen. To provide a basis for comparison, 5 percent contrast sensitivity measurements were also made on a high-speed screen. Measurement conditions were the same as for the gadolinium oxysulfide screen, except the current was reduced to 1 mA to avoid saturating the isocon tube. Results of the histogram analysis are shown in Table 1.

Fiber-Optic Screen. The fiber-optic screen was composed of commercial luminescent glass with individual fiber dimensions of 0.025 mm x 0.025 mm (0.001 in. x 0.001 in.).

Measurement conditions were the same as for the $\text{Gd}_2\text{O}_2\text{S:Tb}$ film, except the large x-ray tube was used to allow measurements over the range 30 to 300 kV (the small tube is limited to 160 kV maximum). Results of the histogram analysis are shown in Table 2.

Table 1 HIGH-SPEED SCREEN CONTRAST SENSITIVITY AND SIGNAL-TO-NOISE RATIO

Integrated Frames	Gd ₂ O ₂ S:Tb Film		High-Speed Screen	
	C	S/N	C	S/N
1	0.628	0.09	0.548	0.10
2	0.421	0.13	0.254	0.21
4	0.282	0.19	0.198	0.27
8	0.171	0.31	0.131	0.41
16	0.213	0.25	0.115	0.46
32	0.097	0.55	0.080	0.67
64	0.118	0.45	0.060	0.89
128	0.050	1.07	0.47	1.4
256	0.043	1.24	0.033	1.63
512	0.032	1.69	0.022	1.99
1024	0.026	2.57	0.017	3.22

Table 2 COMMERCIAL FIBER-OPTIC SCREEN CONTRAST SENSITIVITY AND SIGNAL-TO-NOISE RATIO

Frames	kV: mA:	30	40	50	75	100	125	150	175	200	225	250	275	300
		9	13.5	15	15	13	6	5	3	2	4	3	3	3
(A) 5% Contrast Sensitivity														
2	-	0.0740	0.4801	0.1673	0.1053	0.1227	0.1508	0.1443	0.1773	0.2068	0.2830	0.2112	0.1881	0.2632
4	-	0.2047	0.3461	0.1210	0.0885	0.0989	0.1166	0.1171	0.1311	0.1705	0.1466	0.1391	0.1697	0.1876
8	-	0.1281	0.2852	0.0735	0.0702	0.0855	0.1090	0.1056	0.1010	0.1206	0.1368	0.1144	0.1336	0.1506
16	-	0.0798	0.1531	0.0718	0.0501	0.0582	0.0679	0.0678	0.0817	0.0973	0.0836	0.0815	0.1007	0.1003
32	-	0.0961	0.1168	0.0585	0.0382	0.0443	0.0570	0.0538	0.0615	0.0684	0.0640	0.0647	0.0724	0.0786
64	-	0.0671	0.0598	0.0418	0.0323	0.0331	0.0426	0.0384	0.0422	0.0505	0.0471	0.0451	0.0540	0.0559
128	-	0.0578	0.0716	0.0357	0.0235	0.0244	0.0301	0.0292	0.0337	0.0363	0.0380	0.0376	0.0428	0.0412
256	-	0.0407	0.0386	0.0294	0.0263	0.0192	0.0221	0.0205	0.0242	0.0276	0.0260	0.0263	0.0287	0.0339
512	-	0.0374	0.0389	0.0205	0.0129	0.0154	0.0194	0.0180	0.0180	0.0207	0.0200	0.0219	0.0229	0.0279
1024	-	0.0307	0.0198	0.0166	0.0123	0.0114	0.0129	0.0133	0.0140	0.0165	0.0153	0.0164	0.0193	0.0230
(B) Signal-to-Noise Ratio														
2	-	-	0.11	0.32	0.51	0.44	0.35	0.37	0.30	0.26	0.19	0.25	0.28	0.20
4	0.27	0.15	0.44	0.44	0.60	0.54	0.46	0.46	0.41	0.31	0.36	0.38	0.31	0.28
8	0.43	0.19	0.73	0.73	0.76	0.62	0.49	0.51	0.53	0.44	0.39	0.47	0.40	0.35
16	0.70	0.35	0.74	0.74	1.05	0.92	0.79	0.79	0.65	0.55	0.64	0.53	0.53	0.53
32	0.58	0.46	0.91	0.91	1.40	1.20	0.94	0.99	0.87	0.78	0.83	0.83	0.74	0.70
64	0.83	0.89	1.28	1.28	1.65	1.61	1.25	1.29	1.26	1.06	1.13	1.18	0.99	0.96
128	0.96	0.74	1.49	1.49	2.27	2.19	1.77	1.82	1.58	1.47	1.41	1.42	1.25	1.30
256	1.37	1.38	1.81	1.81	2.92	2.78	2.41	2.61	2.20	1.93	2.05	2.03	1.86	1.58
512	1.49	1.37	2.61	2.61	4.13	3.46	2.75	2.96	2.97	2.58	2.67	2.44	2.33	1.91
1024	1.81	2.69	3.21	3.21	4.32	4.79	4.12	4.00	3.80	3.23	3.50	3.25	2.76	3.32

Inspection of the contrast sensitivity equation (4-1) shows that the closer C approaches zero, the better the contrast resolution. Inspection of Table 2(A) shows the best values of C at 75 kV for 2-128 frames and 100 kV for 256-1024 frames. Also, at all kVs, C consistently improves as the number of integrated frames increases, as might be expected because of the corresponding signal-to-noise ratio increases, as shown in Table 2(B).

3.3.4.2 One Percent Contrast Sensitivity Measurements. Additional measurements, using a 1 percent shim, were made on gadolinium oxysulfide film No. 1-83, a particulate fine detail screen, the glass fiber-optic screen, and a 1/4-in.-thick plate of clear commercial glass. The absorber thickness varied between 0.090 and 2.50 in., depending upon kV, so as to represent about three half-value layers. Only five shim thicknesses were available, so each shim-absorber combination was used for three different kV values. The number of integrated frames was fixed at 256 for this series. Results are shown in Tables 3 through 6. There is considerable scatter in the results, consistent with the relatively low signal-to-noise ratios observed.

3.3.4.3 Effect of Variation of the Shim/Absorber Ratio on Contrast Sensitivity. The shim/absorber ratio $\Delta l/l$ appears in Eq. (4-1) for the contrast sensitivity C . To determine the effect upon C of varying the value of $\Delta l/l$, a series of measurements was performed on the regular and fine commercial particulate screens.

For the regular particulate screen, the absorber was kept constant at 0.5 in. The shim thicknesses used were 0.0008, 0.0031, 0.0041, 0.0058, 0.008, 0.015, 0.025, 0.040, and 0.0625 in., corresponding to variation of $\Delta l/l$ by nearly three orders of magnitude. The measurements were performed at 100 kV, 2 mA, using 256-frame integration and subtraction, as for the earlier measurements. Results are summarized in Table 7 and plotted in Fig. 22.

For the fine particulate screen, the absorber thickness was 1.50 in. and shim thicknesses 0.001, 0.008, 0.015, 0.020, and 0.025 in. Measurements were

Table 3 ONE PERCENT CONTRAST SENSITIVITY OF Gd₂O₂S:Tb FILM,
ONE PERCENT SHIM

kV	mA	Shim (in.)	Absorber (in.)	C	S/N
30	2	0.001	0.090	0.361	0.031
40	3	0.001	0.090	0.123	0.090
50	4	0.001	0.090	0.068	0.164
75	4	0.008	0.750	0.068	0.156
100	6	0.008	0.750	0.090	0.119
125	7	0.008	0.750	0.062	0.172
150	9	0.015	1.50	0.055	0.181
175	10	0.015	1.50	0.056	0.180
200	9	0.015	1.50	0.062	0.162
225	8	0.020	2.00	0.049	0.202
250	7.5	0.020	2.00	0.057	0.175
275	7	0.020	2.00	0.038	0.267
300	7	0.025	2.50	0.084	0.119

Table 4 CONTRAST SENSITIVITY OF PARTICULATE FINE SCREEN, ONE PERCENT SHIM

kV	mA	Shim (in.)	Absorber (in.)	C	S/N
30	9	0.001	0.090	0.210	0.053
40	13	0.001	0.090	2.22	0.005
50	3	0.001	0.090	0.060	0.185
75	5	0.008	0.750	1.74	0.006
100	5	0.008	0.750	0.028	0.381
125	5	0.008	0.750	0.026	0.414
150	5	0.015	1.50	0.021	0.468
175	5	0.015	1.50	0.020	0.511
200	4	0.015	1.50	0.022	0.462
225	4	0.020	2.00	0.022	0.463
250	4	0.020	2.00	0.023	0.439
275	4	0.020	2.00	0.018	0.554
300	4	0.025	2.50	0.024	0.416

Table 5 CONTRAST SENSITIVITY OF GLASS FIBER-OPTIC SCREEN, ONE PERCENT SHIM

kV	mA	Shim (in.)	Absorber (in.)	C	S/N
30	10	0.001	0.090	0.060	0.18
40	13	0.001	0.090	0.047	0.24
50	4	0.001	0.090	0.202	0.06
75	4	0.008	0.750	0.124	0.09
100	4	0.008	0.750	0.049	0.22
125	4	0.008	0.750	0.020	0.53
150	4	0.015	1.50	0.027	0.37
175	4	0.015	1.50	0.019	0.51
200	4	0.015	1.50	0.018	0.56
225	4	0.020	2.00	0.014	0.74
250	4	0.020	2.00	0.009	1.06
275	4	0.020	2.00	0.011	0.94
300	4	0.025	2.50	0.013	0.86

Table 6 CONTRAST SENSITIVITY OF GLASS PLATE, 1/4 in. THICK, ONE PERCENT SHIM

kV	mA	Shim (in.)	Absorber (in.)	C	S/N
30	4	0.001	0.090	1.45	0.008
40	2	0.001	0.090	0.072	0.154
50	4	0.001	0.090	0.094	0.118
75	4	0.008	0.750	0.109	0.097
100	4	0.008	0.750	0.031	0.344
125	4	0.008	0.750	0.037	0.288
150	4	0.015	1.50	0.017	0.607
175	4	0.015	1.50	0.015	0.658
200	4	0.015	1.50	0.015	0.688
225	4	0.020	2.00	0.010	1.04
250	4	0.020	2.00	0.011	0.92
275	4	0.020	2.00	0.010	0.97
300	4	0.025	2.50	0.014	0.69

Table 7 $\Delta l/l$ VARIATION, REGULAR PARTICULATE SCREEN

Shim Thickness	C	S/N
0.0016	0.017	0.094
0.0062	0.021	0.300
0.0082	0.025	0.329
0.0116	0.052	0.223
0.016	0.028	0.566
0.020	0.034	0.597
0.030	0.026	1.135
0.080	0.029	2.792
0.125	0.044	2.863

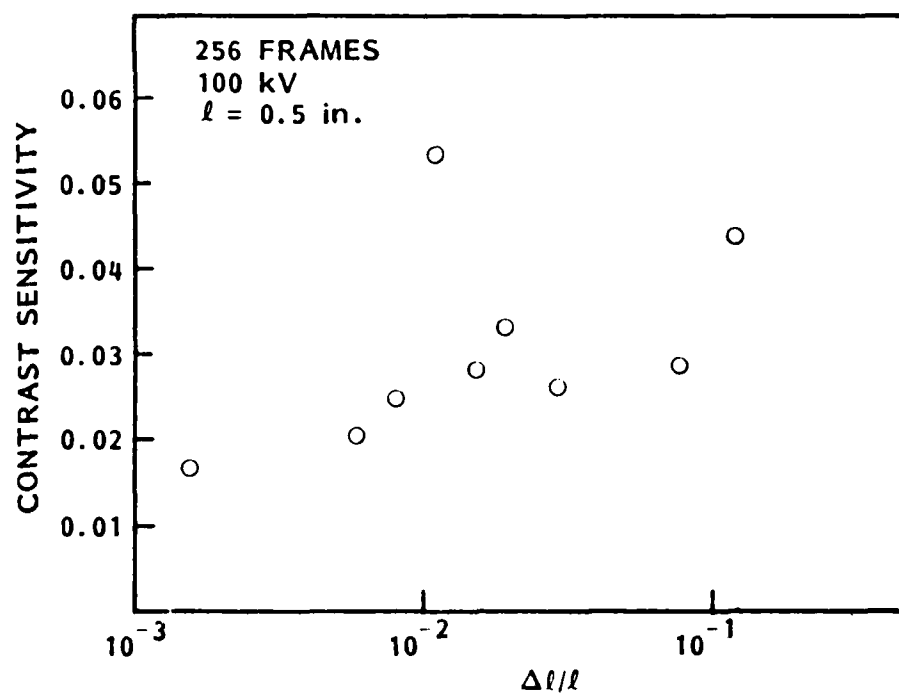


Fig. 22 Contrast Sensitivity Versus Shim/Absorber Ratio for a Regular Particulate Screen

performed at 150 kV, 4 mA, again using 256-frame integration and subtraction. Results are summarized in Table 8 and plotted in Fig. 23.

Figures 22 and 23 indicate that C changes little or not at all with variation of $\Delta I/I$, whereas the signal-to-noise ratio, S/N , most definitely increases as $\Delta I/I$ increases. Under the conditions of measurement, S/N is derived from the difference in light intensity (i.e., signal strength) between the masked and unmasked regions, and thus corresponds to the difference in contrast as ordinarily understood.

3.4 EXTERNAL FACTORS AFFECTING X-RAY CONVERTER PERFORMANCE

There are many factors in the external setup that might affect the accuracy of measurements of the performance and physical properties of the x-ray converter devices. Some of the more important ones and precautions to reduce their effects are as follows.

3.4.1 Geometrical Unsharpness

Because the x-ray focal spots of most commercially available x-ray sources are finite, projecting the focal spot through a test sample on a converter device causes the x-ray image to spread according to the geometrical arrangement of

Table 8 $\Delta I/I$ VARIATION, FINE PARTICULATE SCREEN

Shim Thickness	C	S/N
0.00067	0.049	0.014
0.0053	0.035	0.153
0.010	0.045	0.224
0.014	0.054	0.243
0.017	0.030	0.555

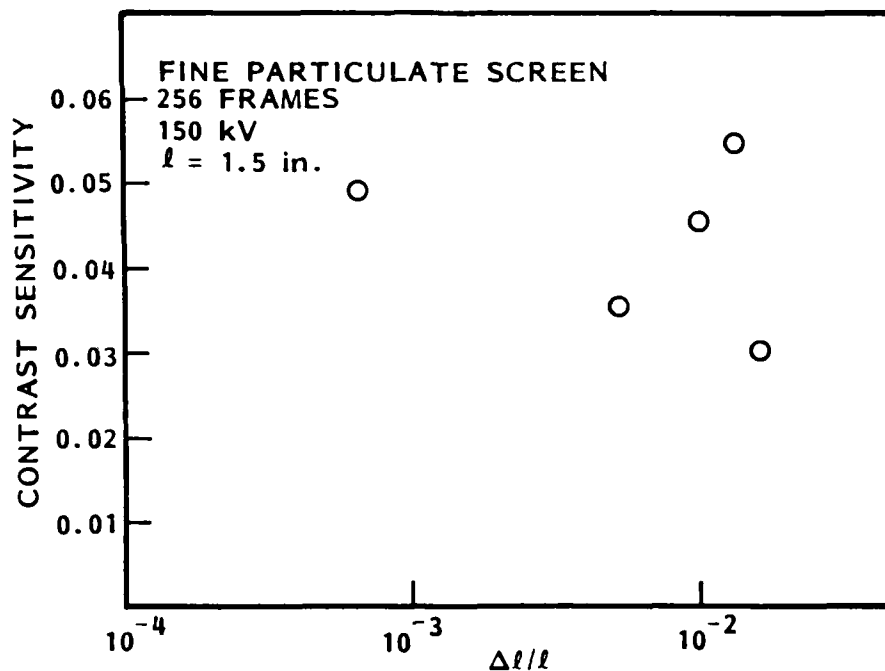


Fig. 23 Contrast Sensitivity Versus Shim/Absorber Ratio for Fine Particulate Detail Screen

the x-ray source, sample body, and the converter. Reducing the ratio between the sample-to-converter distance and the source-to-sample distance will reduce the geometrical sharpness. However, the x-ray flux arriving at the converter device also decreases according to the inverse square law, and consequently reduces the image quality if the exposure time is kept constant.

3.4.2 Spectral Distribution of the X-Ray Source

The spectral distribution of the x-ray beam will also effect the conversion efficiency in the x-ray converter device. A higher energy x-ray photon produces more light photons in the converter. However, higher energy x-rays are less attenuated by the converted material, so that increased x-ray energy does not necessarily produce more visible light. The x-ray spectral distribution depends upon the materials used in constructing the x-ray tube and on the external filtration in the x-ray beam. The x-ray spectrum will

also vary with the material composition and thickness of the object being examined. These factors must be controlled systematically in order to compare data from different devices.

3.4.3 Spectral Distribution of the Visible Light

The visible light generated in the x-ray converter is characterized by its spectral distribution and depends upon the converter material. The Lockheed proprietary fluorescent glass, commercial fluorescent glass, and commercial particulate screen all have narrow emission bands in the green spectral region. Their spectra are shown in Fig. 3-24. These spectra were taken with a Cary 14 Spectrophotometer using a 0.5-mm slit width. The spectra were taken with different gains to observe the fine structure in each material. The increased breadth and different relative peak heights within each sample illustrate that the activator ions in the glass samples occupy a number of different sites in the glass with surroundings most likely different from those found in the particulate screens. Other phosphors may emit a broad band of light in other regions of the spectrum. The low-light-level TV camera has its own spectral-response characteristic curve. For meaningful comparison of devices with different emission spectra, the resultant image data must be corrected by calibrating the camera for the different devices.

3.4.4 Performance of the Measuring Equipment

To measure the performance of a converter device, the measuring equipment must have much better performance than the device being measured. Thus, the measuring equipment must require the converter devices to have much higher resolution, dynamic range, and contrast sensitivity than the converter device to be tested.

The principal image-measuring equipment used in this laboratory is an isocon camera followed by an image processing computer. This system shows excellent dynamic range and contrast sensitivity because of the specially selected isocon cameras. However, the isocon does not have 10 lp/mm resolution in a

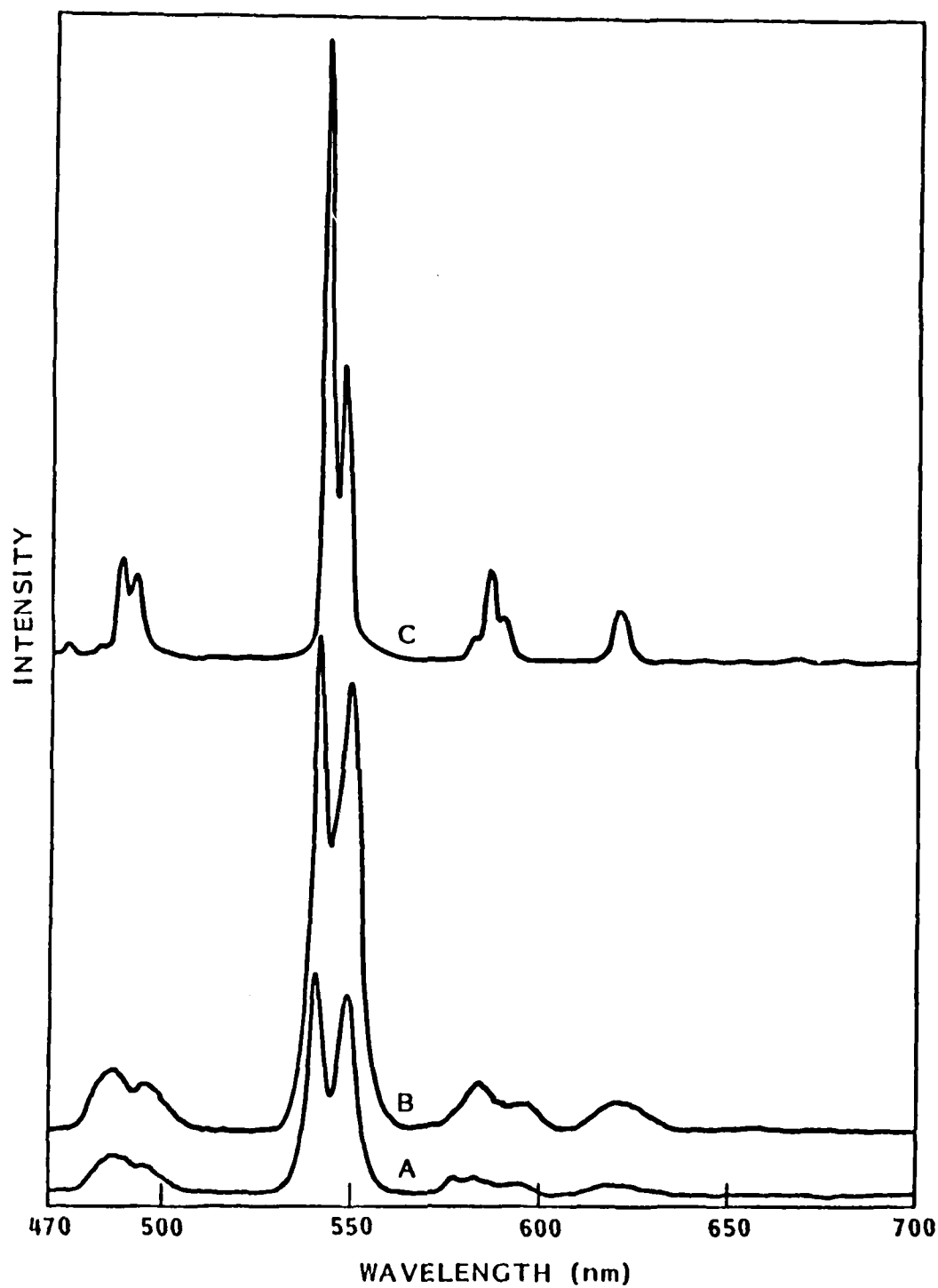


Fig. 24 Spectral Emissions of (A) Lockheed Proprietary Fluorescent Glass, (B) Commercial Fluorescent Glass, and (C) Commercial Proprietary Screen

10 x 12 in. field of view, and when the image is enlarged to bring up the resolution, the optics can introduce more transmission loss and distortion. These features were considered in using the RTR System for doing converter performance measurements so that the image quality achieved by the x-ray converter was not degraded. The resulting 10-20X magnification for high-definition resolution measurements was accurate for performance testing but not for general viewing.

Another area that received extra consideration was the system linearity. When the image brightness changes, the digitized intensity level (0-255) should always correspond independent of image position, average brightness, magnification, etc. The responses of the lens, isocon tube, camera, shading controls, video amplifier, and video digitizer are not perfectly linear. In measuring converter performance, care had to be taken to compare devices taken in as similar circumstance as possible. LMSC is pursuing the RTR system linearization with an internal research program. The MTF performance measurements using step-response method had the most variability due to nonlinearities. The MTF performance figures were backed up by images of a Funk grid (variable-frequency lead bar patterns) which confirmed the results presented.

3.4.5 Scattered Radiation

Since only the x rays directly transmitted through the sample under test carry useful information, the scattered x rays generated in the body of the sample must be reduced. Scattered x rays arriving at the converter device contribute to noise and reduce the signal-to-noise ratio in the final radiographic image. Common practice is to insert a metallic sheet or a filter between the sample and the converter. This filter will preferentially attenuate the scattered x rays, which have lower energies than the direct x-ray beam.

The attenuation of the scattered x rays relative to that of the direct beam is also different, due to differences in the material composition and the screen thickness of different converter devices. In evaluating the performance of

different devices, the filtering conditions must also be specified, especially in the higher x-ray energy ranges.

3.4.6 Radiation Damage of Converter Materials

Most converter materials are susceptible to radiation damage by x rays. If the threshold of radiation damage is low, the converter will not be useful for RTR applications, unless the material is cheap and device fabrication is easy so that the damaged device can be replaced periodically.

The glass screen materials were shown to be highly radiation resistant due to the refractory nature of the crystals.

Recently an extensive study on the radiation damage to glass screens was completed in this laboratory. Coloration was observed after exposure to 10^6 rad. However, the coloration did not markedly reduce either the conversion efficiency or the transmission coefficient of the green light produced by x ray. The coloration can also be annealed by heating the glass to about 300°C . Since the glass screens can be annealed easily, they can be used in the RTR System continually without replacement.

3.5 PERFORMANCE OF LOW-LIGHT-LEVEL VIDEO CAMERAS

Several video camera systems were evaluated for low-light-level characteristics for possible use in the breadboard high-resolution real-time radiography system in conjunction with the candidate high-resolution screens. The video cameras were the compact, rugged, medium-light-level type, which were optically coupled to a light intensifier to achieve a low-light-level sensitivity comparable to that of the more bulky, delicate isocon tube cameras.

The image intensifier was a Varo 25-mm second-generation microchannel inverter tube. The Varo intensifier incorporated an adjustable gain control and an automatic brightness limiter. Its transfer characteristics, shown in Fig. 25, were measured at maximum and minimum gain settings with a Pritchard photometer

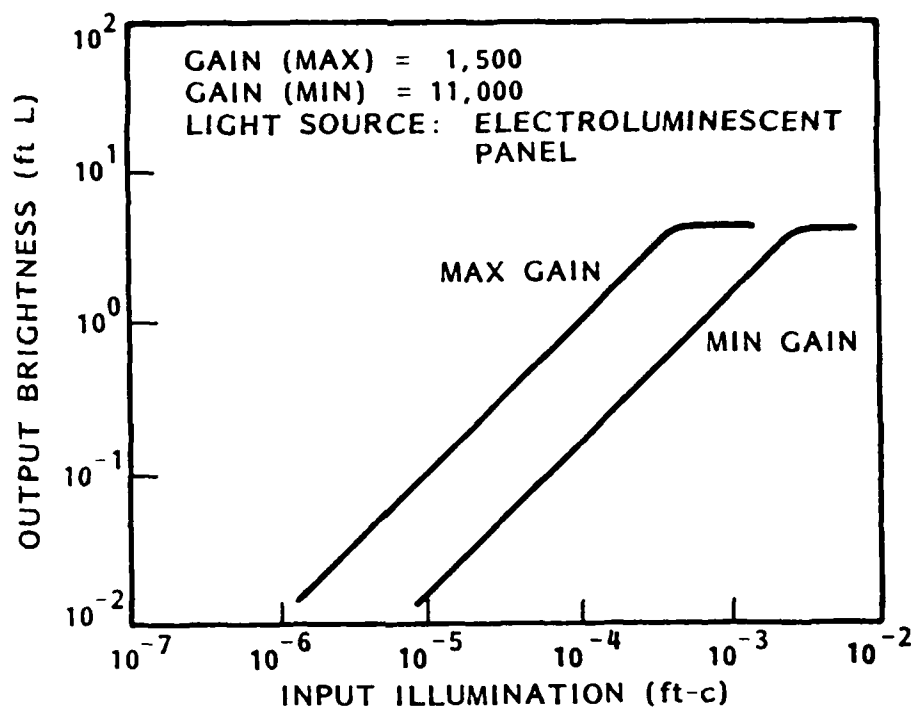


Fig. 25 Varo 25-mm Image-Intensifier Transfer Characteristics

and an electroluminescent panel as a light source. The response of the Varo intensifier was linear for all input illumination below the threshold levels at which the automatic brightness-limiting function set in. A luminance gain of 11,000 was obtained at the maximum gain setting and 1,500 at the minimum gain. The limiting resolution values at the intensifier output were measured as a function of scene brightness with a Marconi resolution chart and are shown in Fig. 26. A 65-mm f/0.65 lens was used as the objective lens.

The output of Varo intensifier was lens-coupled to an Ikegami ITC-82 camera fitted with a vidicon tube (8541B) and to a Fairchild CCD 3000 solid-state camera. The coupling lens was a 42-mm f/1.2 camera lens. The limiting resolutions of the intensifier/camera combinations were measured as a function of scene brightness (see Fig. 26). For comparison, the limiting resolutions of the cameras without the intensifier are also shown. The curves show that there is considerable loss in resolution in the Varo/Ikegami system. The degradation is attributed to the inefficient lens coupling to and from the

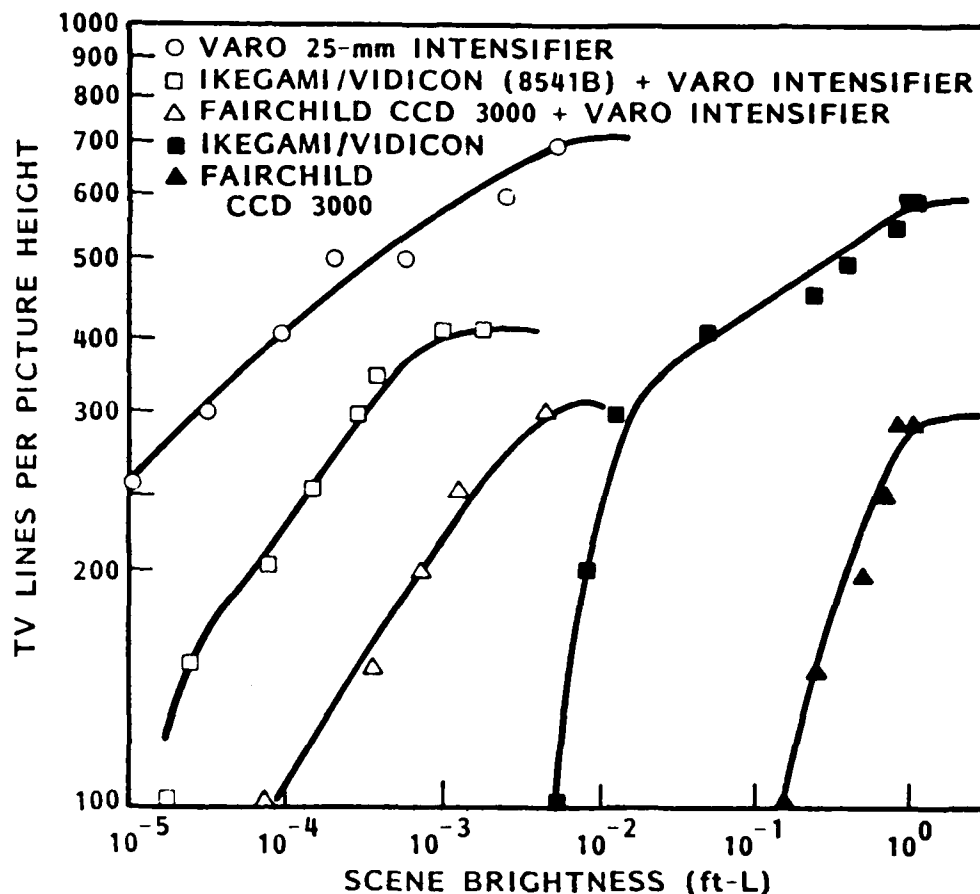


Fig. 26 Limiting Resolution Versus Scene Brightness

intensifier. Significant improvement in resolution should be realized with better lens couplings and a larger diameter image intensifier.

The poor performance of the Varo/Fairchild camera system is primarily due to the inherent low resolution of the Fairchild CCD camera. Higher resolution as well as higher sensitivity CCD cameras which are becoming more available should improve the performance of intensifier/CCD camera system.

Additional camera performance analysis is reported in section 4.1.4 for selecting the camera for the breadboard high-resolution RTR system.

3.6 SUMMARY AND CONCLUSIONS

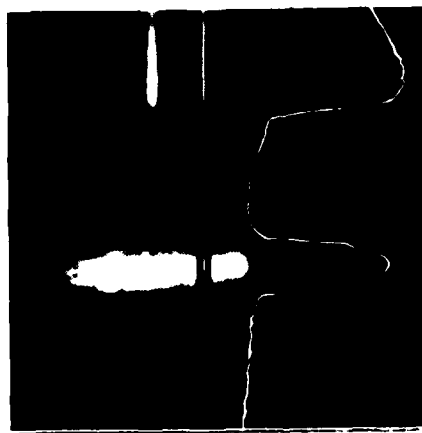
Several particulate and glass x-ray-fluorescent screens were evaluated for spatial resolution, brightness, and contrast sensitivity to determine the optimum screen to use in different energy ranges. These included fine, medium, regular, and high-speed particulate screens and commercial fluorescent glass. A new fluorescent glass screen, produced according to a LMSC-proprietary formula, was also evaluated and compared to the commercially available screens.

The new proprietary glass was designed to maintain the higher spatial resolution characteristic of glasses while improving the efficiency of x-ray-to-light conversion to produce a glass with brightness and resolution greater than the commercially available high-resolution particulate screens. The new glass is 12 in. x 12 in. x 1/4 in. In the first attempt to produce this glass on a "best effort" basis, some occlusions and air bubbles were present.

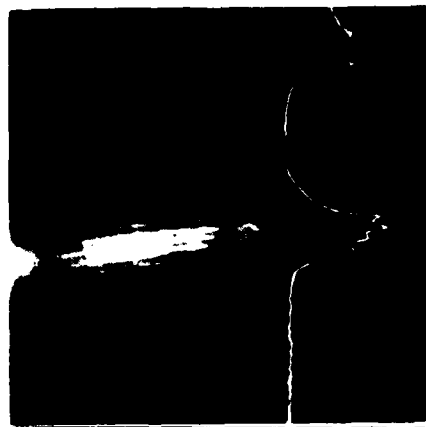
The resolution of the screens was reported in Section 3.3. Figures 27 and 28 show bar pattern images taken with several of the screens. These x-ray images were acquired using very high optical magnification, to minimize the effect of the finite camera resolution, and no geometric magnification, to minimize the effect of focal spot unsharpness. In Fig. 27, the tick marks on the right represent 16, 18, and 20 lp/mm from top to bottom. An intensity profile was taken through the 20-lp/mm pattern with the profile plotted in the lower half of the figures. The fine particulate screen is near the resolution limit at 20 lp/mm, while the glass screens still give sharp images. In Fig. 28, the pattern for each screen was moved to an area where the bar pattern could be resolved. The range of lp/mm resolutions included in each image is noted under each one.

The light output and contrast sensitivity of the screens were evaluated using two different x-ray sources to allow coverage of the full 20- to 400-kV energy range. The measurements in the energy region from 60 to 400 kV used a Seifert

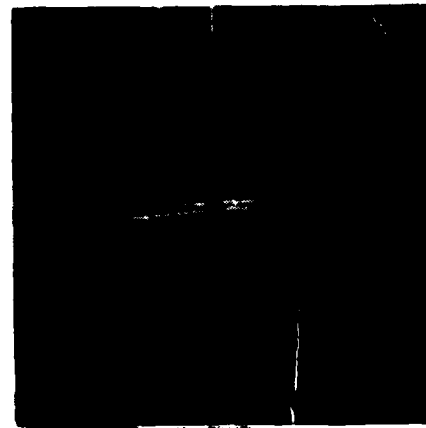
PROFILE AT 20 lp/mm



FINE PARTICULATE



1/4-in. GLASS
F.O. MIRRORED

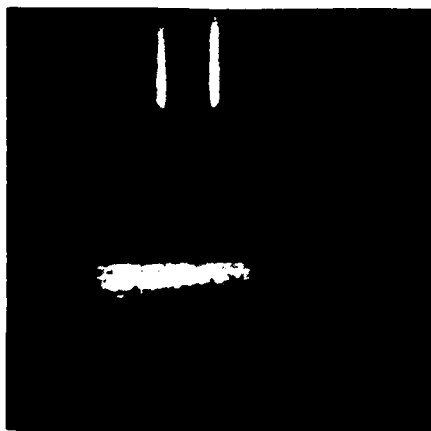


NEW GLASS
1/4 in., MIRRORED

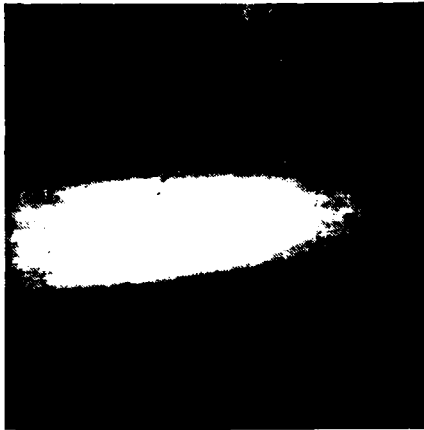


NEW GLASS
1/4 in. THICK

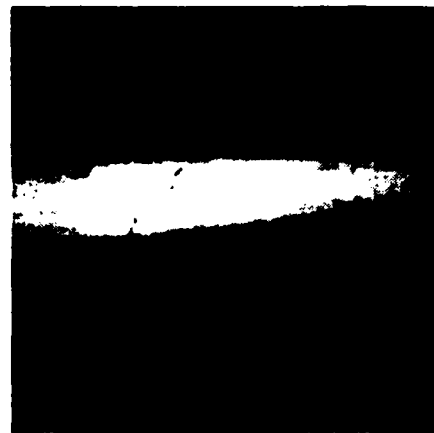
Fig. 27 Screen Resolution Comparison Examples



FINE PARTICULATE
14-20 μ p/mm



REGULAR PARTICULATE
8-10 μ p/mm



MEDIUM PARTICULATE
10-18 μ p/mm



HIGH-SPEED PARTICULATE
5 μ p/mm

Fig. 28 Screen Resolution Comparison Examples

420-kV tube with 7-mm beryllium filtrations; the 20- to 60-kV measurements used a Seifert 60-kV source with 0.4-mm beryllium filtration.

The light output from the screens was measured using a Pritchard 1980A photometer. The incident exposure at the screen was measured using a Victoreen 500 radiometer. The measurement technique is shown schematically in Fig. 2. The screen output was normalized to the incident exposure resulting in a relative output in (mft-L)/(mRs) as a function of energy. The results from the 60- to 400-kV measurement are shown in Fig. 29, while those from 20 to 60 kV are shown in Fig. 30. There is a scale difference between these two figures due to the difference in intrinsic filtration of the two sources used. Additional filtration was added to the 60-kV source and relative light outputs were obtained that were in better than 10 percent agreement with the previous results, proving that scale difference is only because of the filtration difference.

The contrast sensitivity data from 100 to 400 kV were reported in section 3.3.4. The data from 20 to 60 kV are presented here. At each kV, images were acquired of an absorber of 0.5-in. lucite with a shim of 0.032-in. lucite covering half the field of view. Then an image of just the absorber was acquired and subtracted from the absorber-plus-shim image.

Histogram analysis was performed on the shim and no-shim areas of the subtracted image to provide mean and standard-deviation intensity values for the corresponding areas as depicted in Fig. 21. Using this data, the contrast sensitivity C was calculated as

$$C = \frac{\Delta l}{l} \frac{(\sigma_1^2 + \sigma_0^2)^{1/2}}{(m_1 - m_0)}$$

where Δl and l are the shim and absorber thicknesses, m_1 and m_0 the mean intensities from the no-shim and shim areas, respectively, and σ_1 and σ_0 the corresponding standard deviations. This contrast sensitivity is defined

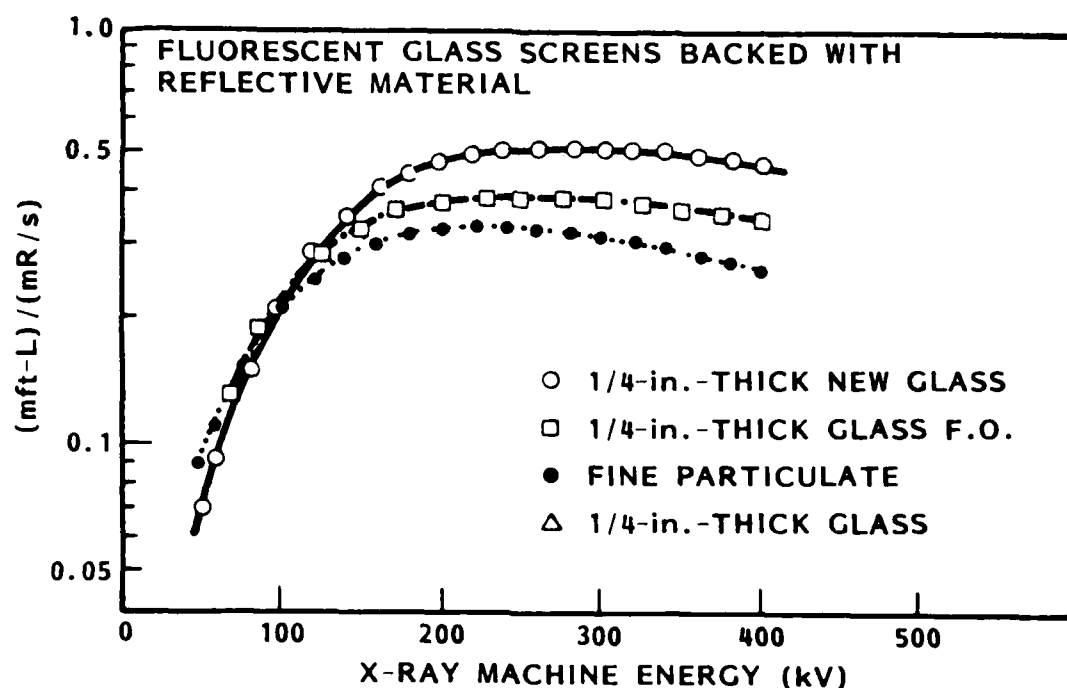


Fig. 29 Screen Efficiency Versus Tube Voltage

such that the smaller the value of C , the better the contrast sensitivity. The results of the low-energy (20 to 60 kV) analysis are given in Table 9.

The conclusion is that, above 100 kV, the new proprietary glass gives approximately twice the light output as other glasses and the high-resolution fine particulate screen. Below 100 kV, the efficiency of the glasses drops off more rapidly than that of the particulate screens. At all energies, the spatial resolution of the glass is better than for particulate screens. Thus, in deciding the optimum screen to use, one must determine the required resolution, sensitivity, and kV required for the item being examined.

3.7 FIGURES OF MERIT CONVERTER PERFORMANCE

The figure of merit (FM) as defined in section 3.2.5 ($FM = MTF \times EQE$), although a function of both spatial frequency and tube voltage, provides a meaningful basis for comparing image-conversion devices.

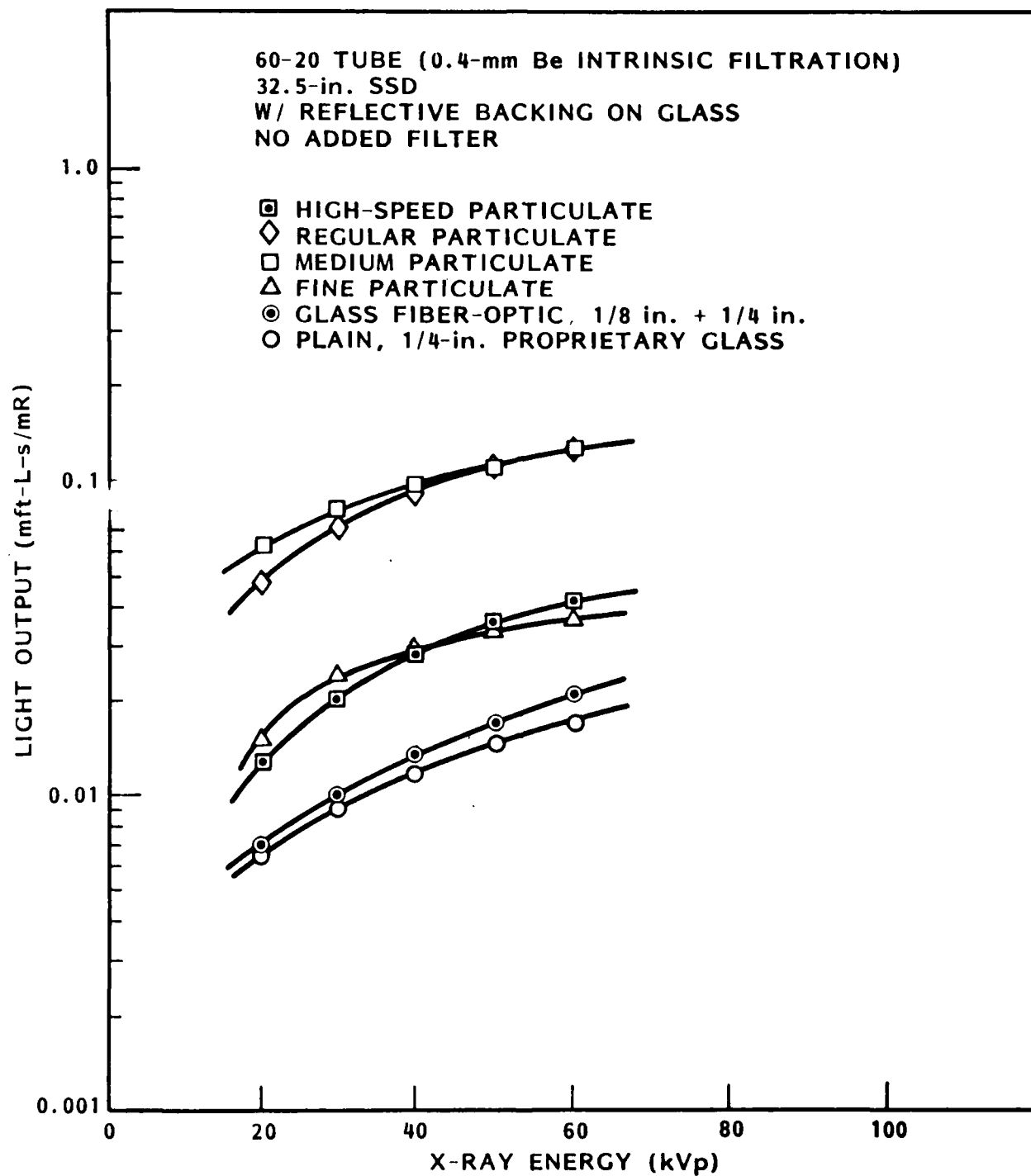


Fig. 30 Screen Light-Output Measurements

Table 9 LOW-ENERGY CONTRAST SENSITIVITY MEASUREMENTS

Exposure Screen	20 kV 15 mA	40 kV 5 mA	60 kV 3 mA
LMSC GLASS**	0.36	0.19	0.13
COMMERCIAL GLASS**	0.18	0.17	0.13
Fine Particulate	0.074	0.109	0.077
Medium Particulate	0.054	0.078	0.094

*Units are dimensionless, see text

**1/4-in.-thick glass with reflective surface

Figure 31 shows FM versus spatial frequency for four of the converter screen materials evaluated under this contract.

The fine particulate screen has the best FM for spatial frequencies below 6 lp/mm; the commercial glass plate has the best FM for frequencies above 6 lp/mm.

The regular FM for the gadolinium oxysulfide (GOS) film is attributable to the small film thickness which reduces the EQE. Interestingly, the GOS curve nearly exactly parallels that of the commercial glass. It is believed that is a characteristic of the optical uniformity of the film and glass, and suggests that all luminescent materials that are free of optical imperfections have identical MTF curves and differ essentially only in their EQE curves.

A summary of the conclusion is given in Table 10. These considerations indicate that the RTR system should be of modular construction, allowing insertion of the screen that is optimum for the given application.

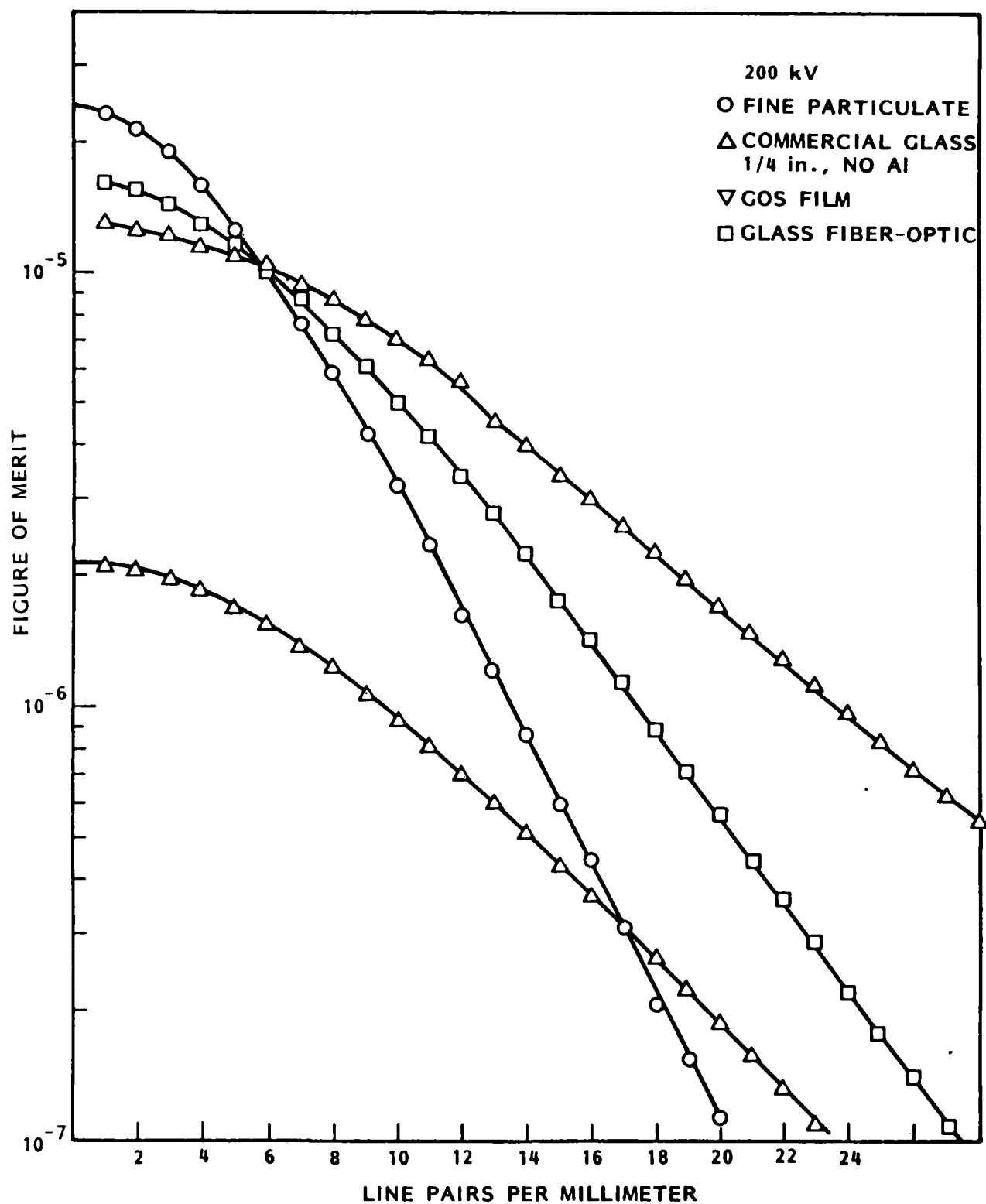


Fig. 31 Figures of Merit for Converter Screen Materials

Table 10 FIGURE OF MERIT CONCLUSION

Energy Range (kV)	Relative X-Ray Flux Available	X-Ray Converter Screen	Maximum Resolution Required (lp/mm)
100-300	High	Commercial Glass	24
20-100	High	Fine Particulate	20
20-300	Medium	Medium Particulate	10
20-300	Low	Medium Particulate	6

Section 4

TASK II - BREADBOARD RTR SYSTEM

In this phase of the program, a breadboard of a high-resolution real-time radiography system was constructed and performance tested. The breadboard system performance will be demonstrated for the NDT industry after this final report draft is due.

4.1 CONSTRUCTION OF THE BREADBOARD HIGH-RESOLUTION RTR SYSTEM

The first step in the construction of a breadboard RTR system was to derive a design philosophy from the program goals, requirements, and objectives. The design philosophy is that the operator will use the RTR system the same way a radiographer uses film. The radiographer reads a film x-ray image by first viewing the overall image and noting the essential features and flaws. The density range of the film usually requires lighting adjustments for observing the entire image. Then the radiographer reexamines the key features and flaws with magnification and amplifies his notes. This design philosophy led to the breadboard RTR system operating strategy.

The RTR breadboard will acquire an x-ray image of the object over the full field of view so the operator can observe the essential features. The operator will be able to improve the acquired overview image by adjusting the brightness and contrast and applying image-enhancement features which are available interactively from the image processor. The operator will position a square cursor on the screen to indicate each area of interest and will then magnify or zoom in to acquire a microview image of each interesting feature or suspected flaw. Optical magnification of the screen places all of the video lines in the microview and gives true magnification with more detail. The cursor location and size on the overview will indicate the area of interest being examined in the microview. The effective magnification will be

indicated on the display. Brightness, contrast, and image enhancements can also be applied to improve the perceptability in the magnified microviews.

The performance goals (Table 11) and the design strategy are the basis for selecting the individual subsystems of the breadboard RTR system. The critical components are the x-ray source, x-ray converter screen, lens, video tube and camera controller, camera and lens positioner, host computer, image-processor system, software, display, image printer, object positioner, and overall configuration.

4.1.1 X-Ray Source

The energy range to be tested (20 to 300 kVp) could not be produced in a stable manner by one x-ray source. By using three Sieffert x-ray sources, the entire range could be covered in a stable manner with maximum power and minimum focal-spot size.

Table 12 gives the x-ray source specifications. Using the Seifert 420-kVp system gave coverage from 70 to 300 kVp. Substituting the Seifert 160-kV system gave higher resolution due to the smaller focal spot but the output was not stable below 50 kVp. The Seifert 60-kVp system had to be used for 20 kVp to get enough power, but the focal spot is large. All three sources were used for 60 kVp to provide a comparison of how the inherent filtration, focal-spot size variations, and construction differences affected the image quality and performance data.

Table 11 BREADBOARD HIGH-RESOLUTION RTR SYSTEM PERFORMANCE GOALS

Features	Baseline	Actual
Energy Range	20 to 300 kVp	20 to 420 kVp
Resolution	>10 lp/mm	>20 lp/mm
Dynamic Range	1000	1000
Contrast Sensitivity	< 1 percent	< 1 percent
Area = 10 x 12 in.	25 x 30 cm	25 x 30 cm

Table 12 X-RAY SYSTEM SPECIFICATIONS

SEEFERT

ISOVOLT-PROGRAM

ISOVOLT EQUIPMENT				ISOVOLT TUBEHOUSINGS							
Type	Voltage kV	Range and stability of operation values		Exposure time min	Type 2)	Maximum tube voltage (kV)	Max. tube current (mA) at max. tube voltage		Effective focal spot size (mm)	Inherent filtration (mm)	Emergent beam angle
		Output current mA	Stability of current %				operating	range			
60/30	60 and 30 kV in steps of 1 kV	max. 50 limited by type of tube starts at 1 mA ± 0.5%	∞ and 0.3 - 12	60/30	60	—	20	—	12 x 15	0.4 mm Be	30°
160 M1	160 and 100 kV in steps of 10 kV	1.25 ± 0.3% in steps of 1 mA	∞ and 0.1 - 99.9	160 M1	160	4	19	0.4 x 0.4	30 x 30	10.8e	40°
420/10	420 and 100 kV in steps of 1 kV	1.25 ± 0.3% in steps of 1 mA	∞ and 0.1 - 99.9	420/10	420	4	10	18 x 18	45 x 45	70.8e	40°

1. All equipment of the ISOVOLT line the control AS 2 is
 2. Any tubehousing used with one of the ISOVOLT models
 can be used with any controls of the same model
 3. The tubehousing 60/25 was designed for the inspection
 of extremely low absorbing workpieces (such as CFK
 materials). Tubehousing 60/25 combined with one of our
 X-ray diffraction units of the ISO DEBYEFLEX line give an
 excellent operational range

4.1.2 X-Ray Converter Screen

The x-ray converter screen had to provide a minimum resolution of 10 lp/mm, a dynamic range of at least 1000, and a contrast sensitivity of 1 percent or better, cover an area of 12 x 10 in., and give enough light intensity for the video camera to function. The screen chosen was the medium particulate, which barely met all the requirements. Other screens and glasses (shown in Table 10) offer advantages for specific applications and should be implemented as required. Since screen changes were imminent, the screen mount was designed so the screens could be interchanged.

4.1.3 Lens

The lens couples the light emitted by the x-ray converter screen to the video camera. The light-collection efficiency of the lens is low. For a particulate screen, the light is emitted in a Lambertian distribution. A lens that is 3.37 in. in diameter and 30 in. from the screen has an efficiency given by

$$E = \frac{D^2}{4L^2} = \frac{(3.37)^2}{4(30)^2} = 0.0032$$

The collection efficiency is further reduced by transmission efficiency of about 80 percent to give an overall efficiency of 0.25 percent. For a glass screen, the distribution is non-Lambertian so the efficiency is more difficult to compute. The result for glass screens is also a small number. This makes the lens the least efficient element in the imaging chain; therefore, it is very important to use a state-of-the-art lens. The lens selected is a 60-mm focal length, f/0.7 as described in Table 13. This lens gives very low distortion and is frequently used on Real-Time Radiographic (RTR) systems. The lens is shown mounted on the video camera in Fig. 32. The bellows between the Isocon and lens have been removed to clarify the view.

Table 13 LENS SPECIFICATION, LENS 60-mm f/0.7

Specifications (Calculated by wavelength e-line)	
Focal length	60.15 mm
Maximum relative aperture	1:0.69
Lens construction	8 components, 9 elements
Magnification	-1/7.8
Object-to-image distance	689.38 mm (at best focus point) (27.15 in.)
Wavelength range	
for color correction	400 - 700 mμ
Image format covered	45 mmφ
Angular field of view	36.7° (at best focus point)
Clear aperture of front glass	85.8 mmφ
Clear aperture of rear glass	44.4 mmφ
Overall length	
lens only	161.6 mm
from front vertex to focal plane	166.08 mm
Back focal distance (-)	-4.37 mm (in air) (0.172 in.)
Distance from front vertex to front principal plane	4.45 mm
Distance from rear vertex to rear principle plane	64.517 mm
Optical interval	
for two principal points	92.83 mm
Glass compensation (face plate)	3.4 mm (Ne = 1.51825)

This fixed-focal-length (nonzoom) lens can be adjusted for various fields of view by varying the screen-to-lens distance (Z-F) and the low light level camera photocathode-to-lens distance (F). The camera-to-screen distance is Z. Figure 33 shows the relationship between field size, Z-F, and F. The adjustment of field size and focus requires a complex control system and is



Fig. 32 Side View of Lens Manipulator System

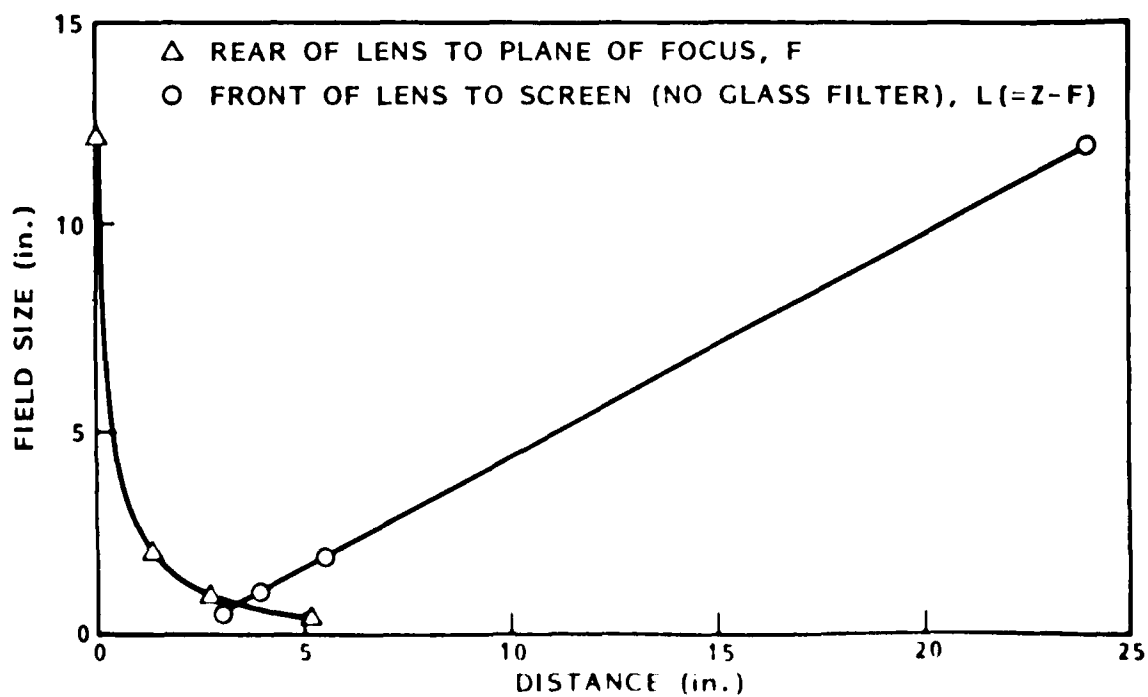


Fig. 33 Requirements to Focus Lens for Each Field Size

implemented with two-axis digital position controllers interfaced to the host computer. The operator selects the field size and the computer directs the movement. The operator can make fine adjustments with a two-axis joystick control. The details of this part of the camera positioners are discussed in section 4.1.5.

As the field of view is reduced, the brightness of the light illuminating the Isocon photocathode is reduced by

$$B_M = \frac{B}{(M + 1)^2}$$

where

- B = the brightness of the scene at infinite distance, ft-L
- B_M = the brightness of the magnified scene, ft-L
- M = magnification = image size/object size, no units

In bright scenes the camera's automatic gain control compensates for brightness changes due to magnification changes. For high magnifications, the reduction in light exceeds the camera's gain range. Thus, more x-ray flux is required for high magnifications to avoid a noisy image.

4.1.4 Camera

Several video-camera candidates were tested for resolution as a function of scene brightness, as shown in Fig. 34. The Isocon image tube in a Penn Video camera and control unit was selected due to its superior resolution and low-light-level capabilities. Image Isocon tubes are available from RCA and ITV. Figure 35 gives some Isocon performance data. The Penn Video camera and controller was designed to work with Isocon image tubes. Penn Video supplies special functions such as shading and thermal control, as shown in Table 14. The combined performance definitely meets the breadboard performance goals. At 10^{-5} ft-L, the Isocon gives a horizontal resolution of 800 TV lines. At

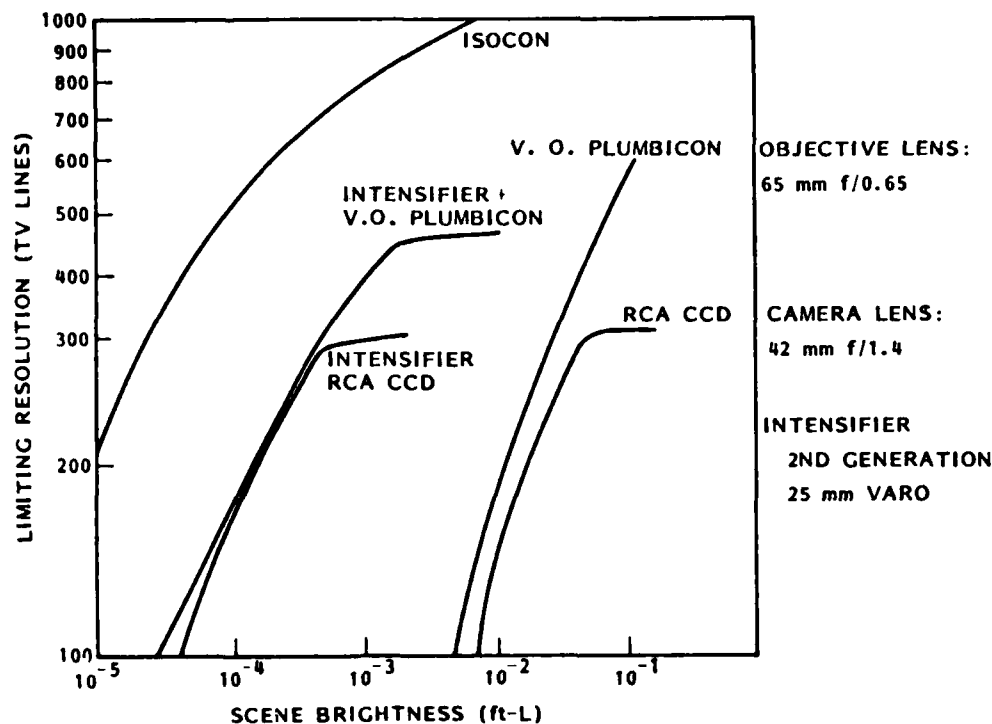


Fig. 34 Limiting Resolution Characteristics of Low-Light-Level Cameras

10⁻² ft-L, well over 1000 horizontal TV lines are visible, and it is common to get over 1200 horizontal TV line from Isocon cameras.

The vertical resolution was limited to 525 lines at 30 frames/s by the camera controller circuitry, the bandwidth of the video digitizer, and the image-processor synchronization. To get the correct vertical resolution, the Isocon camera was modified by Penn Video to produce twice as many vertical lines, or 1050 lines. To keep the bandwidth and sampling rate of the video digitizer the same, the frame rate was adjusted to 7.5 frames/s. The bandwidths are:

$$512 \text{ pixels horizontal} \times 512 \text{ pixels vertical} \times 30 \text{ frames/s} = 7,864,320 \text{ pixels/s}$$

$$1024 \text{ pixels horizontal} \times 1024 \text{ pixels vertical} \times 7.5 \text{ frames/s} = 7,864,320 \text{ pixels/s}$$

Performance Characteristics Range Values[§]

With conditions shown under Typical Operating Values, picture highlights at knee of the light transfer characteristic, 525 line scanning, interlaced 2:1, frame time of 1/30 second, and 1.4" (35.5 mm) picture diagonal with 4x3 aspect ratio.

	RCA C21204			
	Min.	Typ.	Max.	
Photocathode Radiant Responsivity at 400 Nanometers	—	80	—	mA/W
Photocathode Luminous Responsivity (2856 K tungsten source) [†]	60	100	—	μA/lm
Signal-Output Current (Peak-to-peak) [§]	4	7	—	μA
Photocathode Illumination at 2856 K Required to Reach "Knee" of Light Transfer Characteristic	—	.02	.03	lm/ft ²
Photocathode Irradiance at 400 nm Required to Reach "Knee" of Transfer Characteristic	—	1.4x10 ⁻⁴	—	W/m ²
Signal-to-Noise Ratio [‡] :				
Signal to noise-in-signal for highlights	36	38	—	dB
Highlight signal to dark current noise	46	—	—	dB
Amplitude Response (Contrast transfer) at 400 TV Lines Per Picture Height (Per cent of response to large-area black to large-area white transition) [¶]	70	85	—	%
Limiting Resolution:				
At center of picture	950	1200	—	TV Lines
At corner of picture	800	950	—	TV Lines
Lag-Per Cent of Initial Signal Output Current 1/20 Second After Illumination is Removed	—	5	10	%
Shading (Uniformity) [¶] :				
Black level:				
Variation of output current with tube capped (per cent of maximum highlight signal)	—	1	3	%
White level:				
Variation of highlight signal (per cent of maximum highlight signal)	—	15	20	%

Spurious Signal (Blemish) Tests

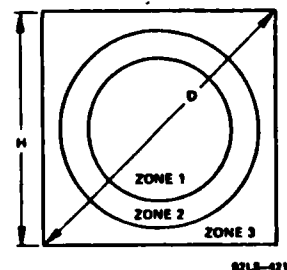
This test is performed using a uniformly diffused white test pattern that is separated into three zones as shown in Figure 1. The tubes are operated under the conditions specified under Typical Operating Values. The tubes are adjusted to provide maximum picture resolution. Spurious signals are evaluated by size which is represented by equivalent numbers of raster lines in a 525 TV line system. Allowable spot size for each zone is shown in Table. To be classified as a spot, a contrast ratio of 1.5:1 must exist for white spots and 2:1 for black spots.

Equivalent Number of Raster Lines	Zone 1 Allowed Spots	Zone 2 Allowed Spots	Zone 3 Allowed Spots
Over 6	0	0	0
Over 4	0	0	4
Over 1	2	6	10
1 or less	•	•	•

Minimum separation between any 2 spots greater than 1 raster line is limited to 16 raster lines.

*Spots of this size are allowed unless concentration causes a smudged appearance.

C21203, C21204



C21203A, C21204A

D: Active Target Diameter

H: Raster Height (4x3 Aspect Ratio)

Zone 1: Diameter = H/2, Area ≈ 15%

Zone 2: Diameter = H, Area ≈ 45%

Zone 3: Area ≈ 40%

Figure 1 — Spurious Signal Zones

Fig. 35 Isocon Image Tube Performance

Table 14 PENN VIDEO ISOCON CAMERA FUNCTIONS

+500-V Regulator
 -900-V Regulator
 Focus Regulator
 Thermal Limit
 Horizontal Control
 Vertical Deflection
 Sync Generator
 Shading Line Driver
 Shading A Board
 Shading B Board
 Shading C Board
 Shading Mixer
 Pedestal Control
 Video Processor
 Camera Control Unit
 Preamp
 Cathode Blanking
 H. V. Regulator
 Horizontal Deflection
 Camera Head

Corresponding modifications were required in the video digitizer, image processor, and software.

Assuming that four pixels are required to distinguish one line pair (lp) without aliasing in a digitized image, we can calculate the theoretical resolution of the modified camera versus field of view for two light levels, as shown in Table 15. The 800 TV lines correspond to a light level of 10^{-3} ft-L, and 1024 lines to a light level of 10^{-2} (from Fig. 34). It can be seen that zooming to a 1.0-in. field of view should produce the desired spatial resolution of 10 lp/mm.

Table 15 RESOLUTIONS FOR 800 AND 1024 TV LINES FOR VARIOUS FIELDS OF VIEW

Field of View (in.)	Resolution (lp/mm)	
	For 800 TV Lines	For 1024 TV Lines
0.4	19.6	25.2
0.5	15.7	20.2
1.0	7.9	10.1
1.5	5.2	6.7
2.0	4.0	5.0
3	2.6	3.4
4	2.0	2.5
6	1.3	1.7
8	1.0	1.3
10	0.8	1.0
12	0.7	0.8

Other minor modifications were also made to the camera in order to cool it. The standard blower did not move with the camera as it was moved around by the manipulator. A muffin fan fitted to the back of the camera has provided adequate vibration-free cooling. Extra care was taken since the camera is sensitive to microphonics under some circumstances.

Since the camera faces the x-ray source, it is shielded within a 1/8-in. lead jacket and the lens system is protected with a leaded glass filter, 1 cm thick, which also contributes to the shielding for the camera. Experiments have shown that, at energies less than 400 keV, the shielded camera system can tolerate head-on exposures. In the past, some glasses have required periodic treatment to eliminate hazing effects of long-term large radiation dosages.

4.1.5 Camera Positioner

The breadboard camera positioner consists of an X-stage, Y-stage, Z-stage, and F-stage. The X-stage positions the camera horizontally with respect to the x-ray converter screen. The Y-stage positions the camera vertically. The

Z-stage adjusts the camera-to-screen distance which adjusts the field of view. The F-stage adjusts the focus by adjusting the isocon image tube photocathode-to-lens distance. All of the stages use dovetail ways and are driven by a lead screws with antibacklash nuts.

A Compumotor stepper motor with digital controllers actuates the lead screws to form a precision 4-axis digital positioning system. It is capable of positioning a 200-lb load within ± 0.001 -in. reproducibility and within 0.008 in. of the absolute position. The actual load is about 120 lb worst case. The layout is shown in Figs. 36 and 37. All axes have limit switches which deactuate only the axis and direction causing a limit condition.

The Compumotor digital controls can control position, speed, acceleration, and deceleration. Control is by preset thumbwheel switches, two-axis joysticks (X and Y on one and F and Z on the other), or as commanded by the host computer. The interface to the host computer is through a serial RS232 interface daisy chained to all four Compumotor controllers, as shown in Fig. 38.

4.1.6 Host Computer System

The host computer interfaces include the image processor, positioners, memories, and the operator. Its functions are interpreting the operator's commands, calculating positioning commands, and directing image acquisition, processing, storage, and retrieval.

Since these functions are relatively straightforward, the most important considerations in selecting a host computer are the availability of peripheral devices, interfaces and drivers, software support, and the suitable image-processing hardware and software. The most heavily supported, most widely used scientific host computers with compatible image-processing subsystems are the Digital Equipment Corp (DEC) minicomputers such as the DEC LSI 11/23. A SMS 1000 computer package including the host was acquired from Scientific Micro Systems (SMS). The SMS 1000 includes a 40-Mbyte 5-1/4-in. Winchester, an 8-in. floppy, a Q bus interface to the image processor, and series RS232 ports for control, monitoring communications, and a terminal. A



Fig. 36 Top View of Manipulator

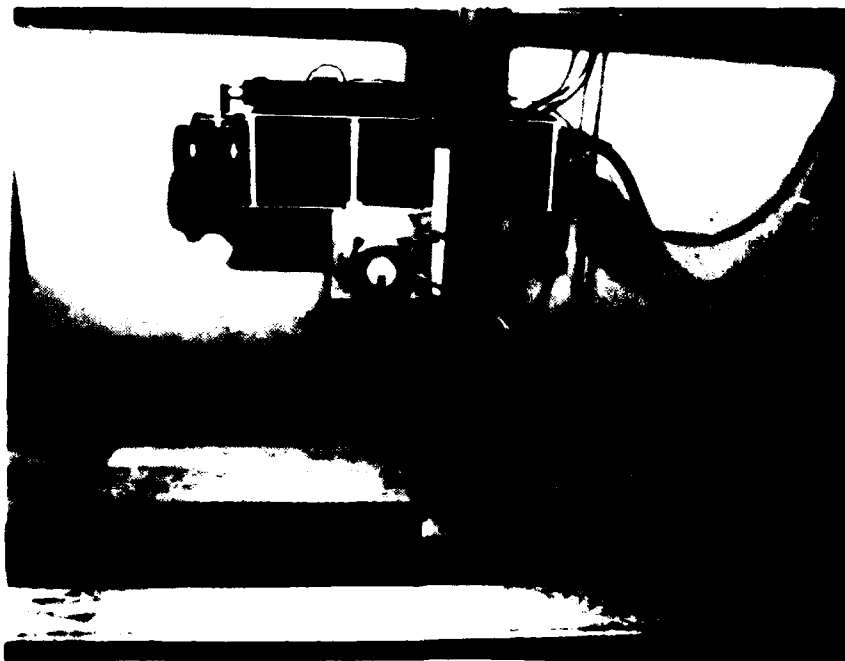
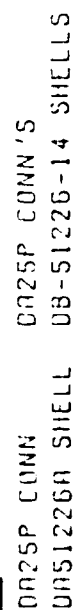


Fig. 37 Side View of Manipulator



block diagram of the SMS 1000 is shown in Fig. 39. The host is shown in the upper part of Fig. 40.

Each image is 1024 x 1024 pixels x 3 bits per pixel or 1 Mbyte per image. This means only 39 images plus software can be stored on the Winchester. This number was deemed adequate for breadboard testing. An image can be transferred to a pair of floppy disks for digital archiving. Floppies are very inefficient and not cost effective, since each floppy holds only 615,424 bytes formatted.

4.1.7 Image Processor

The image processor operates on 1024 x 1024 pixels per image and at least two image buffers are needed for the breadboard system. The image processor system selected is a Recognition Concepts, Inc. RC-1 Image Board, as shown in Fig. 40. A block diagram of the system is shown in Fig. 41. The system contains memory management, image display controller, digital-to-video converter, pipeline image processor, histogram module, formatter module, video digitizer, video input options, digital interface ports, video look up tables, annotation overlay, cursor generator, interactive controller, image processor, software, and diagnostics.

The memory is segmented into 4 buffers. Each buffer is 1024 x 1024 pixels with 16 bits per pixel. The memory is organized as follows: Buffer 1: 1024 x 1024 pixels/image with 16 bits per pixel. Buffer 2: 1024 x 1024 pixels/image with 16 bits per pixel. Buffer 3: 1024 x 1024 pixels/image with 16 bits per pixel. Buffer 4: 1024 x 1024 pixels/image with 16 bits per pixel.

The image display controller selects the image to be displayed and generates its corresponding video output. It determines the position of the image on the screen and moves them in x and y directions.

The digital-to-video converter takes the image data from the image display controller, modifies it with overlay, histogram, and other features, and generates an analog video output.

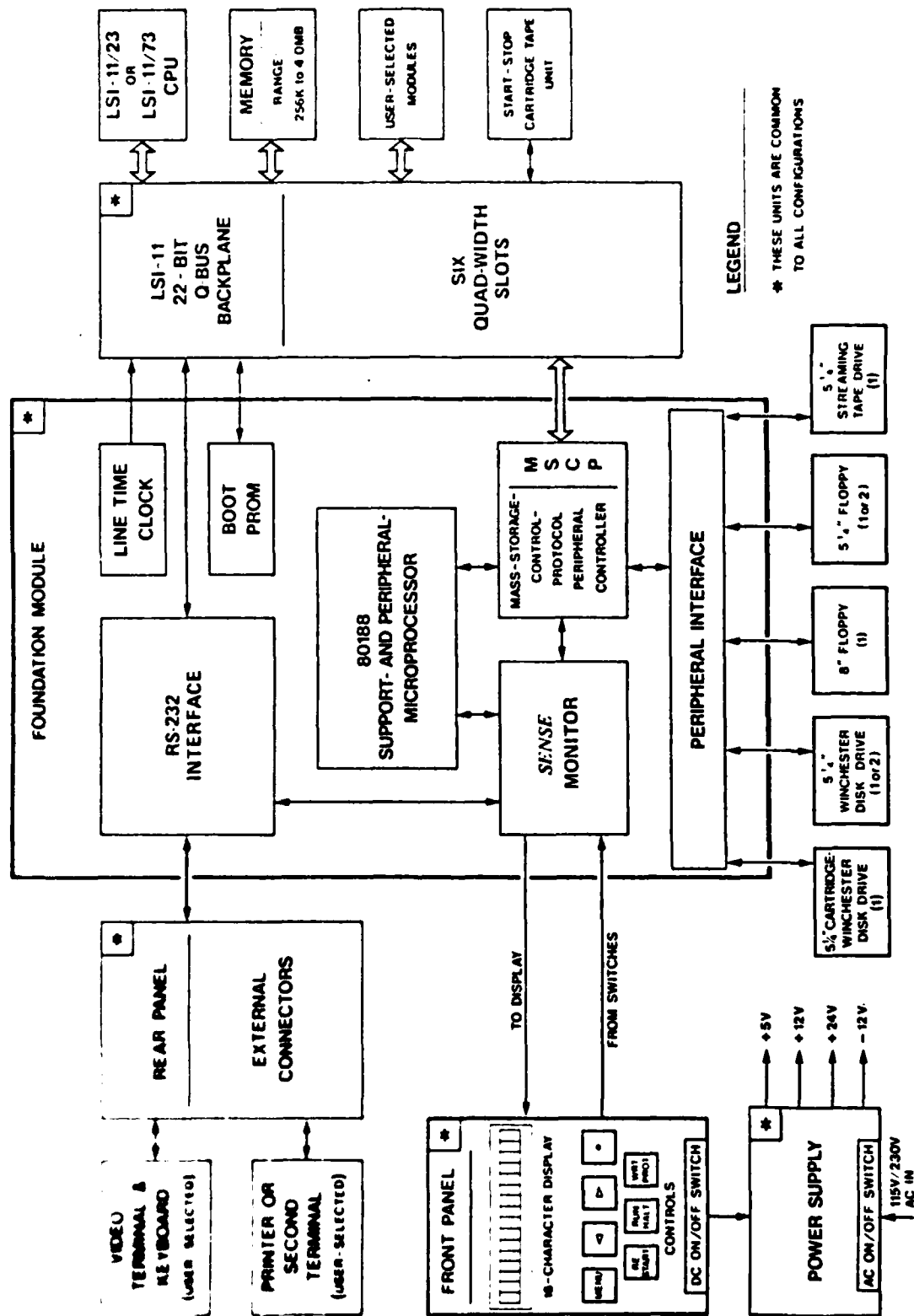


Fig. 39 Functional Block Diagram of the Computer System



Fig. 40 Front View of Computer and Image Processor

The pipeline image processor (PIP) takes advantage of the 12-Mbytes/s data throughput of each of the image data channels by providing input and output data selection, arithmetic and Boolean operations, and true 8x8 multiplication of image data from image memories, external digital input, video signal digitizers, or selected constants. Each of these complex operations can be done on one or two entire images in a single frame time or 1/30 s (33.3 ms). Combinations of PIP functions do image processing such as edge and feature enhancement, image smoothing or sharpening, interpolated zoom, spatial convolutions, and functional mapping operations such as log-antilog division and transcendental functions.

The histogram module permits the acquisition in a 256-level histogram of an 8-bit image in two video frame times (66.6 ms).

The formatter module speeds spatial resolution reduction in order to employ image memory for a larger series of images such as in animation and multiview imaging.

The video digitizer adjusts the gain and offset of a 525-line video input signal and then converts it to digital data at 30 frames/s. Each frame time, a 512 x 512-pixel image is produced in digital memory with 8, 10, or 12 bits of precision. The video digitizer was modified for the RTR breadboard to digitize a 1050-line video input and produce a 1024 x 1024-pixel digital image at 7.5 frames/s. This maintains the nominal average digitizing rate and bandwidth. Noise can be further reduced by integrating the images as they are required.

Video input options facilitate digitizing external video sources such as video tape by providing a time base corrector, phase-lock loop, and external video synchronization.

The digital port interface provides a flexible mechanism for acquiring digital data in a wide variety of formats up to 2048 x 2048 and nonstandard data rates up to 12.5 Mbytes/s. External synchronization signals are used to direct both image format and transferring image data.

Video look-up tables are used to scale the digital intensity value of the entire image in a single frame time. They are available in sizes from 256 x 8 bits up to 4096 x 16 bits. The tables can be loaded from a software file, manually by the joystick, or automatically by a program involving a histogram- optimization algorithm.

The annotation overlay provides 80 columns or 25 lines on alphanumeric image annotation in black, white, or colors as appropriate.

The cursor generator provides two cursors overlaying the image field, which may be independently rendered visible or made to blink. The cursors can take the form of a rectangle, full-screen crosshairs, or small crosshairs. The position may be controlled by the joystick or under software direction and the coordinates may be read or written.

The joystick (or trackball) is a two-axis controller with additional push-button switches and a potentiometer. Example functions include interactive adjustment of brightness and contrast, positioning the cursor to indicate the area of interest to perform a histogram or profile, or roving with a magnified view in a large digital image.

The pixel processor, designated VPP, is a self-contained microcomputer for high-speed access and processing of pixel values in an image memory. It is useful in generating vector displays and calculating intensity profiles.

RCI and TAU provide comprehensive software package called RTIPS (real-time image processing software), which will be discussed in section 4.1.8.

4.1.8 Software

The software is under the control of the Digital Equipment Corporation (DEC) operating system RT-11 which is designed for a single user doing real-time control and computation. RT-11 is an old operating system which has been largely replaced by RSX-11M and VMS operating systems for multiusers, but RT-11 is adequate, extremely well supported, and already in use for other projects in the LMSC Lab. The DEC 11/23 host computer used a Fortran compiler.

Recognition Concepts, Inc. and TAU, Inc. provide comprehensive real-time image-processing software (RTIPS) packages for the Trapix image-processing system. Based on convenient, mnemonic commands, the RTIPS system provides the user with facilities to capture, process, store, and retrieve images. Image-processing operations may be concatenated into complex series or

tailored to a particular application, by either building a command file of the desired complexity or invoking the function as subroutines in a master program.

The software written for the high-resolution RTR breadboard system encompasses the design strategy of having an overview and microview. The major functions of the software are:

Manual Operation. The menu is used in manual mode to acquire an overview image. The RTR system is then zoomed in to acquire microview images with the size and location controlled interactively by the operator using the joystick and menu. The location and area being examined in the microview are shown on the overview. Image processing such as controlling the brightness, contrast, and edge enhancement can be applied by the operator.

Automatic Operation. A programmable automatic scan plan divides the overview into grids of any field size from overview to microview. The operator then chooses the grids of interest and programs them to be raster scanned in a back-and-forth fashion. It will also perform any of the image-enhancement methods available in the software as it scans. This is a very useful technique for laborious repetitive inspection procedures.

Initialization. Initialization sets the system parameter, such as manipulator speed, overview field size, microview field size, and type of image-acquisition algorithm, such as pairs subtraction. It works with manual positioning and then resets the position registers to zero. This process can be automated.

Overview. The system automatically moves to the overview location, which can then be adjusted by the operator. A 1024 overview image is acquired and stored. A 512 overview is displayed by averaging 4 pixels.

Define Microview. The operator positions the microview. A 1024 microview is acquired. The display shows the center 512 pixels. A cursor box on the overview will indicate the size and location of the microview and the area

being viewed. Field-of view and location tables and equations are being defined for this purpose.

Microview. Previous image files must be manually erased before starting. An automatic overwrite will be incorporated. The microview location being viewed is automatically indexed through a two-dimensional array of microviews with selected X and Y distance intervals. The image must be viewed by retrieving them and using the image processing mode.

Microview Pairs Scan. Microview pairs scan is the same as scan microview, except pairs of images separated by DX and DY are acquired, subtracted, and stored.

Hyper Scan. Hyper scan simply remembers a series of microviews and acquires them serially.

Image Processing. Image processing is determined by the operator manually.

Roaming Magnification. Roaming with magnification will be done mechanically with the X, Y, Z, and F manipulators.

4.1.9 Displays

The video display monitors used on the high-resolution RTR breadboard system varied in resolution from about 500 lines to over 1200 lines. The particular RCI Inapix 55128 image processor being used supported only 512 x 512 pixel/image with 8 bits/pixel video output. To display a 1024 x 1024 pixel/image file, it is necessary to either subsample the image to get a displayable file or show only one quadrant of the 1024 x 1024 image at a time. Both display compromises eliminate most of the advantage of the high-resolution overview. To get around this problem during breadboard evaluation, the overview was examined with full resolution by quadrants to locate areas of interest. Then the entire subsampled overview is displayed to show the location of the microview being examined.

The microview must also show a 512 x 512 subsection of the 1024 x 1024 pixels/image being acquired. The breadboard microview is displayed by showing the center of the microview data. This shows an image with less area than would be visible with a higher resolution monitor, and therefore it only slows down the operator in examining microviews.

The displays are all monochrome since monochrome offers the best resolution, brightness, contrast range, and since pseudocolor in high-quality x-ray images is considered distracting by most radiographers.

A very-high-resolution display system, being tested by LMSC under an LMSC-funded research program, will be used for the industry demonstration. The Azuray Inc. 2048 x 2048 pixels/image with 8 bits/pixel display system gives virtually film quality resolution with very good brightness and contrast due to its unique eight-electron-beam CRT.

4.1.10 Video Image Printer

The Honeywell Video Graphic Recorder, Model VGR 4000 (Fig. 42) is used to print breadboard RTR images with 512 x 512 pixels/image. The video graphic recorder produces an 8.5 x 11-in. black-and-white page or continuous-tone image copies from static sources of video raster scan data. Conductive-backed dry silver media in roll form produces records as single-page copies. A single fiber-optic cathode-ray tube, maintaining direct contact with the photographic media, produces all data traces. The copy time is 14 s, including a 4-s thermal development. The image density can vary from 0.2 to 1.4 optical density units (ODU) with a resolution of 5.9 lines/mm at 1.0 ODU. At 60-Hz field rate, it accepts interlaced video up to 1119 lines per frame and noninterlaced video up to 665 lines per field. The video output from the Trapix image processor was limited to 525 lines, so no attempts were made to print images with a 1024 x 1024 pixel image.

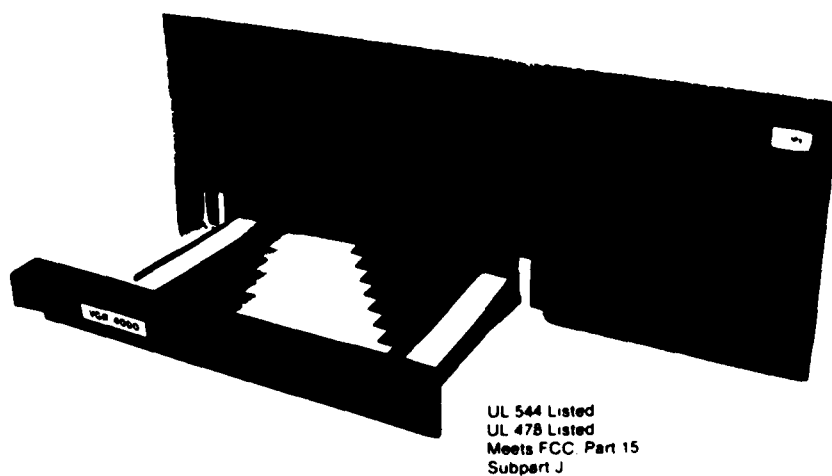


Fig. 42 Honeywell Video Graphic Recorder

4.1.11 Object Positioner

The object being x-rayed has to be supported and positioned by translation in the X and Y axes. In many cases the object also needs to be rotated or aligned interactively. The breadboard camera enclosure was originally planned to be supported by a large laboratory jack. The camera moved vertically to align with the fixed height of the object and the x-ray source. This arrangement was found to be unstable and was modified. The camera positioner is independent of the object positioner and was unaffected.

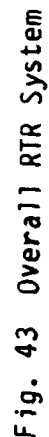
The breadboard camera enclosure is mounted on a fixed-height table. The object positioner and x-ray source are mounted on the laboratory jack. The x-ray source is elevated to align with the center of the x-ray converter screen. The object positioner adjusts the position of the object in the X and Y axis and rotates about the Y axis. It is manually controlled with push-button switches and speed-control potentiometers. Because the positioner is not under computer control, positioning is not reproduceable. Future object positioners should have digital as well as manual positioning capabilities and include rotation about the X axis.

4.1.12 Overall Configuration

The overall system, shown in Fig. 43, includes the x-ray source, object positioner, and camera enclosure in the shielded x-ray room, with cables running to the operator's console outside the x-ray room.

The x-ray source is fixtured for a horizontal beam with the fixture on the laboratory jack. The jack height is adjusted so the x-ray beam is aimed directly at the center of the x-ray converter screen, which is vertical on the end of the breadboard camera enclosure.

The object positioner is on the laboratory jack between the x-ray source and x-ray converter screen, near the screen. This allows the object being examined to be translated in the X and Y axes and rotated about the Y axis. The camera enclosure contains the 4-axis camera positioner on the horizontal base. The isocon camera is mounted on the camera positioner and is aimed toward the x-ray converter screen which is on the end of the camera enclosure. The 4 x 4 x 8 ft camera enclosure is constructed from plywood with two-by-four and angle-iron bracking. Tape and black drapes were required to make the enclosure light-tight when required. The x-ray converter screen mount shown in Fig. 44 provides relatively quick changing of screen materials. Since the isocon camera has many cables, a festooning system is mounted on the inside top of the enclosure to allow movement as shown in Fig. 45. The camera waste heat is dissipated into the air in the camera



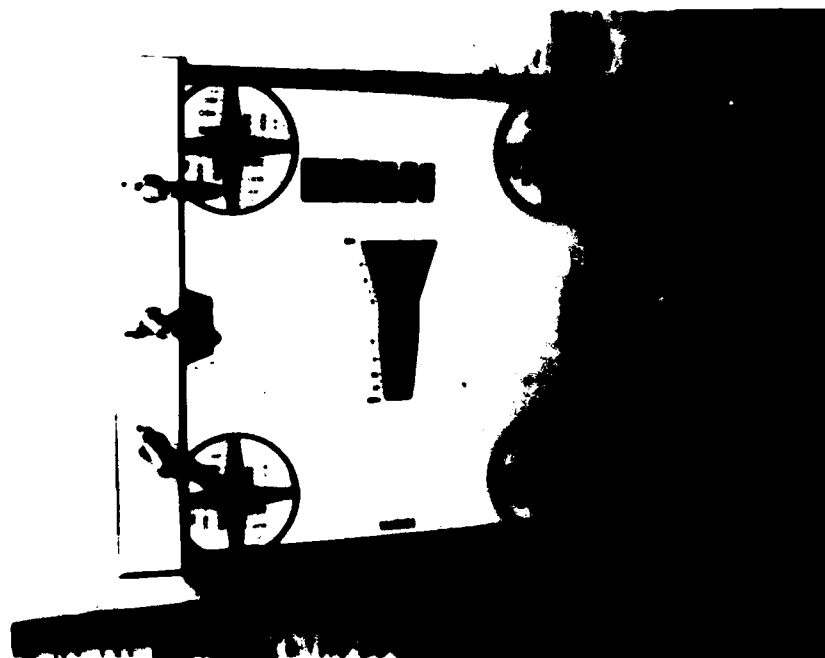


Fig. 44 Back View of Fluorescent Screen Bulkhead



Fig. 45 Front View of Fluorescent Screen Bulkhead

care must be taken not to induce microphonic noise when the camera is moved. The camera enclosure has been operated in our laboratory for over 100 hours without overheating.

The camera system are given in Fig. 46. The cables connecting the operators console include eight video cables, two camera cables, one multiconductor cable for the video camera controller cables, and an antenna cable.

In addition to the x-ray controllers, the computer controllers for camera positioning and the Trax image processor, the system includes a VG4000 video image printer, the video camera, two monochrome video display units, and optionally a videotape recorder.

The x-ray converter screen, the RTR system. The resolution as a function of field of view, the techniques, procedures, and optimization was done for film exposure geometry. The same exposure geometry was used for x-ray images of penetrameter wedges were taken with the RTR system. Comparisons indicated the

analog output was about 1250 lines at the center of the image and about 950 lines at the edges of

NO-A187 187

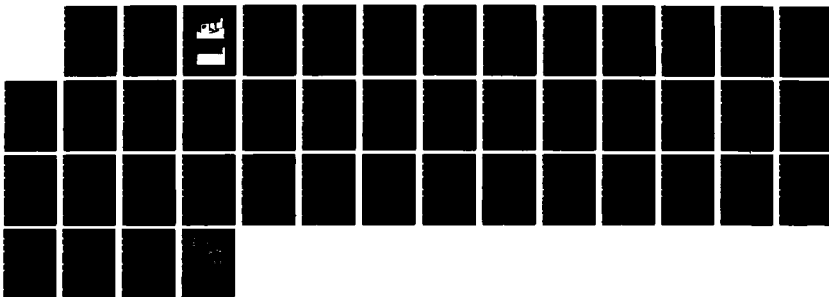
HIGH-RESOLUTION REAL-TIME RADIOGRAPHY (RTR) SYSTEM
DESIGN(UD) LOCKHEED MISSILES AND SPACE CO INC PALO ALTO
CA RESEARCH AND D L M KLYNN ET AL JUL 87
LMSC-D067282 AFMAL-TR-87-4035

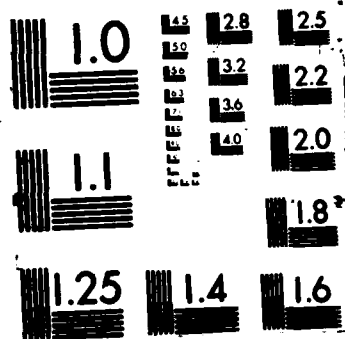
2/2

UNCLASSIFIED

F/G 14/2

NL





		REP RATE			
	CKI	FREQ.	PERIOD	PULSE	
COMP	HD	5555.5	118US	10.2US	
	VD	7.353	136MS	11MS	
	II	BLNK	2237.14	470US	350US
COMI	V	BLNK	7.353	136MS	124MS
	V	SYNC	7.353	136MS	3.6MS
	II	SYNC	5555.5	118US	8.4US

SYS: 1015 X 1015 LINES

FIELDS/FRAME 1-1

CAMERA: W/1 TUBE S/N

BEAM -40.3
G4 224
A 241
B 203
SEP 96.9
G2A 84.4
PC (-785)
AL1 1.79
AL2 -1.08
TGT 2.29

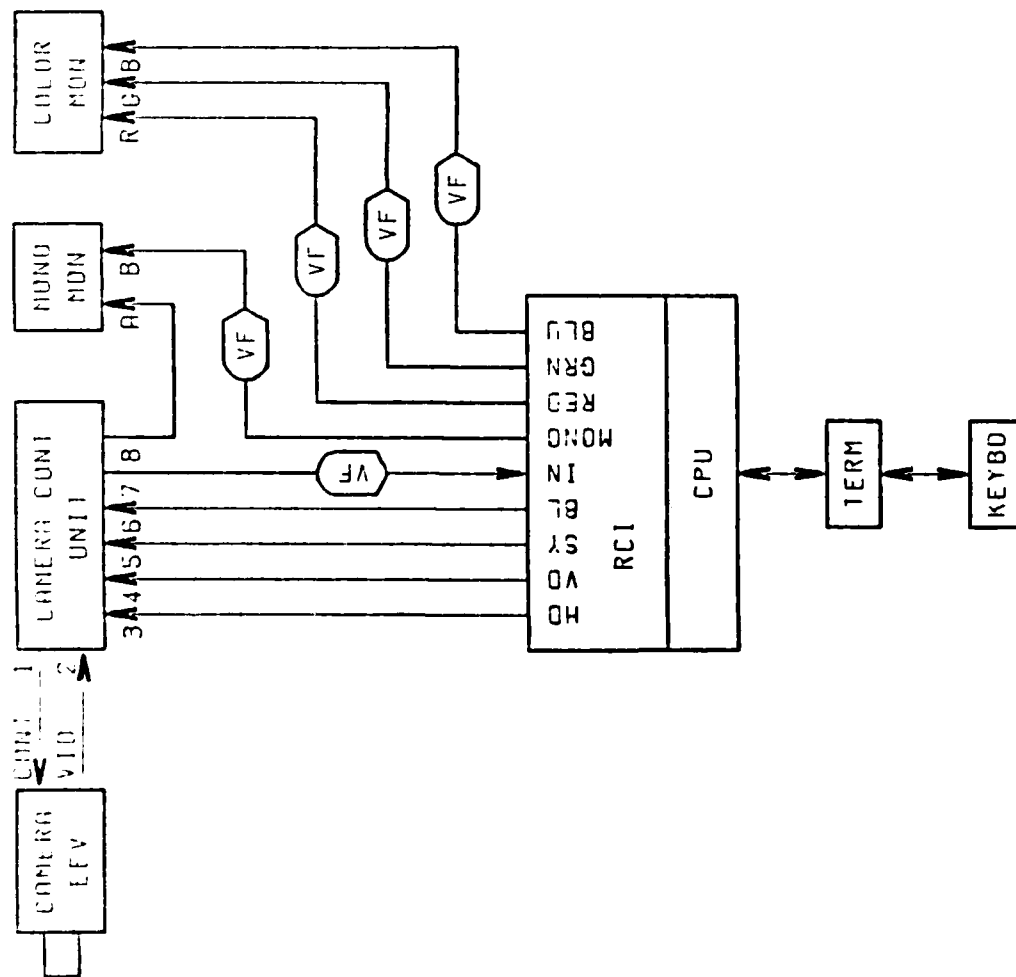


Fig. 46 Computer, Camera, and Operator Console Electrical Wire and Cable Interconnect Configuration



Fig. 47 Front View of Operator's Console Work Area



Fig. 48 Front View of Indexers and Joysticks for X, Y, Z, and F

the image. The 1024 x 1024 pixel/image data acquisition captures these resolutions in digital form. The vertical resolution is limited by the number of lines which is 1024 in this case. The standard resolution RTR system has the same high horizontal resolution but is digitized to 512 x 512 pixels/image. For the same field of view the 1024 image show about twice the resolution as the 512 x 512 pixel images. However, by zooming-in, the optical magnification on the standard 512 line RTR system can be adjusted to give the same resolution as the 1024-line RTR system. This holds true for fields of view larger than one inch and is therefore acceptable for these performance tests where the smallest objects are penetrameters about 2 in. long.

The 512 x 512 pixel/image system was tested with a medium particulate screen by inspecting a Funk grid MTF lead target. The x-ray generator was 80 kVp, 8 mA. The x-ray tube had a 0.4-mm focal spot and 1.0 mm of beryllium inherent filtration. The x-ray tube was tilted about 10 deg toward the x-ray beam's heel to reduce the effective focal spot size. The focal spot-to-screen distance was 33 in. and the object-to-screen distance was about 1 in. The modulation on the 10 lp/mm bars was visible with a 0.4-in. field of view only after integrating 256 frames and then increasing the display contrast by a factor of 10 or more.

Practically speaking, the 512 x 512 pixel/image RTR system is much better supported by auxiliary subsystems such as real-time analog display monitors, a video waveform monitor, a video tape recorder, video image printer, and numerous image processing enhancement algorithms. Even though the system resolution was marginal with the 512 x 512 pixel/image RTR system it was used for all remaining comparisons. This is acceptable because it was shown that the 1024 x 1024 pixel images give about twice the resolution. All of the support subsystems can be acquired or built for 1024 x 1024 pixel images when a production system is assembled.

4.2.2 Dynamic Range

A dynamic range of 1000-to-1 for film means that objects are perceptible over a range of light intensities of 1000-to-1 or 3.0 optical densities units. A

representative dynamic range measurement was made at 100 kV for the 512 x 512 pixel/image RTR system and for film, by inspecting aluminum penetrameters on an aluminum step wedge. Kodak Industrex M film was used with 74°F manual processing consisting of development 5 min, rinse 0.5 min, fix 5 min, rinse 30 min, and drying in warmed forced air. The film was inserted into cardboard holders for exposing. Densities were measured with a Macbeth TD504 densitometer. Images were examined by two readers independently with variable intensity full field and apertured high intensity film viewer to show detail for densities in the range of 0.5 to 5.0.

To produce a film density of about 2.5 for the 0.5-in. aluminum thickness the exposure was 100 kVp, 1.0 mA, 2.2 min, 2.2 mA · min as shown in Table 16. The film densities shown on Table 16 are plotted on Fig. 49. A central 3.0 density units range was selected from 1.74 to 4.74 to represent the 1000-to-1 dynamic range. These densities correspond to aluminum thicknesses of 0.750 and 0.255 in.

A similar image was made using the RTR system with an exposure of 100 kV, 2.0 mA, and integrating 256 frames. All of the filtration, field of view, focal spot size, and geometry were identical to the set-up for film. The digital image was analyzed using a histogram program. A joystick adjustable size and location cursor box is placed on the image of the aluminum step of interest. The program calculates the histogram and statistics of the data in the cursor box. The resulting signal levels are plotted on Fig. 50. The original image data is plotted along with a plot of how the same image data can look after digitally adjusting the gain and offset. Additional gain and offset adjustments can be used to help the operator to perceive subtle contrast differences. The original image as acquired showed the penetrameters and all of the steps of aluminum from 0.125 to 1.000 in. This demonstrates that the RTR system is equal to or exceeds a 1000-to-1 dynamic range of film.

4.2.3 Penetrameter Sensitivity

The penetrameter sensitivity of the RTR system and film were compared. Both sets of images were prepared in accordance with the Radiographic Inspection

Table 16 FILM DATA

Processing: Development 5 min, Rinse 0.5 min, Fix 5 min, Rinse 30 min, Temperature 74°F

Energy (kVp)	Current (mA)	Time (min)	Exposure (mA min)	Object Material	Optical Density (ODU)							
					Object Thickness (in.)							
Film = Kodak Type M without screens												
X-ray = Sieffert 60 with 1.2-mm focal spot. FS-film = 37.5 in. O-film = 1.5 in.												
20	15.0	2.0	30.0	Plastic	6.05	6.04	3.09	2.99	2.12	1.51	1.10	0.79
Film = Kodak Type M without screens												
X-ray = Sieffert 160 with 0.4-mm focal spot. FS-film = 34 in. O-film = 1.5 in.												
60	2.0	3.5	7.0	Aluminum	6.05	5.49	3.37	2.47	1.90	1.51	1.23	1.07
100	1.0	2.2	2.2	Aluminum	6.06	4.85	3.44	2.69	2.15	1.74	1.43	1.21
140	1.0	1.3	1.3	Aluminum	6.05	5.08	3.69	2.96	2.45	2.02	1.69	1.37
Film = Kodak Type M with 0.005 inch Lead screens on both sides of the film												
X-ray = Sieffert 420 with 1.8-mm focal spot. FS-film = 47 in. O-film = 1.5 in.												
180	2.0	8.2	16.4	Steel	6.22	5.26	3.00	2.07	1.53	1.23	1.00	0.86
220	1.0	7.6	7.6	Steel	6.00	4.47	2.89	2.09	1.61	1.31	1.10	1.00
260	1.0	5.0	5.0	Steel	6.17	4.62	3.00	2.25	1.70	1.45	1.19	1.02
300	1.0	3.4	3.4	Steel	6.15	4.50	3.07	2.30	1.78	1.41	1.18	0.99

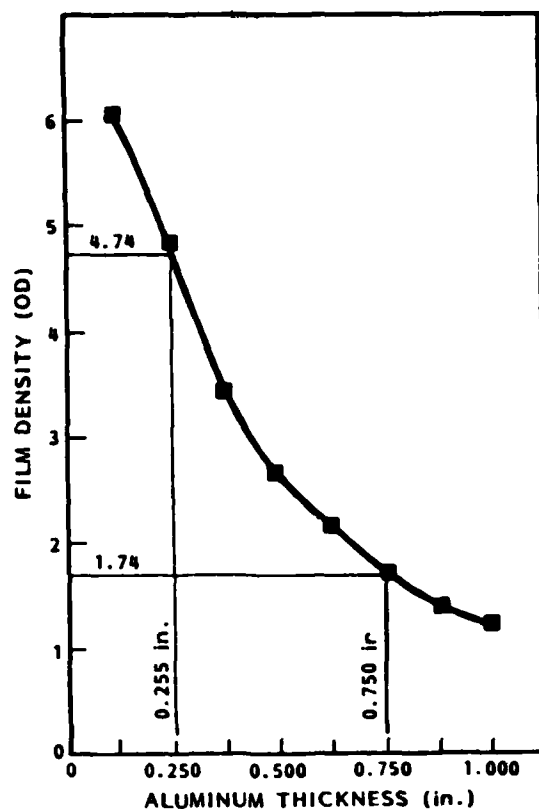


Fig. 49 Film Density Versus Aluminum Thickness For 100-kV, Type M Film

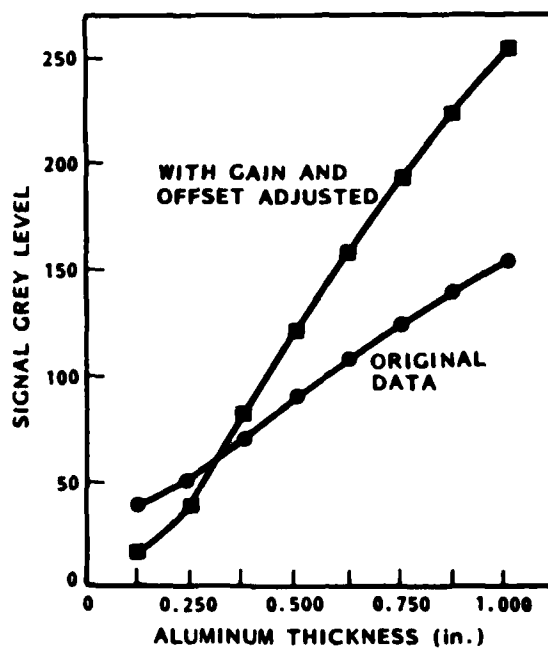


Fig. 50 Digital Level Versus Aluminum Thickness For 100-kV, 2-mA, RTR System

Standard MIL-STD-453C which describes the application of penetrometer image quality indicators to measuring penetrometer sensitivity.

Kodak Industrialex M film was used with 74°F manual processing consisting of development of 5 min, rinse 0.5 min, fix 5 min, rinse 30 min, and drying in warmed forced air. The film was inserted into cardboard holders for exposing. The exposure techniques are given in Table 16. Film densities must be in the 2.0-to-4.0 range as required by MIL-STD-453C. Object thicknesses corresponding to the correct density range are given in Table 16. Penetrometer sensitivity data for film in the correct density range is given on Tables 26-33.

The RTR images were made using approximately the same imaging set-up as film. The main difference was an extra 1.5 in. of object-to-screen distance for the RTR images due to the thickness of the screen and film mounts. The x-ray kV was the same as film but the current was adjusted to suit the RTR system. Images were digitized to 512 x 512 pixels/image with 8 bits/pixel. Although the entire object step wedge could be seen if desired, the penetrometer hole detectability judgements were made with optical magnification which limited the horizontal field of view to about 2 in. This corresponds to about 0.004 in. per pixel. The smallest holes are 0.010 in., therefore, at least three pixels subtend all holes. Image noise was reduced by integrating 256 frames. The object position was shifted by approximately 0.005 in., and a second image was integrated. The shift distance wasn't as consistent as it could be if a digitally controlled stepper motor had been used for the object positioner. The two images were digitally subtracted to minimize nonuniformities in x-ray flux, screen brightness, lens brightness, photocathode sensitivity and shading adjustments on the camera controller. Brightness and contrast were adjusted and the images was judged by the operator. Each image was printed on dry silver using the Honeywell VGR4000 and the penetrometer holes visible on the CRT monitor were marked on the image print. Each inspection took less than one minute. The resulting RTR system penetrometer sensitivity data is given on Tables 17 through 24.

Table 17 RTR PENETRATOR DATA

Technique = 20 kVp, 20 mA
 Focal spot size = 1.2 x 1.5 mm
 Focus-to-screen = 34 in.
 Object-to-screen = 3 in.
 Filter = 0.4 mm Be (inherent)
 Object and penetrometer = Plastic
 Screen type = Medium-Speed Particulate
 (No Backing)

Minimum Detectable Hole Size (in. and xT)

Object Thickness (in.)	Penetrometer Thickness, T (in.)						
	0.005	0.010	0.015	0.020	0.025	0.030	0.035
0.125	0.040 4T	0.040 4T	0.030 2T	0.020 1T	0.025 1T	0.030 1T	0.035 1T
0.250	0.040 4T	0.040 4T	0.030 2T	0.020 1T	0.025 1T	0.030 1T	—
0.375	0.040 4T	0.040 4T	0.030 2T	0.020 1T	0.025 1T	0.030 1T	—
0.500	0.040 4T	0.040 4T	0.030 2T	0.020 1T	0.025 1T	0.030 1T	—
0.625	0.040 4T	0.040 4T	0.030 2T	0.020 1T	0.025 1T	0.030 1T	—
0.750	0.040 4T	0.040 4T	0.060 4T	0.040 2T	0.025 1T	0.030 1T	—
0.875	N	0.040 4T	0.060 4T	0.080 4T	0.050 2T	0.030 1T	0.035 1T
1.000	P	P	0.030 2T	0.080 4T	0.100 4T	0.060 2T	0.035 1T

P = Penetrometer outline is visible
 N = Not visible
 — = No data taken

Table 18 RTR PENETRATOR DATA

Technique = 60 kVp, 7-20 mA
 Focal spot size = 1.5 x 0.4 mm
 Focus-to-screen = 34 in.
 Object-to-screen = 3 in.
 Filter = 0.7-1.0 mm Be (inherent)
 Object and penetrometer = Aluminum
 Screen type = Medium-Speed Particulate
 (No Backing)

Minimum Detectable Hole Size (in. and xT)

Object Thickness (in.)	Penetrometer Thickness, T (in.)						
	0.005	0.010	0.015	0.020	0.025	0.030	0.035
0.125	0.010 1T	0.010 1T	0.015 1T	0.020 1T	—	—	—
0.250	0.040 1T	0.020 2T	0.015 1T	0.020 1T	—	—	—
0.375	0.040 4T	0.010 1T	0.015 1T	0.020 1T	—	—	—
0.500	0.040 4T	0.010 1T	0.015 1T	0.020 1T	—	—	—
0.625	0.040 4T	0.010 1T	0.015 1T	0.020 1T	—	—	—
0.750	0.040 4T	0.020 2T	0.015 1T	0.020 1T	—	—	—
0.875	0.040 4T	0.040 4T	0.015 1T	0.020 1T	—	—	—
1.000	0.040 4T	0.020 2T	0.015 1T	0.020 1T	0.025 1T	—	—

P = Penetrometer outline is visible
 N = Not visible
 — = No data taken

Table 19 RTR PENETRATOR DATA

Technique = 100 kVp, 7 mA
 Focal spot size = 1.8 x 1.8 mm
 Focus-to-screen = 44 in.
 Object-to-screen = 4 in.
 Filter = 7.0 mm Be (inherent)
 Object and penetrometer = Aluminum
 Screen type = Medium-Speed Particulate
 (No Backing)

Minimum Detectable Hole Size (in. and xT)

Object Thickness (in.)	Penetrometer Thickness, T (in.)						
	0.005	0.010	0.015	0.020	0.025	0.030	0.035
0.125	0.040 4T	0.020 2T	0.015 1T	0.020 1T	0.025 1T	0.030 1T	0.035 1T
0.250	0.040 4T	0.020 2T	0.015 1T	0.020 1T	0.025 1T	0.030 1T	0.035 1T
0.375	0.040 4T	0.010 1T	0.015 1T	0.020 1T	0.025 1T	0.030 1T	0.035 1T
0.500	0.040 4T	0.020 2T	0.015 1T	0.020 1T	0.025 1T	0.030 1T	0.035 1T
0.625	—	0.040 4T	0.015 1T	0.020 1T	0.025 1T	0.030 1T	0.035 1T
0.750	—	0.040 4T	0.015 1T	0.020 1T	0.025 1T	0.030 1T	0.035 1T
0.875	—	0.020 2T	0.015 1T	0.020 1T	0.025 1T	0.030 1T	0.035 1T
1.000	—	—	—	0.020 1T	0.025 1T	0.030 1T	0.035 1T

P = Penetrometer outline is visible
 N = Not visible
 — = No data taken

Table 20 RTR PENETRATOR DATA

Technique = 140 kVp, 10 mA
 Focal spot size = 1.8 x 1.8 mm
 Focus-to-screen = 44 in.
 Object-to-screen = 4 in.
 Filter = 7.0 mm Be (inherent)
 Object and penetrometer = Aluminum
 Screen type = Medium-Speed Particulate
 (No Backing)

Minimum Detectable Hole Size (in. and xT)

Object Thickness (in.)	Penetrometer Thickness, T (in.)						
	0.005	0.010	0.015	0.020	0.025	0.030	0.035
0.125	0.010 1T	0.010 1T	0.015 1T	0.020 1T	—	—	—
0.250	P	0.010 1T	0.015 1T	0.020 1T	—	—	—
0.375	P	0.020 2T	0.015 1T	0.020 1T	—	—	—
0.500	P	0.010 1T	0.015 1T	0.020 1T	—	—	—
0.625	P	0.040 4T	0.015 1T	0.020 1T	—	—	—
0.750	0.040 4T	0.020 2T	0.015 1T	0.020 1T	—	—	—
0.875	—	0.020 2T	0.015 1T	0.020 1T	—	—	—
1.000	—	0.010 1T	0.015 1T	0.020 1T	0.025 1T	—	—

P = Penetrometer outline is visible
 N = Not visible
 — = No data taken

Table 21 RTR PENETRATOR DATA

Technique = 180 kVp, 10 mA
 Focal spot size = 1.8 x 1.8 mm
 Focus-to-screen = 46 in.
 Object-to-screen = 4 in.
 Filter = 7.0 mm Be (inherent)
 Object and penetrometer = Steel
 Screen type = Medium-Speed Particulate
 (No Backing)

Minimum Detectable Hole Size (in. and xT)

Object Thickness (in.)	Penetrometer Thickness, T (in.)						
	0.005	0.010	0.015	0.020	0.025	0.030	0.035
0.125	0.010 1T	0.010 1T	0.015 1T	0.020 1T	0.025 1T	0.030 1T	0.035 1T
0.250	0.020 2T	0.010 1T	0.015 1T	0.020 1T	0.025 1T	0.030 1T	0.035 1T
0.375	0.020 2T	0.010 1T	0.015 1T	0.020 1T	0.025 1T	0.030 1T	0.035 1T
0.500	0.040 4T	0.020 2T	0.015 1T	0.020 1T	0.025 1T	0.030 1T	0.035 1T
0.625	0.040 4T	0.040 4T	0.015 1T	0.020 1T	0.025 1T	0.030 1T	0.035 1T
0.750	P	0.040 4T	0.015 1T	0.020 1T	0.025 1T	0.030 1T	0.035 1T
0.875	0.040 4T	0.040 4T	0.060 4T	0.020 1T	0.025 1T	0.030 1T	0.035 1T
1.000	P	0.040 4T	P	P	0.050 2T	—	—

P = Penetrometer outline is visible
 N = Not visible
 — = No data taken

Table 22 RTR PENETRATOR DATA

Technique = 220 kVp, 5-8 mA
 Focal spot size = 1.8 x 1.8 mm
 Focus-to-screen = 44 in.
 Object-to-screen = 4.5 in.
 Filter = 7.0 mm Be (inherent)
 Object and penetrometer = Steel
 Screen type = Medium-Speed Particulate
 (No Backing)

Minimum Detectable Hole Size (in. and xT)

Object Thickness (in.)	Penetrometer Thickness, T (in.)						
	0.005	0.010	0.015	0.020	0.025	0.030	0.035
0.125	0.040 4T	0.020 2T	0.015 1T	0.020 1T	0.025 1T	0.030 1T	0.035 1T
0.250	0.010 1T	0.010 1T	0.015 1T	0.020 1T	0.025 1T	0.030 1T	0.035 1T
0.375	0.040 4T	0.020 2T	0.015 1T	0.020 1T	0.025 1T	0.030 1T	0.035 1T
0.500	0.020 2T	0.020 2T	0.015 1T	0.020 1T	0.025 1T	0.030 1T	0.035 1T
0.625	0.040 4T	0.020 2T	0.015 1T	0.020 1T	0.025 1T	0.030 1T	0.035 1T
0.750	0.040 4T	0.040 4T	0.015 1T	0.020 1T	0.025 1T	0.030 1T	0.035 1T
0.875	0.040 4T	0.010 1T	0.015 1T	0.020 1T	0.025 1T	0.030 1T	0.035 1T
1.000	—	—	0.060 4T	0.040 2T	0.050 2T	—	—

P = Penetrometer outline is visible
 N = Not visible
 — = No data taken

Table 23 RTR PENETRATOR DATA

Technique = 260 kVp, 7 mA
 Focal spot size = 1.8 x 1.8 mm
 Focus-to-screen = 45 in.
 Object-to-screen = 4 in.
 Filter = 7.0 mm Be (inherent)
 Object and penetrometer = Steel
 Screen type = Medium-Speed Particulate
 (No Backing)

Minimum Detectable Hole Size (in. and xT)

Object Thickness (in.)	Penetrometer Thickness, T (in.)						
	0.005	0.010	0.015	0.020	0.025	0.030	0.035
0.125	P 4T	0.040 4T	0.015 1T	0.020 1T	0.025 1T	0.030 1T	0.035 1T
0.250	P	0.020 2T	0.015 1T	0.020 1T	0.025 1T	0.030 1T	0.035 1T
0.375	P	0.020 2T	0.030 2T	0.020 1T	0.025 1T	0.030 1T	0.035 1T
0.500	P	0.010 1T	0.015 1T	0.020 1T	0.025 1T	0.030 1T	0.035 1T
0.625	P	0.010 1T	0.015 1T	0.020 1T	0.025 1T	0.030 1T	0.035 1T
0.750	0.040 4T	0.020 2T	0.015 1T	0.020 1T	0.025 1T	0.030 1T	0.035 1T
0.875	P	P	0.015 1T	0.020 1T	0.025 1T	0.030 1T	0.035 1T
1.000	P	0.020 2T	0.015 1T	0.020 1T	0.025 1T	0.030 1T	0.035 1T

P = Penetrometer outline is visible
 N = Not visible
 — = No data taken

Table 24 RTR PENETRATOR DATA

Technique = 300 kVp, 4-6 mA
 Focal spot size = 1.8 x 1.8 mm
 Focus-to-screen = 45 in.
 Object-to-screen = 3 in.
 Filter = 7.0 mm Be (inherent)
 Object and penetrometer = Steel
 Screen type = Medium-Speed Particulate
 (No Backing)

Minimum Detectable Hole Size (in. and xT)

Object Thickness (in.)	Penetrometer Thickness, T (in.)						
	0.005	0.010	0.015	0.020	0.025	0.030	0.035
0.125	0.010 1T	0.010 1T	0.015 1T	0.020 1T	0.025 1T	0.030 1T	0.035 1T
0.250	0.010 1T	0.010 1T	0.015 1T	0.020 1T	0.025 1T	0.030 1T	0.035 1T
0.375	0.020 2T	0.010 1T	0.015 1T	0.020 1T	0.025 1T	0.030 1T	0.035 1T
0.500	0.020 2T	0.010 1T	0.015 1T	0.020 1T	0.025 1T	0.030 1T	0.035 1T
0.625	P	0.010 1T	0.015 1T	0.020 1T	0.025 1T	0.030 1T	0.035 1T
0.750	P	0.040 4T	0.015 1T	0.020 1T	0.025 1T	0.030 1T	0.035 1T
0.875	0.040 4T	0.010 1T	0.030 2T	0.020 1T	0.025 1T	0.030 1T	0.035 1T
1.000	0.040 4T	0.040 4T	0.060 4T	0.020 1T	0.025 1T	0.030 1T	0.035 1T

P = Penetrometer outline is visible
 N = Not visible
 — = No data taken

A comparison of the penetrometer sensitivities of RTR and film images can be accomplished by comparing Tables 25 through 32 with 17 through 24, respectively by kV. The penetrometer sensitivity of film and RTR images can also be seen on plots of penetrometer thickness versus object thickness in Figs. 51 through 58. The smallest penetrometer hole visible is expressed as a function of the penetrometer thickness (T). The only exception is the 0.005-in. penetrometer which has a 0.010-in. diameter for the 1T hole. Figure 51 shows that at 20 kV, film is a little more sensitive in detecting the 1T and 2T holes. Figures 52 through 54 show that from 60 to 140 kV, film and RTR are about equal for 1T holes, and film has an advantage on seeing 2T holes. Figures 55 through 58 show that in the 180 to 300 kV range, RTR is equal to or better than film for all penetrometer hole sizes. The useable density range of 2.0 to 4.0 defined by MIL-STD-453C severely limits the range of object thicknesses that may be evaluated. The eye is capable of detecting high contrast objects on film over a wider density range, perhaps densities of 0.5 to 4.5, but there may not be adequate contrast sensitivity over the entire range to detect subtle objects. The RTR system had no difficulty examining the test object thicknesses from below 0.125 to over 1.000 in.

4.3 INDUSTRY RTR DEMONSTRATION

A demonstration of the 1024 x 1024 pixel/image RTR breadboard system was held in November 1986 at the LMSC facility. Air frame and engine hardware specimens were inspected with the breadboard RTR system. The RTR image quality was compared with that of film radiographs. The demonstration included 1024 x 1024 pixel/image acquisition, optical zoom, storage, retrieval scan plan sequencing, image processing, 512 x 512 pixel/image overview display, and a 512 x 512 pixel/image microview display. A 2048 x 2048 pixel/image Azuray display was acquired and integrated with the breadboard RTR system as part of LMSC's internally funded research program. The Azuray display demonstrated the real advantage of 1024 x 1024 pixel/image resolution radiography over 512 x 512 pixel/image resolution by providing either a larger field of view at the same resolution or the same field of view at higher resolution. An RTR 2048 x 2048 pixel x-ray image was acquired by combining four adjacent images and displayed for the first time.

Table 25 FILM PENETRATOR DATA

Technique = 20 kVp, 15 mA, 2.0 min, 30 mA · min
 Focal spot size = 1.2 x 1.5 mm
 Focus-to-screen = 34 in.
 Object-to-screen = 3 in.
 Filter = 0.4 mm Be (inherent)
 Object and penetrometer = Plastic
 Film and screen type = Kodak Industrialex M Film
 (No Backing)

Minimum Detectable Hole Size (in. and xT)

Object Thickness (in.)	Penetrometer Thickness, T (in.)						
	0.005	0.010	0.015	0.020	0.025	0.030	0.035
0.125							
0.250							
0.375	0.040 4T	0.020 2T	0.015 1T	0.020 1T	0.025 1T	0.030 1T	0.035 1T
0.500	N	0.040 4T	0.015 1T	0.020 1T	0.025 1T	0.030 1T	0.035 1T
0.625	N	0.020 2T	0.015 1T	0.020 1T	0.025 1T	0.030 1T	0.035 1T
0.750							
0.875							
1.000							

P = Penetrometer outline is visible
 N = Not visible
 — = No data taken

Table 26 FILM PENETRATOR DATA

Technique = 60 kVp, 2.0 mA, 3.5 min, 7.0 mA · min
 Focal spot size = 1.5 x 0.4 mm
 Focus-to-screen = 34 in.
 Object-to-screen = 3 in.
 Filter = 0.7-1.0 mm Be (inherent)
 Object and penetrometer = Aluminum
 Film and screen type = Kodak Industrialex M Film
 (No Backing)

Minimum Detectable Hole Size (in. and xT)

Object Thickness (in.)	Penetrometer Thickness, T (in.)						
	0.005	0.010	0.015	0.020	0.025	0.030	0.035
0.125							
0.250							
0.375	0.020 2T	0.010 1T	0.015 1T	—	—	—	—
0.500	0.020 2T	0.010 1T	0.015 1T	0.020 1T	—	—	—
0.625							
0.750							
0.875							
1.000							

P = Penetrometer outline is visible
 N = Not visible
 — = No data taken

Table 27 FILM PENETRAMEETER DATA

Technique = 100 kVp, 1 mA, 2.2 min, 2.2 mA · min
 Focal spot size = 1.8 x 1.8 mm
 Focus-to-screen = 44 in.
 Object-to-screen = 4 in.
 Filter = 7.0 mm Be (inherent)
 Object and penetrameter = Aluminum
 Film and screen type = Kodak Industrialex M Film
 (No Backing)

Minimum Detectable Hole Size (in. and xT)

Object Thickness (in.)	Penetrameter Thickness, T (in.)						
	0.005	0.010	0.015	0.020	0.025	0.030	0.035
0.125							
0.250							
0.375	0.020 2T	0.010 1T	0.015 1T	—	—	—	—
0.500	0.020 2T	0.010 2T	0.015 1T	0.020 1T	—	—	—
0.625	N	0.020 2T	0.015 1T	0.020 1T	0.025 1T	—	—
0.750							
0.875							
1.000							

P = Penetrameter outline is visible
 N = Not visible
 — = No data taken

Table 28 FILM PENETRATOR DATA

Technique = 140 kVp, 1 mA, 1.2 min, 1.2 mA · min
 Focal spot size = 1.8 x 1.8 mm
 Focus-to-screen = 44 in.
 Object-to-screen = 4 in.
 Filter = 7.0 mm Be (inherent)
 Object and penetrometer = Aluminum
 Film and screen type = Kodak Industrialex M Film
 (No Backing)

Minimum Detectable Hole Size (in. and xT)

Object Thickness (in.)	Penetrometer Thickness, T (in.)						
	0.005	0.010	0.015	0.020	0.025	0.030	0.035
0.125							
0.250							
0.375	0.040 4T	0.010 1T	0.015 1T	—	—	—	—
0.500	0.020 2T	0.020 2T	0.015 1T	0.020 1T	—	—	—
0.625	N	0.020 2T	0.015 1T	0.020 1T	—	—	—
0.750	N	N	0.015 1T	0.020 1T	0.025 1T	0.030 1T	—
0.875							
1.000							

P = Penetrometer outline is visible
 N = Not visible
 — = No data taken

Table 29 FILM PENETRAMEETER DATA

Technique = 180 kVp, 2 mA, 7.0 min, 14.0 mA · min
 Focal spot size = 1.8 x 1.8 mm
 Focus-to-screen = 46 in.
 Object-to-screen = 4 in.
 Filter = 7.0 mm Be (inherent)
 Object and penetrameter = Steel
 Film and screen type = Kodak Industrialex M Film with 2 each
 0.005-in. lead screens

Minimum Detectable Hole Size (in. and xT)

Object Thickness (in.)	Penetrameter Thickness, T (in.)						
	0.005	0.010	0.015	0.020	0.025	0.030	0.035
0.125							
0.250							
0.375	0.040 4T	0.020 2T	0.015 1T	—	—	—	—
0.500	0.040 4T	0.020 2T	0.015 1T	0.020 1T	—	—	—
0.625							
0.750							
0.875							
1.000							

P = Penetrameter outline is visible
 N = Not visible
 — = No data taken

Table 30 FILM PENETRATOR DATA

Technique = 220 kVp, 1.0 mA, 7.6 min, 7.6 mA · min
 Focal spot size = 1.8 x 1.8 mm
 Focus-to-screen = 44 in.
 Object-to-screen = 4.5 in.
 Filter = 7.0 mm Be (inherent)
 Object and penetrometer = Steel
 Film and screen type = Kodak Industrialex M Film with 2 each
 0.005-in. lead screens
 (No Backing)

Minimum Detectable Hole Size (in. and xT)

Object Thickness (in.)	Penetrometer Thickness, T (in.)						
	0.005	0.010	0.015	0.020	0.025	0.030	0.035
0.125							
0.250							
0.375	0.040 4T	0.020 2T	0.030 2T	—	—	—	—
0.500	P	0.020 2T	0.020 2T	0.020 1T	—	—	—
0.625							
0.750							
0.875							
1.000							

P = Penetrometer outline is visible
 N = Not visible
 — = No data taken

Table 31 FILM PENETRAMEETER DATA

Technique = 260 kVp, 1 mA, 5.0 min, 5.0 mA · min
 Focal spot size = 1.8 x 1.8 mm
 Focus-to-screen = 44 in.
 Object-to-screen = 4.5 in.
 Filter = 7.0 mm Be (inherent)
 Object and penetrameter = Steel
 Film and screen type = Kodak Industrialex M Film with 2 each
 0.005-in. lead screens

Minimum Detectable Hole Size (in. and xT)

Object Thickness (in.)	Penetrameter Thickness, T (in.)						
	0.005	0.010	0.015	0.020	0.025	0.030	0.035
0.125							
0.250							
0.375	0.040 4T	0.020 2T	0.030 1T	—	—	—	—
0.500	0.040 4T	0.020 2T	0.015 1T	0.020 1T	—	—	—
0.625							
0.750							
0.875							
1.000							

P = Penetrameter outline is visible
 N = Not visible
 — = No data taken

Table 32 FILM PENETRAMEETER DATA

Technique = 300 kVp, 1.0 mA, 3.4 min, 3.4 mA · min
 Focal spot size = 1.8 x 1.8 mm
 Focus-to-screen = 45 in.
 Object-to-screen = 4 in.
 Filter = 7.0 mm Be (inherent)
 Object and penetrameter = Steel
 Film and screen type = Kodak Industrialex M film with two
 each 0.005-in. lead screens.
 (No Backing)

Minimum Detectable Hole Size (in. and xT)

Object Thickness (in.)	Penetrameter Thickness, T (in.)						
	0.005	0.010	0.015	0.020	0.025	0.030	0.035
0.125							
0.250							
0.375	0.020 2T	0.020 2T	0.015 1T	—	—	—	—
0.500	P	0.020 2T	0.030 2T	0.020 1T	—	—	—
0.625							
0.750							
0.875							
1.000							

P = Penetrameter outline is visible
 N = Not visible
 — = No data taken

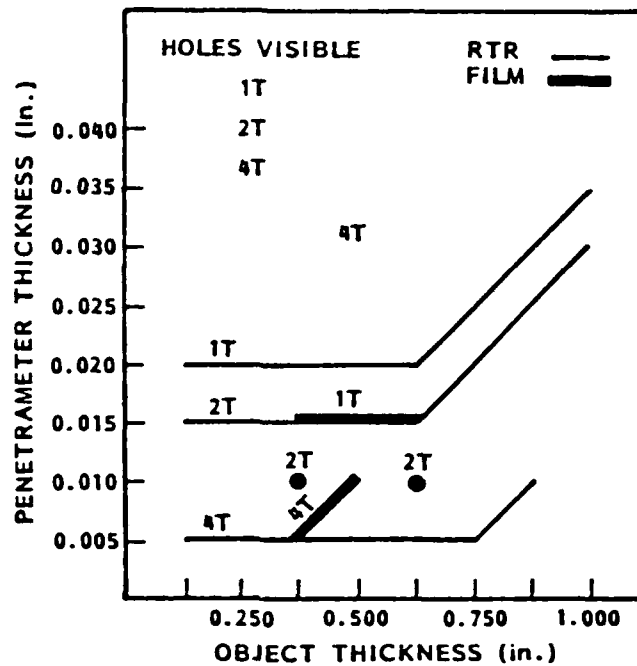


Fig. 51 Penetrator Sensitivity of Film and RTR for 20 kV, Plastic

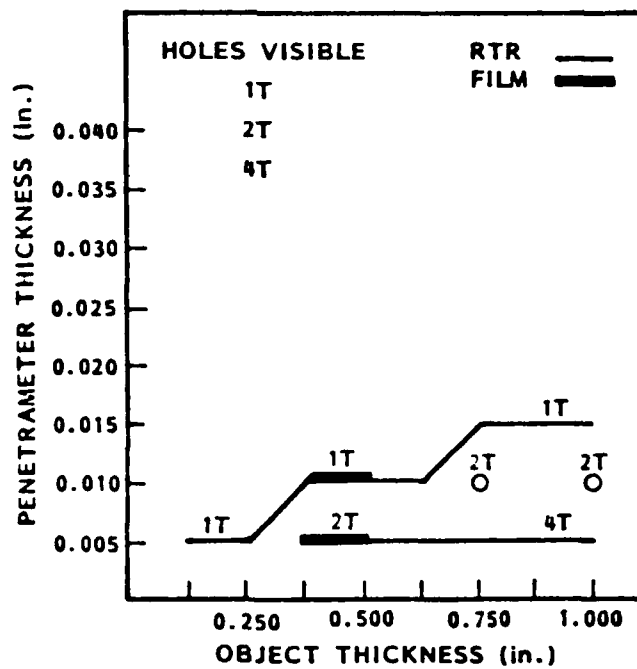


Fig. 52 Penetrator Sensitivity of Film and RTR for 60 kV, Aluminum

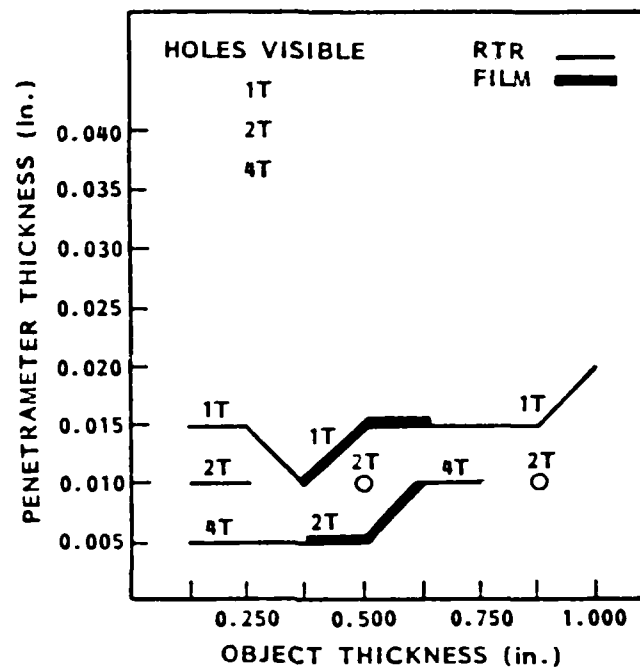


Fig. 53 Penetrameter Sensitivity of Film and RTR for 100 kV, Aluminum

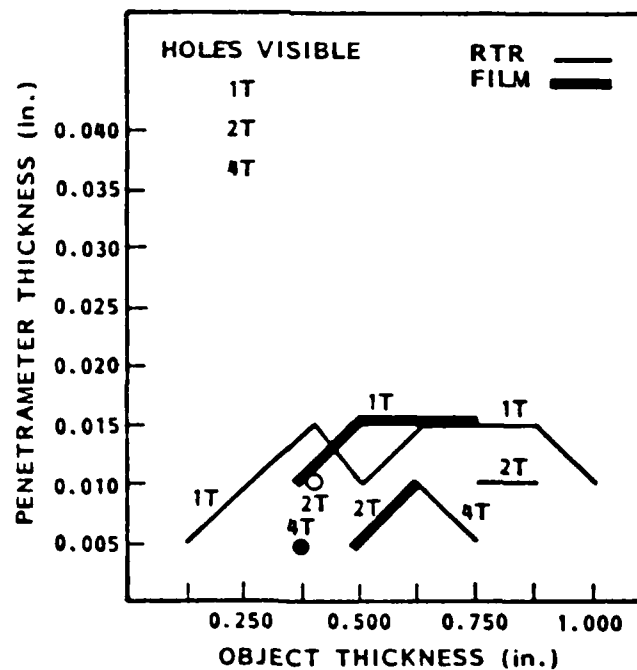


Fig. 54 Penetrameter Sensitivity of Film and RTR for 140 kV, Aluminum

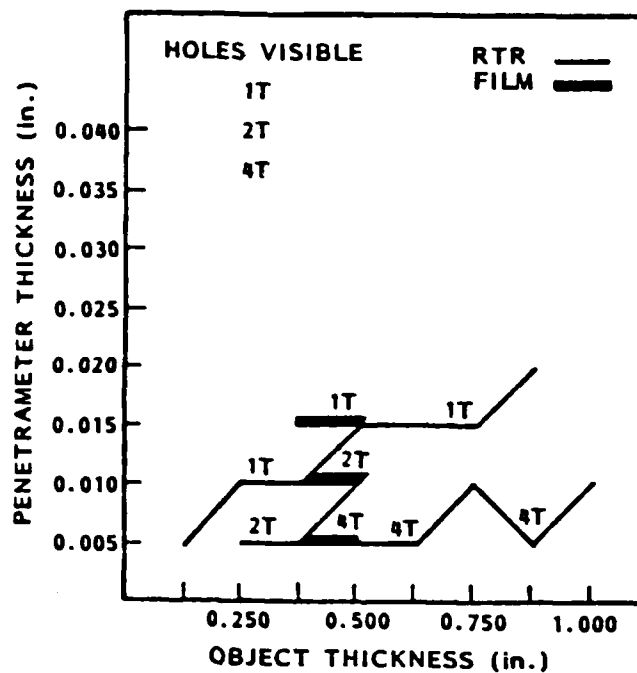


Fig. 55 Penetrameter Sensitivity of Film and RTR for 180 kV, Steel

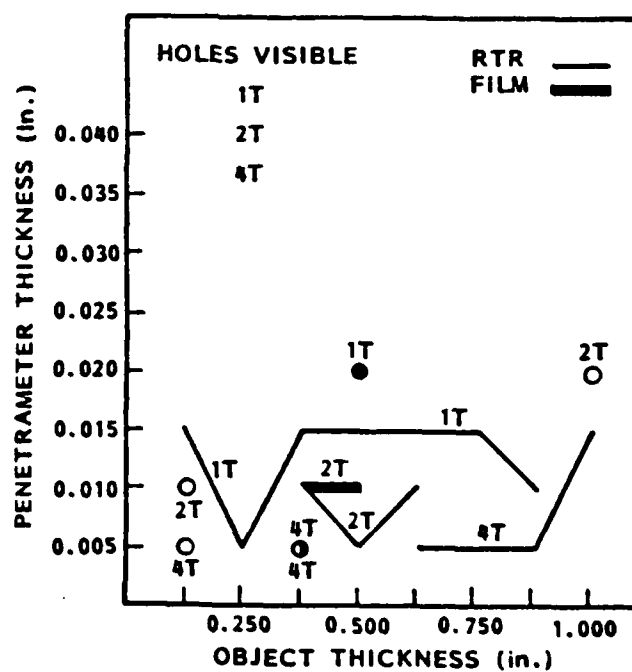


Fig. 56 Penetrameter Sensitivity of Film and RTR for 220 kV, Steel

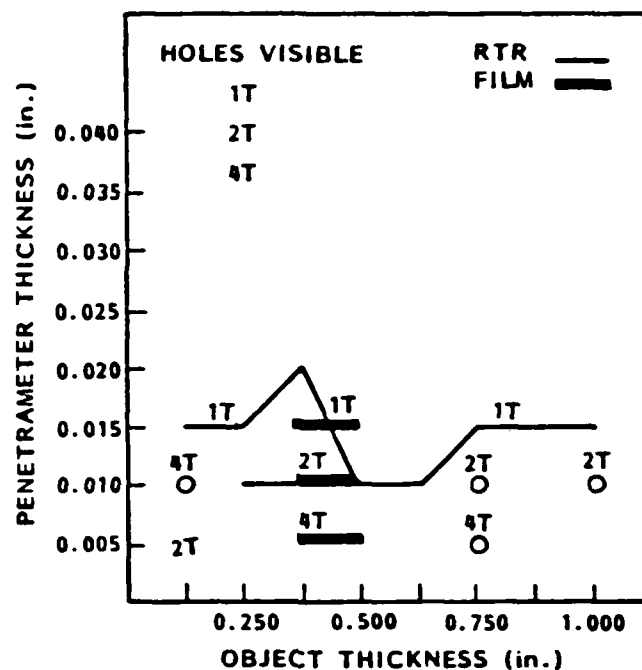


Fig. 57 Penetrameter Sensitivity of Film and RTR for 260 kV, Steel

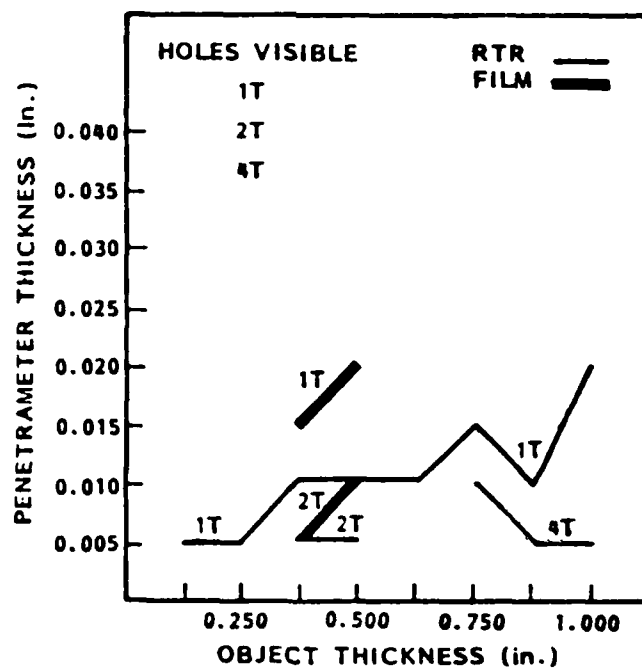


Fig. 58 Penetrameter Sensitivity of Film and RTR for 300 kV, Steel

Section 5

RTR PROTOTYPE SYSTEM DESIGN

A real-time radiography system consists of an x-ray system, a camera system, an image-processing computer, displays, video recorders, digital storage system, an alphanumeric printer, an image printer, and an object manipulation system. The camera is the key system being evaluated during this program; however, all of the systems are required in order to have an RTR system useful for real inspection applications at a manufacturing, remanufacturing, or maintenance facility.

5.1 X-RAY SYSTEM

The x-ray system consists of an x-ray tube, tube housing, collimator, filter, tube positioner, HV generator, cooling, control, and interlocks. A digital control interface can also be useful *when designing* advanced systems. The x-ray source must produce fixed energies between 20 and 300 kVp with sufficient flux to give enough screen brightness, be on nearly all the time, and maintain a small enough focal spot such that resolution is not restricted. So far no system meets all of the above requirements. The Seifert systems on Table 12 with their Digital Interface chassis V24 (RS 232) may be adequate. Multiple x-ray source mechanics and geometries are difficult to design for a general inspection system.

5.2 CAMERA SYSTEM

The camera system consists of the x-ray converter screen, lens, video camera, and camera positioner.

5.2.1 X-Ray Converter Screen

The x-ray converter screen absorbs x-ray photons and emits light photons. Higher efficiency converters tend to give more light output but less resolution. To further improve brightness or resolution, a change in the converter technology is needed. The optimum screen material varies with the inspection application as shown in Table 33; therefore, the prototype system will incorporate easily changeable screens.

5.2.2 Lens

The lens collects the light from the screen and focuses it onto the light-sensitive element of the video camera (photocathode). A light amplifier or image intensifier can be in close proximity to the lens. Since a variety of x-ray converter screens are necessary, the light amplifier is kept independent of the x-ray converter screen. To permit variable optical magnification (zooming in and out), the light amplifier must not be between the converter and lens unless it can provide resolution better than the highest resolution at the highest magnification. Although image intensifiers have improved a lot, none available can meet the size, zoom range, and resolution requirements. If the field of view is eventually expanded as anticipated, then the use of an image intensifier will be impractical. Consequently, the light amplifier is incorporated in the video camera by selecting an extremely low-light-level camera.

The lens then is simply an optical component, optimized for maximum light collection and adjustable in magnification. The present lens is a fixed-focus 60-mm $f/0.7$. This lens, described in section 4.1.3, is close to the state of the art and is selected for the prototype design. Comparable custom lenses are available. Manufacturers of zoom lenses may be capable of building a fast lens or a 20-to-1 zoom ratio, but no attempt has been made to get a quote to design or fabricate such a lens.

Table 33 X-RAY CONVERTER SCREENS FOR VARIOUS APPLICATIONS

The following combinations of applications and screens were found useful:

<u>Application</u>	<u>Screen</u>	<u>Energy</u>	<u>Resolution</u>
Carbon composite structure	Medium particulate	20-60 kVp	10 lp/mm
Aluminum/aluminum honeycomb airfoil	Regular particulate	40-100 kVp	5 lp/mm
Engine components	Glass	100-300 kVp	20 lp/mm

An alternate lens system could consist of two to four fixed lenses, each optimized for a particular field of view and magnification. The lenses could be mounted on a turret. Each lens would require a mechanical fine-focus adjustment. If a motorized focus were required, the turret may not simplify the design. At high magnification the focus is sensitive and will probably require interactive adjustments. An automatic fine focus may be possible.

5.2.3 Video Camera

The video camera tested was an Isocon tube mounted in a Penn Video Camera control unit. It was modified to give over 1024 lines x 1024 pixels resolution at 7.5 frames per second. The bandwidth required by the camera and the video digitizer was the same as when the camera gave 512 x 512 pixels at 60 fields per second (30 interlaced frames per second). The camera specifications are given in section 4.1.4. Included were shading controls which enable the operator to adjust field offset and flatness in the vertical and horizontal planes using analog controls before digitizing. The shading controls help reduce errors due to the nonuniformity of the x-ray flux, screen variability, and camera variability. A waveform monitor is necessary for the proper adjustment of the camera and shading.

The same Isocon tube and Penn Video camera are selected for the prototype. The 7.5 fps gives an adequate information rate but makes viewing the analog

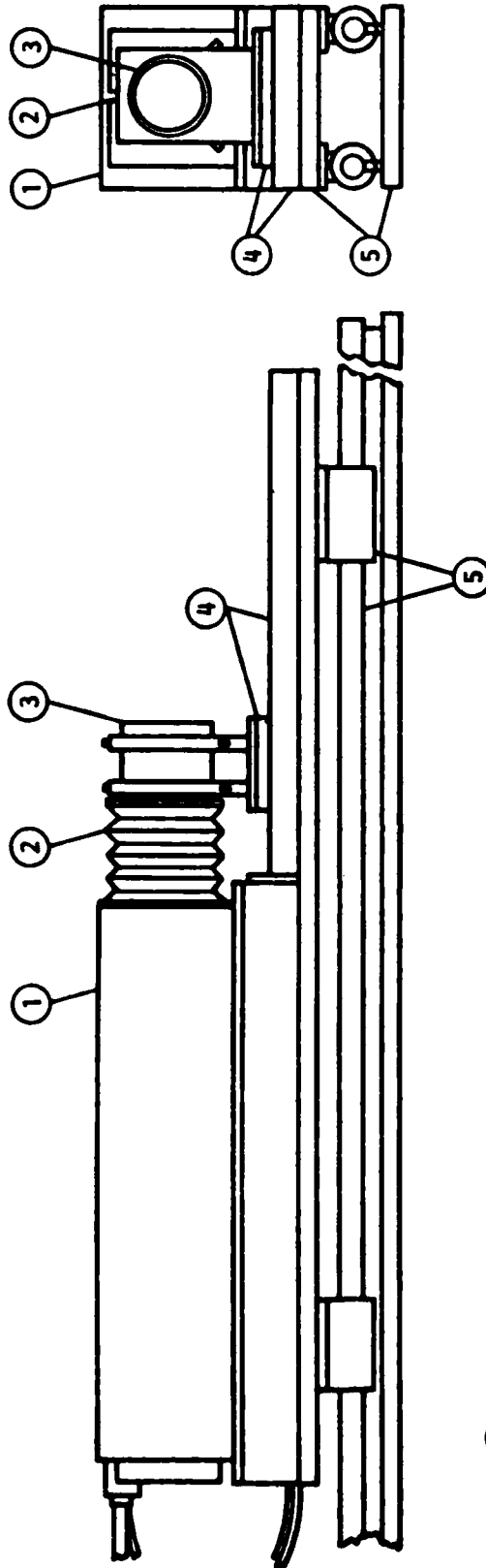
video signal impossible with off-the-shelf equipment. Real-time viewing can be achieved by digitizing the signal and updating the display at 7.5 fps. This means a digital image processing system is required to operate the camera, even for servicing. This mode presented some difficulties when malfunctions were encountered but was fine when the system was operational.

The present shading controls give horizontal, vertical, linear, and parabolic contour corrections in the analog offset domain. These first-order corrections are very helpful in avoiding saturation and in compensating for observed conditions, but rely on the operator's skill. A digital two-axis shading controller could provide the equivalent of a perfectly compensated zero-offset adjustment for each pixel. Extending the concept could provide digital gain compensation to make each pixel appear to have precisely the same gain. The principle is similar to the patented pairs subtraction technique used by the LMSC Hertis.

5.2.4 Camera Positioners

The image size or field is controlled by a Z-stage that adjusts the camera-to-screen distance. The magnification is controlled by a F-stage that adjusts the camera-to-lens distance. The lens is coupled to the camera with bellows which allow a lot of motion, which in turn gives a large zoom range. Demonstrations have made good use of fields of view from 12 in. to under 1 in. A custom zoom lens could be designed for the RTR system, but the usual zoom ratios are limited to between 6:1 and 10:1. The breadboard system has exceed 20:1 zoom ratio. It is likely that lens and camera positioners will have to be built.

The positioning systems are smooth way stages with tight tolerances, such as ball bearings or cross roller bearings. Motion will be provided by a lead screw driven by a stepper motor. Figure 59 shows one possible configuration of the F and Z axis positioners. A digitally controlled positioner will require a stepper motor with a small displacement per step that can still move quickly enough that the operator will not have to wait for it to respond.



- ① ISOCON CAMERA
- ② BELLOWS
- ③ LENS
- ④ F-STAGE
- ⑤ Z-STAGE

Fig. 59 Camera Positioner Configuration

Compumotor makes a series of digitally controlled stepper motors that are adequate.

5.3 IMAGE PROCESSING AND CONTROL COMPUTER

The image-processing-and-control computer consists of a host computer, image-processing computer, video digitizer, and serial interfaces to communicate with the positioners, printers, modem, X-ray systems, and terminals.

5.3.1 Host Computer

The host computer selected is a Digital Equipment (DEC) 11/23 or 11/73 or MicroVax, depending on the type of application. The DEC computer family is largely interchangeable since the buss architecture is similar, and DEC computers are compatible with the widest variety of general purpose hardware and software of any computer. The flexibility of DEC compatability makes designing a system straightforward. The total development-program cost is lowered because hardware and software are off-the-shelf even though the hardware is expensive. If an application requires reproducing many of the overall systems, other more cost-effective host computers and image processors will have to be considered. Noteable, host computers and image processors based on the Motorola 68000 and IBM AT microcomputers are becoming very popular for dedicated applications such as computer-aided design, robot vision, automated inspection, and process control.

5.3.2 Image Processor

The image processor selected for the next stage of system development is the Recognition Concepts, Inc., Trappix Model 55128. This host and image processor combination is similar to those now being used. It is one of the more expensive to purchase but it offers a lot of flexibility and a wide base of support. RCI image processors can be configured to operate with 512 x 512 or 1024 x 1024 pixels per image and with 8, 12, or 16 bits per pixel. They have been programmed to do image enhancement, manipulation, and automatic

recognition in either gray scale or color. This choice assumes that the number of systems to be built will be small enough that the development costs are dominant. For higher-volume applications, several manufacturers make image processing boards compatible with DEC, Motorola 68000, and/or IBM AT based computers.

5.3.3 Video Digitizer

The video digitizer selection is a function of the information rate that must be acquired. RCI provides 8-bit, 10-bit, or 12-bit video rate digitizers. All of the work so far has been done with an 8-bit or 256-gray-levels digitizer. The video goes through software-controlled analog offset and gain corrections before being digitized. The offset and gain parameters can be optimized by the computer, if desired, to make use of the entire gray-scale range. The acquired signals are further integrated to improve the image signal-to-noise ratio. A 10- or 12-bit digitizer should either reduce the number of frames to be integrated and/or improve the image quality. A 12-bit digitizer is also being recommended in an effort to linearize the video-response of the video data acquisition system by passing the acquired 12-bit data through a lookup table during acquisition but before integration. This lookup table could be used to linearize the gray scale or calibrate it in terms of material thickness, number of photons, or other parameters.

5.3.4 Software

The current computer software language is Fortran. The operating system was DEC RT-11 but was recently changed to DEC RSX-11M to allow multiple users, easier programming, and more flexibility. The image-processing software supplied for the RCI Trappex was supplemented by a package by TAU, Inc. This is a widely supported, flexible software system. If the software package were to be rewritten, a UNIX operating system with a C language would probably be preferred. These should allow transporting the software from more flexible and expensive development systems to dedicated lower cost production systems.

5.4 OBJECT MANIPULATION SYSTEM

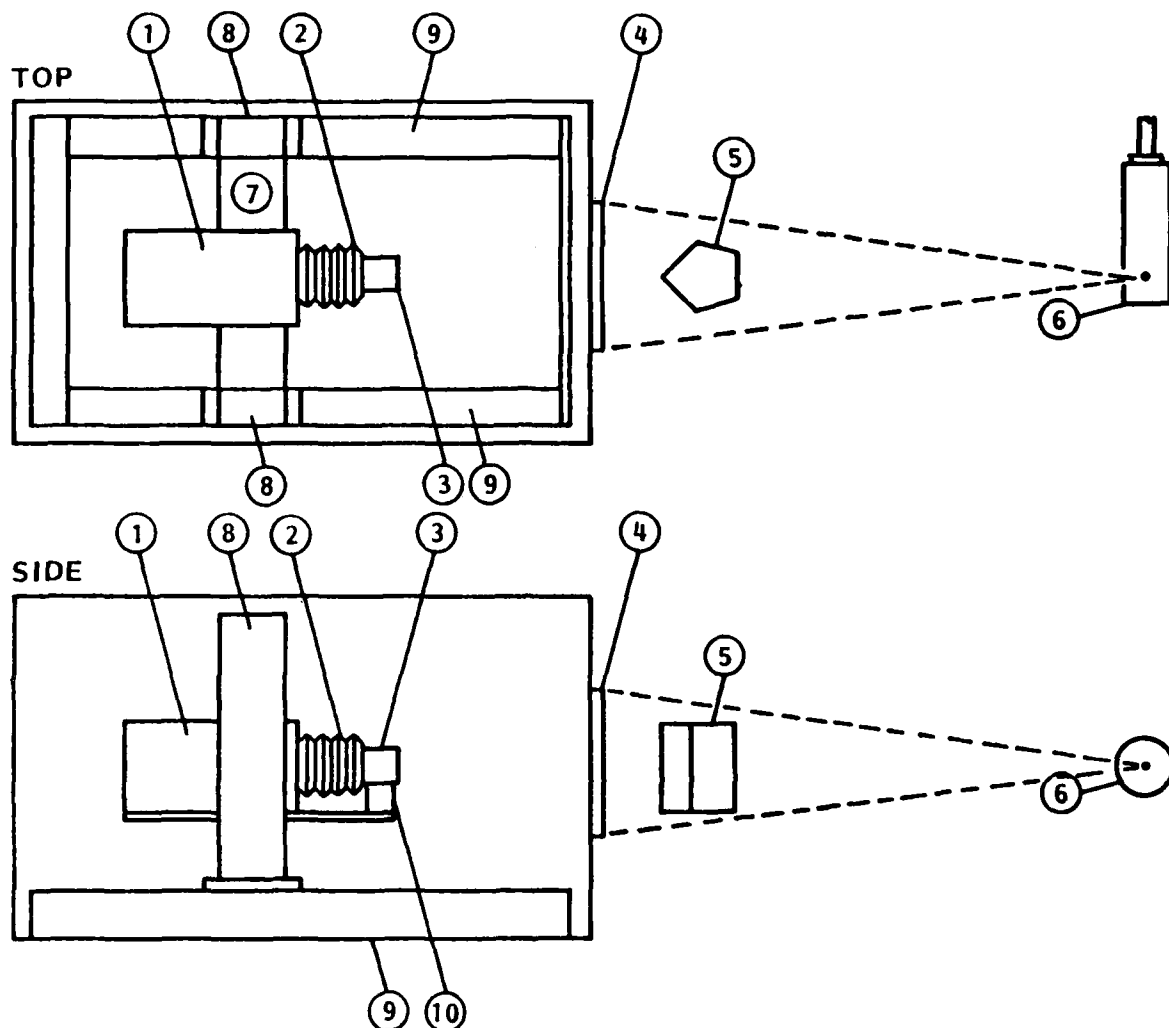
The object manipulator in the original breadboard was merely a platform to hold the object between the x-ray source and the x-ray converter screen as shown in Fig. 50. This system used an X, Y stage to move the Isocon camera to look at various screen locations and a Z, F stage to zoom in to get optical magnification and focus. A manual-switch-controlled positioner was added to align and move the objects being examined. The problems with this layout are:

- Shift-subtraction image acquisition shows the screen and x-ray beam nonuniformities.
- High-energy x-rays are directed at the camera and lens. This may cause electronic damage and browning of the lens glass if unshielded. Lead glass shielding may be quite thick for high energies.
- An object manipulator is still needed to position objects being inspected.
- The Isocon camera is vibration sensitive. This can cause image noise when moving in the X, Y direction, since the motion is coupled directly to the camera. The extra positioners make the camera mount less rigid.

To overcome these problems, the X and Y object positioners were moved outside the camera enclosure as shown in Fig. 61. This configuration allows the camera to be smaller, more rigid, and less sensitive to vibration. The camera can still zoom in on the center of the field of view. Moving the object in X and Y causes the system to emulate a magnifying glass looking at film images. Now shift subtraction moves the object and eliminates all defects except features in the object. The remaining problems with this configuration are:

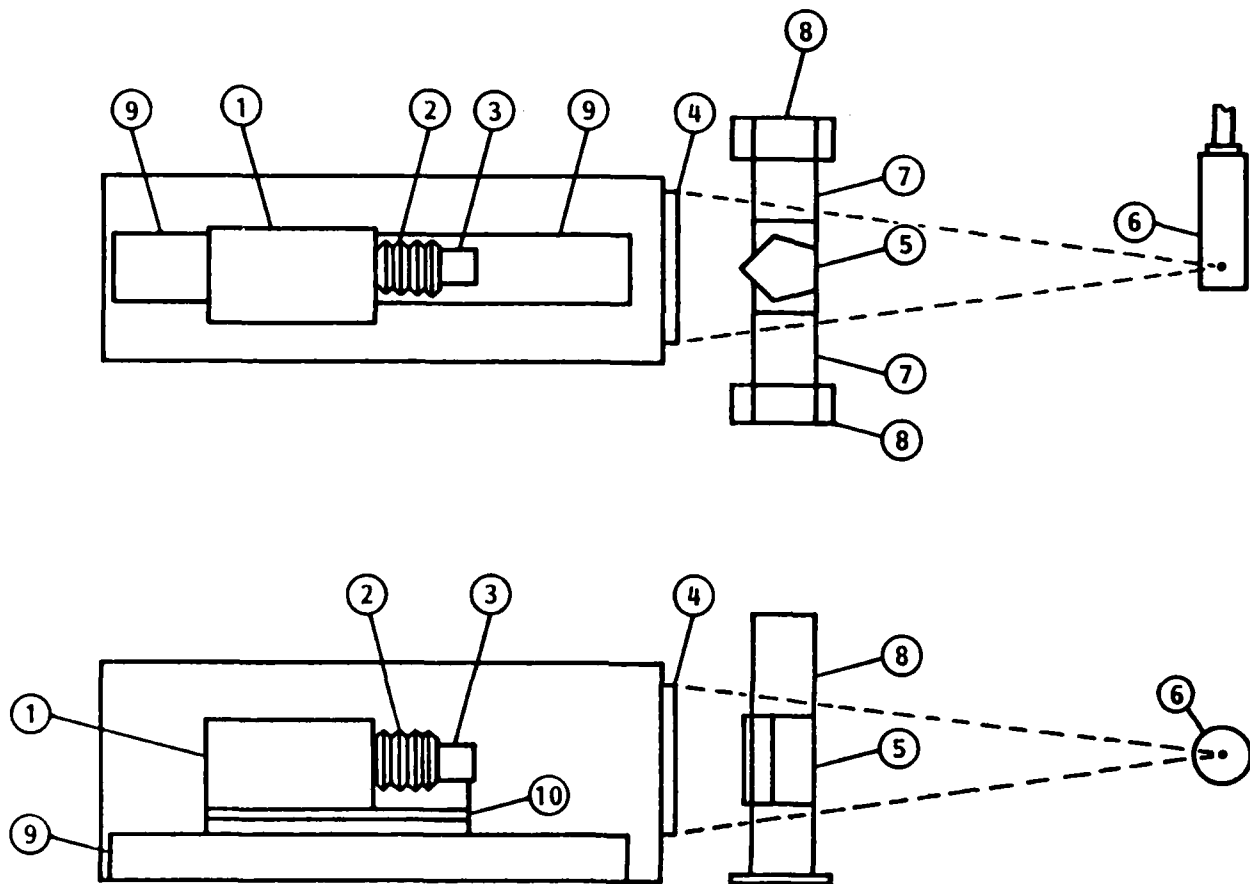
- High-energy x-rays are still directed at the camera and lens.
- The object may be heavy or awkward to manipulate.

The breadboard RTR camera has been shielded for direct exposure to x-rays below 300 kV, and no damage has been observed except eventual lens browning. Lens browning can be reversed by treatment with ultraviolet light. Lens



- | | | |
|----|---------|--|
| 1 | CAMERA | ISOCON LOW-LIGHT-LEVEL VIDEO CAMERA |
| 2 | BELLOWS | ALLOWS ISOCON-TO-LENS MOTION WITHOUT LIGHT LEAKS |
| 3 | LENS | LENS 60 mm f/0.7 |
| 4 | SCREEN | X-RAY-TO-LIGHT CONVERTER FOR APPLICATION |
| 5 | OBJECT | THE OBJECT BEING EXAMINED BY X-RAY |
| 6 | X-RAY | X-RAY HEAD |
| 7 | X-STAGE | LEFT-RIGHT MOTION |
| 8 | Y-STAGE | UP-DOWN MOTION |
| 9 | Z-STAGE | LENS-TO-SCREEN DISTANCE |
| 10 | F-STAGE | CAMERA-TO-LENS DISTANCE |
| 11 | MIRROR | FRONT SURFACE MIRROR |
| 12 | SHIELD | LEAD X-RAY SHIELDING |

Fig. 60 The Camera, Optics, and X Ray: Concept 1



- | | | |
|----|---------|--|
| 1 | CAMERA | ISOCON LOW-LIGHT-LEVEL VIDEO CAMERA |
| 2 | BELLOWS | ALLOWS ISOCON-TO-LENS MOTION WITHOUT LIGHT LEAKS |
| 3 | LENS | LENS 60 mm f/0.7 |
| 4 | SCREEN | X-RAY-TO-LIGHT CONVERTER FOR APPLICATION |
| 5 | OBJECT | THE OBJECT BEING EXAMINED BY X-RAY |
| 6 | X-RAY | X-RAY HEAD |
| 7 | X-STAGE | LEFT-RIGHT MOTION |
| 8 | Y-STAGE | UP-DOWN MOTION |
| 9 | Z-STAGE | LENS-TO-SCREEN DISTANCE |
| 10 | F-STAGE | CAMERA-TO-LENS DISTANCE |
| 11 | MIRROR | FRONT SURFACE MIRROR |
| 12 | SHIELD | LEAD X-RAY SHIELDING |

Fig. 61 The Camera, Optics, and X Ray: Concept 2

browning can be eliminated by shielding with lead glass, however, the optical image quality suffers as the energy range rises. To eliminate the potential high-energy x-ray shielding difficulties, a mirror can be installed in the optical path as shown in Fig. 62. This configuration allows the camera to zoom in and move around to emulate using a magnifying glass on a film image, but only with a limited range. The horizontal field of view could be varied from 12 to 4 in.

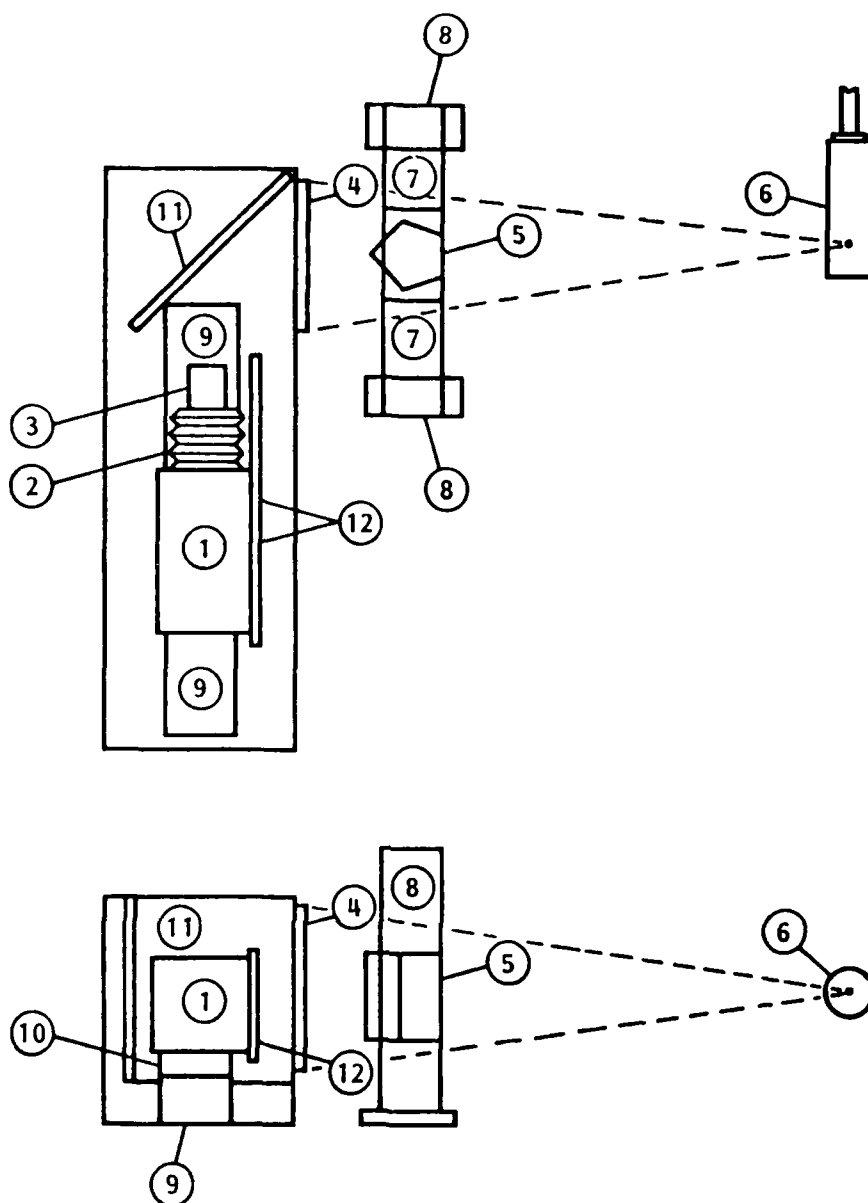
To extend the zoom range, the Z-stage can be mounted on a diagonal as shown on Fig. 63. The difficulty with this design is that zooming in causes the image to move off the center of the object being inspected. A computer-controlled object positioner could be programmed to compensate for zooming in, but the x-ray beam and screen might still vary.

Another way to keep the image centered is to move the mirror when zooming in as shown in Fig. 64. This should give a horizontal field of view from 12 to 3 in. A fast 4:1 or better zoom lens may be acquirable and must be evaluated against the mirror designs. For lower energies, where shielding is not a serious problem, the in-line design in Fig. 60 provides up to 20:1 zoom range.

5.5 OVERALL CONFIGURATION

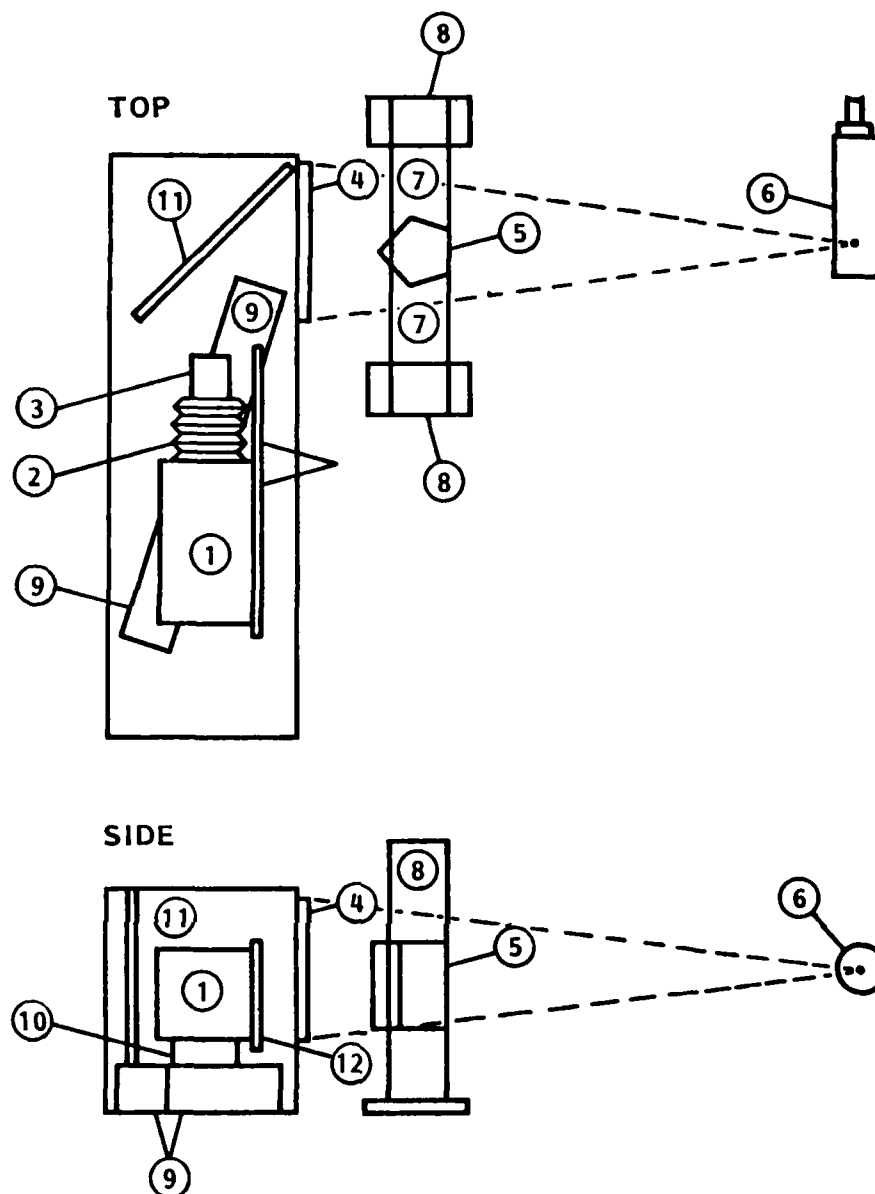
The configuration of the system is divided into the area inside the shielded x-ray room and the operator's area. The x-ray room configuration is dictated primarily by the camera, object configuration, and the type(s) of x-ray sources required for the inspection.

The operator's area is determined by the subsystems selected for the system. A typical operator's console design for a high-resolution real-time radiographic system is shown in Fig. 65.



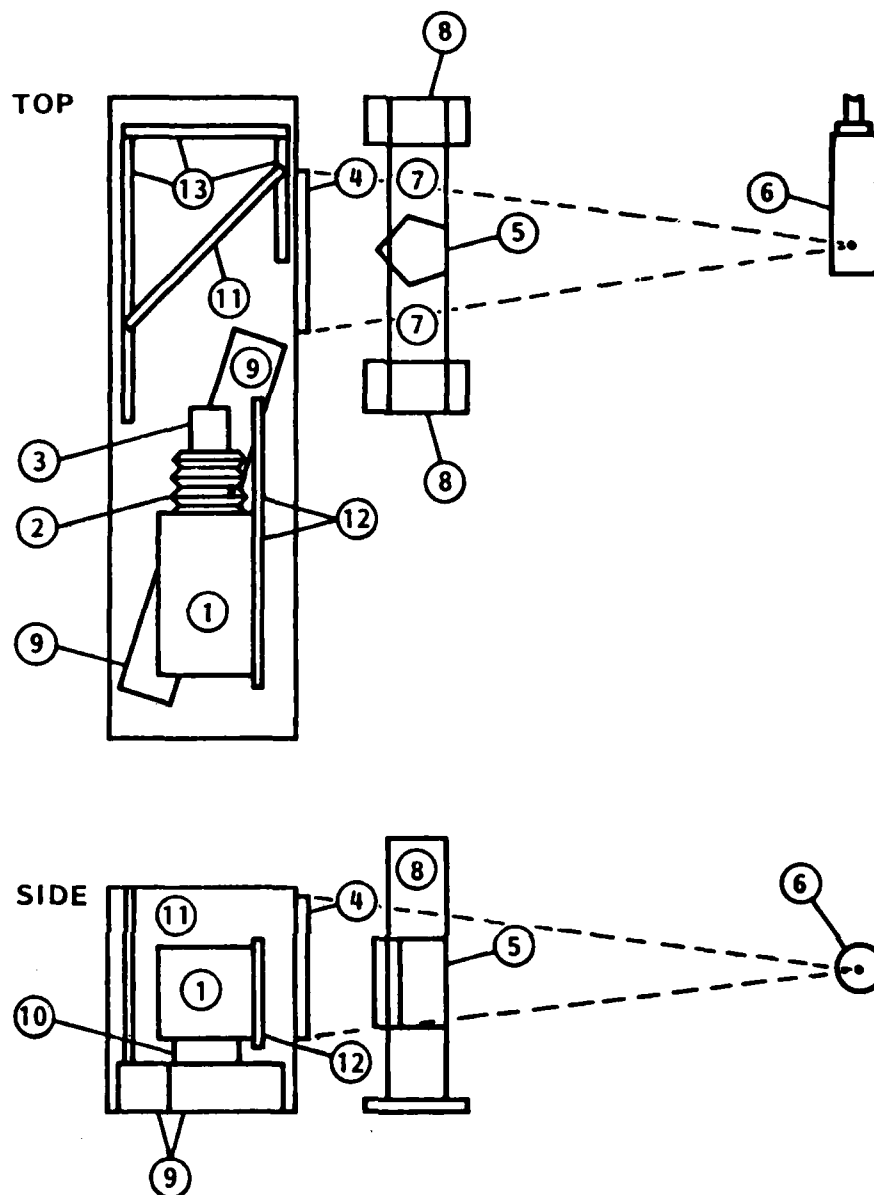
- | | | |
|----|---------|--|
| 1 | CAMERA | ISOCON LOW-LIGHT-LEVEL VIDEO CAMERA |
| 2 | BELLOWS | ALLOWS ISOCON TO LENS MOTION WITHOUT LIGHT LEAKS |
| 3 | LENS | LENS 60 mm f/0.7 |
| 4 | SCREEN | X-RAY-TO-LIGHT CONVERTER FOR APPLICATION |
| 5 | OBJECT | THE OBJECT BEING EXAMINED BY X-RAY |
| 6 | X-RAY | X-RAY HEAD |
| 7 | X-STAGE | LEFT-RIGHT MOTION |
| 8 | Y-STAGE | UP-DOWN MOTION |
| 9 | Z-STAGE | LENS-TO-SCREEN DISTANCE |
| 10 | F-STAGE | CAMERA-TO-LENS DISTANCE |
| 11 | MIRROR | FRONT SURFACE MIRROR |
| 12 | SHIELD | LEAD X-RAY SHIELDING |

Fig. 62 The Camera, Optics, and X Ray: Concept 3



- | | | |
|----|---------|--|
| 1 | CAMERA | ISOCON LOW-LIGHT-LEVEL VIDEO CAMERA |
| 2 | BELLOWS | ALLOWS ISOCON-TO-LENS MOTION WITHOUT LIGHT LEAKS |
| 3 | LENS | LENS 60 mm f/0.7 |
| 4 | SCREEN | X-RAY-TO-LIGHT CONVERTER FOR APPLICATION |
| 5 | OBJECT | THE OBJECT BEING EXAMINED BY X-RAY |
| 6 | X-RAY | X-RAY HEAD |
| 7 | X-STAGE | LEFT-RIGHT MOTION |
| 8 | Y-STAGE | UP-DOWN MOTION |
| 9 | Z-STAGE | LENS-TO-SCREEN DISTANCE |
| 10 | F-STAGE | CAMERA-TO-LENS DISTANCE |
| 11 | MIRROR | FRONT SURFACE MIRROR |
| 12 | SHIELD | LEAD X-RAY SHIELDING |

Fig. 63 The Camera, Optics, and X Ray: Concept 4



- | | | |
|----|---------|--|
| 1 | CAMERA | ISOCON LOW-LIGHT-LEVEL VIDEO CAMERA |
| 2 | BELLOWS | ALLOWS ISOCON-TO-LENS MOTION WITHOUT LIGHT LEAKS |
| 3 | LENS | LENS 85 mm f/0.7 |
| 4 | SCREEN | X-RAY-TO-LIGHT CONVERTER FOR APPLICATION |
| 5 | OBJECT | THE OBJECT BEING EXAMINED BY X-RAY |
| 6 | X-RAY | X-RAY HEAD |
| 7 | X-STAGE | LEFT-RIGHT MOTION |
| 8 | Y-STAGE | UP-DOWN MOTION |
| 9 | Z-STAGE | LENS-TO-SCREEN DISTANCE |
| 10 | F-STAGE | CAMERA-TO-LENS DISTANCE |
| 11 | MIRROR | FRONT SURFACE MIRROR |
| 12 | SHIELD | LEAD X-RAY SHIELDING |
| 13 | M-STAGE | MOVES MIRROR TO CENTER IMAGE |

Fig. 64 The Camera, Optics, and X Ray: Concept 5

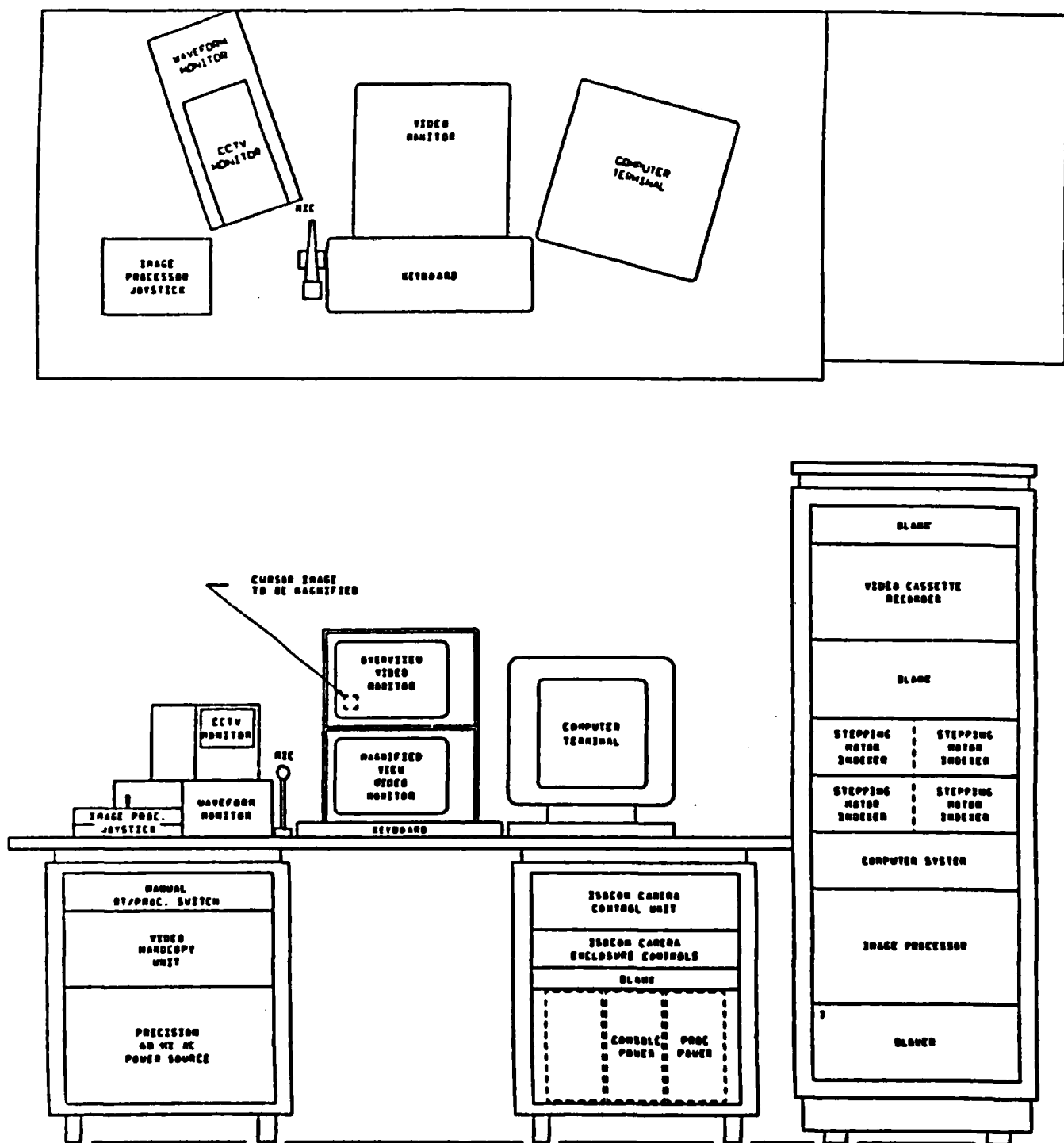


Fig. 65 Operator's Console: Air Force RTR System

END

DATE

FILMED

JAN

1988